ANALYTICAL MODEL FOR CONCRETE ANCHORAGES OF REINFORCING BARS UNDER GENERALIZED EXCITATIONS

by

Vincenzo Ciampi

Visiting Scholar from the University of Rome, Italy

Rolf Eligehausen

Visiting Scholar from the University of Stuttgart,
Federal Republic of Germany

Vitelmo V. Bertero

Professor of Civil Engineering
University of California, Berkeley

Egor P. Popov

Professor of Civil Engineering
University of California, Berkeley

A report on research sponsored by the
National Science Foundation.

Report No. UCB/EERC-82/23
Earthquake Engineering Research Center
College of Engineering
University of California
Berkeley, California
November 1982

50272-101

REPORT DOCUMENTATION PAGE	1. REPORT NO. NSF/CEE-82068	2.	3. Recipient's Accession No. PB83 169532

4. Title and Subtitle
Analytical Model for Concrete Anchorages of Reinforcing Bars under Generalized Excitations

5. Report Date
November 1982

6.

7. Author(s)
V. Ciampi, R. Eligehausen, V. V. Bertero, E. P. Popov

8. Performing Organization Rept. No.
UCB/EERC-82/23

9. Performing Organization Name and Address
Earthquake Engineering Research Center
University of California, Berkeley
47th Street & Hoffman Blvd.
Richmond, Calif. 94804

10. Project/Task/Work Unit No.

11. Contract(C) or Grant(G) No.
(C)
(G) PFR-79-08984

12. Sponsoring Organization Name and Address
National Science Foundation
1800 G Street, N. W.
Washington, D. C. 20550

13. Type of Report & Period Covered

14.

15. Supplementary Notes

16. Abstract (Limit: 200 words)

The model is based on a general local bond stress-slip relationship, derived from the results of a previous extensive study, and on either a bilinear or a simple but sufficiently accurate nonlinear stress-strain relationship for the reinforcing steel bar. An efficient numerical scheme for the integration of the governing differential equation of bond along the embedment length of the bar is presented.

The analytical model is then used to predict the bond behavior of a reinforcing bar embedded in exterior and interior joints of reinforced concrete frames subjected to severe load and/or deformation reversals which simulate the effects of earthquake loading. In these joints, besides confined concrete, the concrete that covers the core is unconfined; therefore, a modified analytical model for these cover regions had to be developed.

The analytical model is also used to conduct a numerical investigation of the influence on anchored bar behavior of (1) type of analytical model of the stress-strain relationship of the reinforcing bar (bilinear vs. nonlinear), (2) severity of hysteretic requirements determined by the number of imposed cycles and the peak values of the steel strains, (3) main mechanical characteristics of steel (namely, yield stress and rate of strain hardening), and (4) anchorage length.

17. Document Analysis a. Descriptors

b. Identifiers/Open-Ended Terms

c. COSATI Field/Group

18. Availability Statement:	19. Security Class (This Report)	21. No. of Pages
Release Unlimited		121
	20. Security Class (This Page)	22. Price

(See ANSI-Z39.18) *See Instructions on Reverse*

OPTIONAL FORM 272 (4-77)
(Formerly NTIS-35)
Department of Commerce

ABSTRACT

This report presents an analytical model for predicting the behavior of single deformed reinforcing bars embedded in confined concrete and subjected to generalized excitations in the range of low cycle fatigue. The model is based on a general local bond stress-slip relationship, derived from the results of an extensive study performed at Berkeley, and on either a bilinear or a simple but sufficiently accurate nonlinear stress-strain relationship for the reinforcing steel bar. An efficient numerical scheme for the integration of the governing differential equation of bond along the embedment length of the bar is presented.

The analytical model is then used to predict the bond behavior of a reinforcing bar embedded in exterior and interior joints of reinforced concrete frames subjected to severe load and/or deformation reversals which simulate the effects of earthquake loading. In these joints, besides confined concrete, the concrete that covers the core is unconfined; therefore, a modified analytical model for these cover regions had to be developed.

The analytically predicted response compares well with the results of a series of tests conducted at Berkeley for monotonic and cyclic loadings.

The analytical model is also used to conduct a numerical investigation of the influence on anchored bar behavior of the following main parameters: (1) type of analytical model of the stress-strain relationship of the reinforcing bar (bilinear vs. nonlinear), (2) severity of hysteretic requirements determined by the number of imposed cycles and the peak values of the steel strains, (3) main mechanical characteristics of steel (namely, yield stress and rate of strain hardening), and (4) anchorage length.

The results of this investigation reported herein are used to offer some practical recommendations regarding the required anchorage length of reinforcing bars in interior and exterior joints. Finally, conclusions are formulated, as well as recommendations for future work.

ACKNOWLEDGEMENTS

The authors are grateful for the financial support provided for this investigation by the National Science Foundation under Grant PFR79-08984 with the University of California, Berkeley. The support of Dr. Ciampi by the Italian Research Council and of Dr. Eligehausen by the Deutsche Forschungs-gemeimschaft are gratefully acknowledged.

F. C. Filippou assisted with the preparation of the report for publication. Gail Feazell made the drawings and prepared them for publication, and Linda Calvin did the typing of the final manuscript. The authors would like to thank them for their help.

TABLE OF CONTENTS

Table of Contents (cont'd) Page

LIST OF FIGURES

LIST OF TABLES

I. INTRODUCTION

1.1 STATEMENT OF PROBLEM

Under severe seismic excitations, the hysteretic behavior of reinforced concrete structures appears to be highly dependent on the interaction between steel and concrete (bond stress-slip relationship) [1]. Tests show that when the developing story displacement ductility ratio is four or more, fixed end rotations caused by slip of the main steel bars along their embedment length in beam-column joints may contribute up to 50 percent to the total beam deflection [2-4]. This contribution must be fully understood and included in the analytical prediction of response. However, in spite of recent integrated experimental and analytical studies devoted to investigating this problem [5], no reliable bond stress-slip laws for generalized excitations are available [6].

This consideration has motivated an extensive experimental study, carried out in Berkeley during the 1979-1981 period, aimed at finding the constitutive bond stress-slip relationships between deformed bars and well confined normal weight concrete. The results of this study are presented in a companion report [7].

At the same time, need for an efficient analytical model capable of predicting the behavior of reinforcing bar anchorages under generalized excitations emerged, and research efforts were directed toward the formulation of such a model. In Ref. [8] a mathematical model of a deformed bar embedded in a concrete block and subjected to generalized cyclic excitations was presented, and this report is a further elaboration on this subject.

1.2 OBJECTIVES AND SCOPE

This report discusses in detail the mathematical model presented in Ref. [8] for reinforcing bars anchored at interior joints as well as its applications. The model is first used to predict analytically the response of anchored beam bars and to compare these predictions with some experimental results presented in [5] and then to generate systematic numerical results for an investigation of the influence of various parameters on the response of an anchored bar.

In Chapter 2 the analytical bond stress-slip law derived from the experimental results reported in [7] is briefly described. In Chapter 3 a model for the stress-strain relationship for a steel bar is formulated. In Chapter 4 a mathematical model is presented for computing the response of an anchored bar, which involves the integration of the governing differential equation of bond. In Chapter 5 the ability of the model to reproduce experimental results is demonstrated. Chapter 6 investigates the influence of variation of parameters on the response. Chapter 7 discusses practical implications of results obtained, and Chapter 8 summarizes the main conclusions and offers some recommendations for future research. The developed computer program is described in Appendix A.

II. LOCAL BOND MODEL

2.1 GENERAL

The constitutive bond stress-slip relationship for deformed bars embedded in normal weight well-confined concrete were derived from an extensive experimental study carried out at Berkeley during 1979-1981. The results of this study are presented in full detail in a companion report [7].

Based on the results of that experimental investigation, an analytical model for the local bond stress-slip law under generalized slip histories was derived and is briefly described in Section 2.2. More details may be found in Ref. [7]. Comparisons of analytical predictions with experimental results are contained in Section 2.3.

The model is valid only for describing the bond behavior in confined concrete regions. However, in view of the purpose of the present investigation, which is to formulate a mathematical model for predicting the behavior of anchorages, an attempt was made to generalize the model to cover the less known behavior of bond in unconfined concrete regions. This is briefly discussed in Section 2.4.

2.2 ANALYTICAL LOCAL BOND STRESS-SLIP MODEL

2.2.1 GENERAL

The assumed bond model is illustrated in Fig. 2.1. Although it simplifies the observed real behavior, it takes into account the significant parameters that appear to control the behavior observed in the experiments. This model, in spite of being simpler than the one proposed in [5], is believed to be more general. The model's main characteristics, illustrated by following a typical cycle (Fig. 2.1), are described below.

When loading the first time, the assumed bond stress (τ) - slip (s) relationship follows a curve valid for monotonically increasing slip, which is called herein "monotonic envelope" (paths OABCD or $OA_1B_1C_1D_1$). Imposing a slip reversal at an arbitrary slip value, a stiff

"unloading branch" is followed up to the point where the frictional bond resistance, τ_f, is reached (path EFG). Further slippage in the negative direction takes place without an increase in τ up to the intersection of the "friction branch" with the curve OA_1' (path GHI). If more slip in the negative direction is imposed, a bond stress-slip relationship similar to the virgin monotonic curve is followed, but with values of τ reduced as illustrated by the path $IA_1'J$, which is part of the curve $OA_1'B_1'C_1'D_1'$ that is called "reduced envelope". When reversing the slip again at J, first the unloading branch and then the frictional branch, with $\tau = \tau_f^+$, are followed up to point N, which lies on the unloading branch EFG (path JLN). At N the "reloading branch" (same stiffness as the unloading branch) is followed up to the intersection with the reduced envelope $OA'B'C'D'$ (path NE'), which is followed thereafter (path E'B'S). If instead of increasing the slip beyond point N more cycles between the slip values corresponding to points N and K are imposed, the bond stress-slip relationship is like that of a rigid plastic model, the only difference being that frictional bond resistance decreases with increasing number of cycles. A similar behavior as described is followed if the slip is reversed again at point S (path STU). To complete the illustration of the model, details about the different branches referred to in the above overall description are given in the following sections.

2.2.2 MONOTONIC ENVELOPE

The simplified monotonic envelope simulates the experimentally obtained curve under monotonically increasing slip. It consists of an initial nonlinear relationship $\tau = \tau_1(s/s_1)^\beta$, valid for $s \leqslant s_1$, followed by a plateau $\tau = \tau_1$ for $s_1 \leqslant s \leqslant s_2$. For $s \geqslant s_2$, τ decreases linearly to the value of the ultimate frictional bond resistance τ_3 at a slip value of s_3. This value s_3 is assumed to be equal to the clear distance between the lugs of the deformed bars. The same bond stress-slip law is assumed regardless of whether the bar is pulled or pushed.

The values s_1, s_2, τ_1, τ_3, and β are chosen to match the experimentally obtained monotonic envelope curve. Some representative numerical values are given in Ref. [7].

2.2.3 REDUCED ENVELOPES

Reduced envelopes are obtained from the monotonic envelope by decreasing the characteristic bond stresses τ_1 and τ_3 through reduction factors, which are formulated as a function of one parameter, called herein the "damage parameter d". For no damage, d=0, the reloading branch reaches the monotonic envelope. For full damage, d=1, bond is completely destroyed (τ=0).

The rationale for this assumption is given by Fig. 2.2, which shows that reloading curves for similar specimens, subjected to different loading histories, appear to form a parametric family of curves.

The deterioration of the monotonic envelope seems to depend on the damage experienced by the concrete, particularly the length of the concrete between the lugs of the bar that has sheared off. This, in turn, is a function of the magnitude of the slip induced in the bar in both directions, the larger the s_{max} and the difference between peak slip values, the larger the damage. Another influence factor is the number of cycles. These parameters can be related to the energy dissipated during the loading and unloading processes. Therefore, it was assumed that the damage parameter d is a function of the total dissipated energy only. However, it has also been taken into account that only a fraction of the energy dissipated during subsequent cycles between fixed peak slip values appears to cause damage, while the other part appears to be used to overcome the frictional resistance and is transformed into heat.

Figure 2.3 illustrates the correlation between the measured damage factor, d, for tests with full reversal of slip as a function of the computed dimensionless dissipated energy factor E/E_o. The proposed function for d is shown as well. In the computation of E, only 50% of the energy dissipated by friction is taken into account. The normalizing energy E_o corresponds to the absorbed energy under monotonically increasing slip up to the value s_3. Although there is some scatter, the agreement between the analytical and experimental results seems acceptable.

No reduction of the current envelope (monotonic or reduced) is assumed for unloading and reloading only (e.g., paths EGE or JLJ in Fig. 2.1). If a cycle is not completed to the

current values of s_{max} or s_{min} (e.g., path GHM), the damage parameter is linearly interpolated between the values valid for the last slip reversal and for the completed cycle (point E and point P in this example). For details, see Ref. [7].

It should be observed that the proposal for calculating the damage parameter as a function of the total dissipated energy is theoretically correct only in the range of the low cycle fatigue; that is, when a small number of cycles at relatively large slip values is carried out. In fact, if a high number of cycles at small slip values is performed, the energy dissipated can be relatively large, but no significant damage is produced and the reloading branch reaches the monotonic envelope again [9]. On the other hand, when limiting our attention to a small number of cycles ($\leqslant 30$), as in the present study, the energy dissipated for cycles between small slip values is rather small and the calculated damage, as a consequence, insignificant.

2.2.4 FRICTIONAL RESISTANCE

The frictional bond resistance after first unloading (τ_f^- in Fig. 2.1) depends upon the peak value of slip, s_{max}, and is related to the value of the ultimate frictional bond resistance of the corresponding reduced envelope (τ_3^- in Fig. 2.1). The relationship found in the tests is shown in Fig. 2.4. However, if cycling is done between fixed values of slip (e.g., between fixed s_{max} and s_{min} in Fig. 2.1), τ_f is reduced more rapidly than the ultimate τ_3 of the corresponding reduced envelope (see Figs. 2.4 and 2.5). Therefore, the analytical function, 0abc, in Fig. 2.4 is used only for the calculation of the frictional resistance for the first slip reversal. For subsequent cycles, τ_f (e.g., τ_f^+ in Fig. 2.1) is reduced from this initial value by multiplying it with an additional reduction factor which depends on the energy dissipated by friction alone. If unloading is done from a larger slip value than the peak slip in the previous cycle (path STU), the new frictional bond resistance (τ_{fu}) is linearly interpolated between two values. The first value is related to τ_3^- of the corresponding new reduced envelope using the analytical function given in Fig. 2.4, and the second value is the τ_f reached in the last cycle (τ_f^+ in Fig. 2.1). This interpolation is done in order to have a smooth transition in the values of τ_f.

2.2.5 CONCLUDING REMARKS

Note that the concept of relating damage to one scalar quantity, like the normalized dissipated energy, has provided a basis for a relatively easy generalization of the bond behavior for random excitations. The bond model selected can easily be extended to cover bond of bars under conditions different from those reported herein, such as different bar diameter, pattern of deformation (lugs), concrete strength, degree of confinement, effect of transverse pressure, etc. This requires that the pertinent experimental data necessary for computing the different parameters, in particular the monotonic envelope, be obtained. If these are not available, the suggestions given in [7] could be used for choosing the required parameters.

2.3 COMPARISON OF ANALYTICAL PREDICTIONS WITH EXPERIMENTAL RESULTS

The local bond stress-slip relationships, obtained using the model described above, are compared in Fig. 2.5 with the experimental results obtained in some of the Berkeley tests. As can be seen, except for the reloading curves near the values of the peak slip between which the specimen was cycled, the agreement is quite good. In general, the model was successful in reproducing most of the experimental results.

2.4 EXTENSION OF THE MODEL TO THE UNCONFINED CONCRETE REGIONS

The bond conditions in a joint vary along the embedment length. For an interior joint, three different regions have been identified in [5] (see Fig. 2.6). They show differences both in the shape of the monotonic envelopes, different for positive and negative slip, and in the rate at which degradation occurs. Of course, there is a gradual variation in the behavior proceeding from an unconfined region to the confined one.

The possibility of extending the analytical model presented here for confined concrete to the unconfined regions, using information contained in [5], is discussed in detail in [7]. The analytical bond model is generalized as follows:

-instead of only one, two different monotonic envelopes are specified, one for positive and one for negative slip values (compare Fig. 2.6);

-the normalizing energy, E_o, used in the computation of damage is chosen as the larger one between E_o^+ and E_o^-. These quantities define the corresponding areas under the monotonic envelopes for positive and negative slip values up to slip value s_3. To take into account different rates of damage in the two directions of loading, the pertinent dissipated energy, E, used for computing the reduced envelopes, is multiplied by an amplification factor b, which is different for the upper and lower curve. The factors b^+ and b^- are specified as input values. Similar rules for the computation of damage apply to the friction part of the curves.

More details regarding the quantification of the various parameters involved, and of their distribution along the anchorage length in an interior beam-column joint, are contained in [7].

III. STEEL MODEL

3.1 GENERAL

Prediction of response of anchored bars under severe seismic excitations requires an accurate model for the stress-strain relationship of reinforcing steel. In fact, since in general the anchorage provided to the bars is sufficient to develop their yield strength, the model should be able to accurately reproduce the inelastic behavior of steel under generalized strain histories.

For this reason, an accurate nonlinear model for steel is presented in Section 3.2 and is compared with some other previously used models. The model described [10] reproduces the experimentally observed cyclic behavior of reinforcing steel bars reasonably well [5].

This model has been used successfully in the numerical investigations which follow. However, in the implementation of the computer program which computes the response of an anchored bar, an option has been left to use, as an alternative, the simple bilinear model referred to in Section 3.4. Reasons for allowing this option are given in Section 3.4.

3.2 NONLINEAR MODEL

The model formulation described here has been used previously [10]. It consists of a nonlinear equation which explicitly expresses stress as a function of strain:

$$\sigma = \hat{\sigma}(\epsilon) \tag{3.1}$$

and of a set of simplified rules which allow reproduction of the behavior under generalized strain histories.

The expression adopted for Eqn. 3.1 was first proposed in [11] and subsequently used in [12]. In a nondimensional form, it can be written:

$$\sigma^* = b\epsilon^* + \frac{(1-b)\,\epsilon^*}{(1+|\epsilon^*|^R)^{1/R}} \tag{3.2}$$

where

$$\sigma^* = \sigma/\sigma_o, \quad \epsilon^* = \epsilon/\epsilon_o \tag{3.2a}$$

for the first loading curve, and

$$\sigma^* = (\sigma - \sigma_i)/2\sigma_o, \quad \epsilon^* = (\epsilon - \epsilon_i)/2\epsilon_o \tag{3.2b}$$

for the first unloading and all subsequent branches.

In the above equations, σ_o and ϵ_o, as shown in Fig. 3.1, are stress and strain at the point where the asymptotes (initial and final) of the curve meet, which approximately correspond to the stress and strain at yield; σ_i and ϵ_i are stress and strain at the latest or current inversion point -- that is, where the last reversal of strain occurred; b is the strain hardening ratio -- that is, the ratio between the slope E_1 of the final symptote and the initial slope E_o; and R is a parameter which influences the shape of the curve and allows a good representation of the Bauschinger effect.

R is considered dependent on the maximum excursion into the plastic range, ϵ_{max}, defined in Fig. 3.1, and takes the form suggested in [12].

$$R = R_o - \frac{a_1 + \epsilon_{max}}{a_2 + \epsilon_{max}} \tag{3.3}$$

where R_o is the value of the parameter R at the first loading curve and a_1, a_2 are parameters to be defined together with R_o.

Equation 3.2b expresses a rule attributed to Masing which states that unloading and reloading curves are twofold magnifications of the first loading curve. They are obtained by a shift of the origin to the point (ϵ_i, σ_i) where the direction of loading was reversed.

However, Masing's rule is not sufficient per se to describe the behavior under generalized strain histories. It has to be properly interpreted and complemented in order to apply to the case being considered here.

But before discussing this point it is worthwhile to compare briefly the model defined by Eqns. 3.2 with the classical Ramberg-Osgood model [15].

$$\epsilon^* = \beta\sigma^* (1 + \alpha |\sigma^*|^{n-1}) \tag{3.4}$$

which has been often used in similar context [4,13,14] to describe the nonlinear behavior of steel in order to indicate the differences and advantages of the present formulation.

Equation 3.4 has several disadvantages compared to Eqn. 3.2. First of all, it has to be solved by an iterative procedure if strains are the independent variables. This disadvantage is particularly felt when the local stress-strain relationship is used, as in the present case, in the context of an iterative procedure where, at each iteration, given a tentative value of the strain, the corresponding value of the stress has to be determined. Since the computations need to be repeated a large number of times, use of explicit expressions as Eqn. 3.2 may be crucial to reduce computational costs. Furthermore, it is disadvantageous for the exponent n in Eqn. 3.4 to control both the mode of transition into the plastic range and the hardening beyond the yield point, while in Eqn. 3.2 these two characteristics are controlled by two independent parameters, R and b. Finally, unlike Eqn. 3.2, Eqn. 3.4 does not have a final asymptote (see also Ref. [16]). Despite these difficulties, models based on Eqn. 3.4 have been used successfully, but at the expense of programming complications and computational cost.

As already indicated, Eqn. 3.2 has to be complemented by a set of rules for unloading and reloading to allow for a generalized loading history. The direct extension of Masing's rule to this case cannot be easily implemented in a computer program because it implies the memorization of all curves followed after any particular branching point, up to returning to the main loop from which that branching originated. The reason for this is that every reversal point, together with the previous one, defines a loop which can be completed or only partially followed before a new reversal occurs. In the second case, a number of internal subloops can possibly originate. However, only when the main loop has been completed can the internal loops be forgotten.

This is illustrated by Fig. 3.2, where the loading history is described by the progression of points of load reversal. When point 6 is reached, the history of loading should have been kept track of for all the points of load reversal from 1 to 5. However, if, starting from 6, the strain is increased monotonically beyond point 3, all the internal subloops defined by load reversals between points 3 to 6 can be forgotten.

This example shows that the number of quantities to be remembered cannot be limited a priori but is dependent on the strain history. This is clearly impractical. The way out is to

adopt some simplified rules, and the common basis of the different variations proposed is the memorization of only a limited number of branches and the acceptance, should it be the case, of some deviation from the "correct" pattern described above. For example, in [14] up to 13 different branches are memorized. In [10], and now here, in order to avoid unnecessary complications, a drastic simplification is used based on the memorization of the parameters defining the following 4 curves (Figs. 3.2 and 3.3):

(a) skeleton curve or monotonic envelope;

(b) upper curve, which is the ascending branch originating at the reversal point with the lowest ϵ value;

(c) lower curve, which is the descending branch originating at the reversal point with the highest ϵ value; and,

(d) current curve, which originates at the most recent load reversal point.

When moving along an ascending branch, in a reloading stage, the current curve (d) is followed up to the point where it intersects curve (b) (point 3 in Fig. 3.2). Thereafter, one follows curve (b) up to the point where the skeleton curve (a) is met (point 1 in Fig. 3.2) and, subsequently, curve (a) is followed. Likewise, when moving along a descending branch, during an unloading stage, the path along the current curve is limited from below by curves (c) and (a).

In Fig. 3.3, for a strain history the same as the one in Fig. 3.2, the path followed using these simplified rules is compared with the "correct" one, which is shown by a dashed line. In this case, the differences are rather small.

The situation is less favorable and the error bigger in the case of Fig. 3.4. On the other hand, if the cycle is rather regular, as in Fig. 3.5a, there is no error involved.

Notice also that the rules used here are very similar to the ones proposed in [13] in connection with a conventional Ramberg-Osgood expression (Eqn. 3.4).

Some final comments need to be made. Some of the previously used models (for exam-

ple, the one used in [4]), though basically based on Eqn. 3.4, include a much more accurate representation of the first loading (or monotonic) curve. A similar generalization is also possible for a model based on Eqn. 3.2. As a matter of fact, this is exactly what has been recently implemented in [17], where the starting expression for describing the steel law is again Eqn. 3.2. Of course, the complexity of the model increases.

Here the above refinements have been considered unnecessary because the interest is focused on the correct reproduction of the overall cyclic response rather than on a very close matching of the first loading path. The nonlinear model presented here has to be considered as a compromise between simplicity and accuracy.

3.3 COMPARISON WITH EXPERIMENTAL RESULTS

The model described in Section 3.2 has been used to compare with some test results presented in [5]. With the following choice of parameters of the model:

$E = 2.04 \times 10^5 N/mm^2$
$R_o = 20$
$a_1 = 18.5$
$a_2 = 0.00015$
$b = 0.017$

the comparison appears to be fairly satisfactory (Figs. 3.5a and 3.5b).

3.4 BILINEAR MODEL

As indicated in the introduction, the option of a simple bilinear model (Fig. 3.6) to describe the cyclic behavior of the steel has been implemented in the computer program. This option has allowed the verification that even if the simplest nonlinear model based on Eqn. 3.2 is used, significantly more expensive computations than the corresponding bilinear model result. The reasons for this are attributed to the fact that the computation of the steel stress using Eqn. 3.2 is more costly than using the bilinear model because it involves checks that have to be made comparing different branches, for each of which the double exponentiation contained in Eqn. 3.2 has to be computed. In addition, the iterative scheme used for solving the

differential equation of bond needs more iterations per step to converge when the local constitutive laws are curvilinear instead of piecewise linear. As a consequence, the overall cost of computation is more than doubled when the nonlinear steel model is used.

As will be discussed in Section 6.2.1, it has been found that in many cases the overall behavior of the anchored bar model, especially the progression of bond damage, which is one of the most important characteristics of such behavior, is not much influenced by the Bauschinger effect in the steel (which is not present in the bilinear model) but depends primarily on the values of the yield point and the slope of the strain hardening branch. A parametric investigation can be conducted more economically when using the bilinear model. The more accurate nonlinear model can be used just to check the reliability of the results obtained using the bilinear model.

IV. ANALYTICAL MODEL FOR AN ANCHORED BAR

4.1 GENERAL

The actual behavior of a bar of finite length embedded in a concrete block can be studied using an idealized one-dimensional mathematical model. The resulting governing ordinary non-linear differential equation may be written as:

$$\frac{dN(x)}{dx} - q(x) = 0 \tag{4.1}$$

where $q = \pi d_b \tau(x)$ and $N = A\,\sigma(x)$, with d_b = diameter of the bar and A = area of the bar cross section. This relation expresses equilibrium of an infinitesimal portion of the bar and connects the axial force in the bar, N, to the resultant per unit length of the bond stresses on the perimeter of the bar, q (see Fig. 4.1). It has to be coupled with the constitutive laws for steel and bond, which can be expressed as:

$$\sigma = \hat{\sigma}(\epsilon(x)) \approx \hat{\sigma}\left(\frac{ds(x)}{dx}\right) \tag{4.2}$$

and

$$\tau = \hat{\tau}(s(x)) \tag{4.3}$$

where $s(x)$ is the slip along the bar. Note that here the influence of concrete deformation on slip has been considered negligible, as commonly assumed; and, as a consequence, the strain in the steel, ϵ, has been set equal to $\frac{ds}{dx}$.

Boundary values are specified at the two end points of the bar. Three different cases, in particular, have been considered (Fig. 4.2).

(1) The displacements (slip) at the two ends are assigned (this is the case, for example, of a pull-push test with displacement control at both ends).

(2) The displacement is assigned at one end only, together with no axial force at the other end (this is the case of a pull test with displacement control at the pulled end).

(3) While at one end the displacement is assigned, at the other end the magnitude of the force is constrained to be equal to the one at the first end (this corresponds to a pull-push test arrangement where the displacement is controlled at one end only, but the pull and push forces are constrained to have the same magnitude).

Different numerical techniques can be used in principle to solve the nonlinear two-point boundary value problem defined by Eqns. 4.1 to 4.3, together with the appropriate boundary conditions. These techniques include finite differences, finite elements, and "shooting techniques". A finite element approach has been tried, for example, with some success, in [5], using constant stress elements for steel and concentrated bond forces (nonlinear springs) at the nodes.

In the present study, a shooting technique has been adopted. It consists of transforming the boundary value problem into an initial value problem in which the unknown boundary condition at one end is guessed in order to produce, after integration along the length, the values of the normal force and displacement at the other end. The computed boundary condition at the far end has to match the specified one, and this provides a nonlinear equation for the unknown boundary condition at the first end; an iterative solution of this equation finally yields the solution of the original problem.

The overall solution process is advanced in an incremental way, where the variations of the assigned boundary conditions, which altogether define the generalized loading, are given in small increments. The procedure is more efficient than the one used in [5] and overcomes the difficulties encountered in that approach.

A more detailed discussion and illustration of the following aspects is presented below:

-the method used to integrate the initial value problem;

-the method of solution for the resulting nonlinear equations;

-the procedure used to estimate a good set of values for the unknown initial condition;

-an alternative iterative scheme which can also be used in connection with the shooting technique;

-the implementation of the described procedures in a computer program.

4.2 INITIAL VALUE PROBLEM

Consider the nonlinear initial value problem recast into the following equations (Fig. 4.1).

$$\frac{dN(x)}{dx} - q(x) = 0 \tag{4.1}$$

$$N(x) = \hat{N}(\epsilon(x)) = \hat{N}\left(\frac{ds(x)}{dx}\right) \tag{4.4}$$

$$q(x) = \pi \cdot d_b \cdot \tau(x), \quad \text{with } \tau(x) = \hat{\tau}(s(x)) \tag{4.5}$$

defined on the interval [O,L] of the real axis x (Fig. 4.3), with the initial conditions:

$$\epsilon(o) = \left(\frac{ds}{dx}\right)_{x=0} = \epsilon_1 \tag{4.6}$$

$$s(x=0) = s_1 \tag{4.7}$$

In order to solve this problem numerically, the interval [O,L] is first divided at the positions (or stations) x_i, (i=1,2,...,n; $x_1 = 0$, $x_n = L$; $\Delta x_i = x_{i+1} - x_i$), by n points into n-1 subintervals, Fig. 4.3.

Once the values N_i, q_i, ϵ_i and s_i of the functions $N(x)$, $q(x)$, $\epsilon(x)$, and $s(x)$ at station i are known, the solution is advanced to the next station i+1 using the following relations:

$$s_{i+1} = s_i + \frac{\epsilon_i + \epsilon_{i+1}}{2} \Delta x_i \tag{4.8}$$

$$N_{i+1}(\epsilon_{i+1}) - N_i - \frac{q_i + q_{i+1}(s_{i+1})}{2} \Delta x_i = 0 \tag{4.9}$$

which express an approximate integration of Eqn. 4.1 on the subinterval $[x_i, x_{i+1}]$. Equation 4.8 would be the exact integration for a linear variation of strains over the i^{th} subinterval and Eqn. 4.9 provides an equilibrium check. When Eqn. 4.8 is substituted in Eqn. 4.9, the latter becomes a nonlinear equation in the only unknown ϵ_{i+1}, whose solution requires repeated evaluation of the functions $N(\epsilon)$, $q(s)$ at point i+1. In fact, what is typically done at each iteration is to:

-use current guess for ϵ_{i+1} to compute s_{i+1}

-evaluate $N(\epsilon_{i+1})$, $q(s_{i+1})$

-use Eqn. 4.9 to check equilibrium

-repeat with a new value for ϵ_{i+1} if the check is not satisfied.

Once ϵ_{i+1} has been determined, and s_{i+1}, N_{i+1}, and q_{i+1} are available, the procedure can be applied to the next subinterval and up to the end point n.

The type of integration scheme used here is implicit and has the disadvantage of requiring at each step (interval) the solution of a nonlinear equation. However, the advantage is that it allows the use of larger steps while maintaining good accuracy and leading to a good solution of the overall problem.

4.3 METHOD OF SOLUTION FOR NONLINEAR EQUATIONS

The problem which has to be solved, according to the formulation given in Sections 4.1 and 4.2, requires solution of nonlinear equations at two levels, which are nested into one another. The implementation of the shooting technique, discussed briefly in Section 4.1, implies the solution of a nonlinear equation with an unknown initial condition. For example, in the case in which the displacements are specified at both ends, this equation takes the form:

$$f(\epsilon_1) = s_n(\epsilon_1) - \bar{s}_n = 0 \tag{4.10}$$

where ϵ_1 is the unknown steel strain at point 1, $s_n(\epsilon_1)$ the value of the displacement at the end point n, computed as a solution of the initial value problem explained in Section 4.2, and $\bar{s}_n$ is the assigned boundary condition at n.

Each evaluation of the left-hand side of Eqn. 4.10 implies, in turn, solution of n-1 non-linear equations in one unknown, due to the choice of an implicit scheme for the integration of the initial value problem (see Section 4.2).

A careful choice of the iteration scheme to be used for the solution of a single nonlinear equation is, for the above reasons, mandatory.

The secant method appears very attractive. In fact, it has a satisfactory rate of convergence (being not much slower than Newton-Raphson's method) and does not require direct evaluation of derivatives. This approach requires two initial approximations, but only one function evaluation is made per step. Given the nonlinear equation $f(x) = 0$ (e.g. Eqn. 4.10) and two initial approximations x^0, x^1, a sequence x^2, x^3, ..., x^n of approximations is computed recursively from the expression (Fig. 4.4):

$$x^{n+1} = x^n - f(x^n)\frac{x^n - x^{n-1}}{f(x^n) - f(x^{n-1})} \tag{4.11}$$

The geometrical interpretation of Eqn. 4.11 is that x^{n+1} is determined as the abscissa of the point of intersection between the secant through the points $(x^{n-1}, f(x^{n-1}))$ and $(x^n, f(x^n))$ and the x axis. The procedure is stopped when a value x is found such that $f(x)$ is zero or less than a prescribed numerical value (tolerance).

A disadvantage of the secant method is that it does not always converge, depending on the initial values x^0 and x^1 and on the shape of the function $f(x)$ near zero. An example is shown in Fig. 4.5a. The function $f(x)$ consists of three branches. While the slopes of the branches (1) and (3) are almost identical, the slope of branch (2), which crosses the x-axis, is much steeper than either of the other branches. Therefore, applying the secant method results in points $(x^{n+1}, f(x^{n+1}))$, which lie either on branch (1) or branch (3) of the curve (i.e., the procedure is nonconvergent).

Numerical examples in the early stages of the research showed that in some critical cases the shape of the function $f(x)$ was similar to the one shown in Fig. 4.5a, and the iteration procedure based on the secant method did not converge. Therefore, an iteration procedure known in the literature as the Illinois Algorithm was adopted. The iteration method is described in detail in [18]. It demonstrates consistently good convergence properties near the root. The principle of the Illinois Algorithm is as follows (Fig. 4.5b).

If the function values of two successive iteration steps (x^{n-1}, x^n) are of different sign $(f(x^{n-1}) \cdot f(x^n) < 0)$, then the value x^{n+1} is computed from Eqn. 4.11. For example, sup-

pose that in Fig. 4.5b the value x^3 was arrived at in this manner. If, on the other hand, those functions the first time are of the same sign ($f(x^{n-1}) \cdot f(x^n) > 0$), then the value of x^{n+1} is taken as the root of the straight line through the points $(x^n, f(x^n))$ and the point $(x^{n-2}, \alpha_1 f(x^{n-2}))$, where $\alpha_1 (0 < \alpha_1 < 1)$ is a parameter. Usually $\alpha_1 = 0.5$ is adopted. This modified step ensures that the function values $f(x^n)$ and $f(x^{n-2})$ are of different sign. In Fig. 4.5b, the modified step was used to compute the value x^4. If, after this modified step, the function values $f(x^n)$ and $f(x^{n+1})$ are of different sign, then the next step is the usual secant step (Eqn. 4.11). Otherwise, the line through the points $(x^{n+1}, f(x^{n+1}))$ and $(x^{n-2}, \alpha_k \cdot f(x^{n-2}))$ is used for the next step, where α_k is taken consecutively as α_1^k, $k = 2, 3, \ldots$, until there is a change of sign in the function $f(x)$. As before, usually one can take $\alpha_1 = 0.5$.

In the example plotted in Fig. 4.5, the secant method does not converge (Fig. 4.5a), while the Illinois Algorithm converges rapidly (Fig. 4.5b).

4.4 PROCEDURE FOR ESTABLISHING FIRST ESTIMATES

The problem of finding a solution of a nonlinear equation is facilitated if a good initial estimate or guess is available for it. In the following the procedure used to establish good first estimates for the solution of the nonlinear equations discussed in Section 4.3 is presented. First of all, because the overall solution process is advanced in increments, all the equations presented so far in this chapter have to be interpreted as equations involving incremental quantities. In particular, Eqns. 4.8 and 4.9 can explicitly be rewritten in these terms and, after defining the local secant stiffnesses for steel (k) and bond stress-slip (r) as:

$$k_i = \hat{k}_i(\Delta\epsilon_i) = \frac{\Delta\hat{N}_i(\Delta\epsilon_i)}{\Delta\epsilon_i}, \quad r_i = \hat{r}_i(\Delta s_i) = \frac{\Delta\hat{q}_i(\Delta s_i)}{\Delta s_i},$$

they become:

$$\Delta s_{i+1} = \Delta s_i + \frac{\Delta\epsilon_i + \Delta\epsilon_{i+1}}{2} \Delta x_i \tag{4.12}$$

$$k_{i+1}\Delta\epsilon_{i+1} - k_i\Delta\epsilon_i - \frac{r_{i+1}\Delta s_{i+1} + r_i\Delta s_i}{2} \Delta x_i = 0 \tag{4.13}$$

Substituting Eqn. 4.12 in Eqn. 4.13, solving with respect to Δs_{i+1}, and substituting back into Eqn. 4.12, one obtains:

$$\Delta s_{i+1} = \left[1 + \frac{(r_i + r_{i+1})\,\Delta x_i^2}{4k_{i+1} - r_{i+1}\Delta x_i^2}\right]\Delta s_i + \frac{\Delta x_i}{2}\left[1 + \frac{4k_i \times r_{i+1}\Delta x_i^2}{4k_{i+1} - r_{i+1}\Delta x_i^2}\right]\Delta \epsilon_i \tag{4.14}$$

$$\Delta s_{i+1} = \alpha_i \Delta s_i + \beta_i \Delta \epsilon_i \tag{4.14a}$$

$$\Delta \epsilon_{i+1} = \frac{2(r_i + r_{i+1})\,\Delta x_i}{4k_{i+1} - r_{i+1}\Delta x_i^2}\,\Delta s_i + \frac{4k_i + r_{i+1} + \Delta x_i^2}{4k_{i+1} - r_{i+1}\Delta x_i^2}\,\Delta \epsilon_i \tag{4.15}$$

$$\Delta \epsilon_{i+1} = \gamma_i \Delta s_i + \delta_i \Delta \epsilon_i \tag{4.15a}$$

These two equations express in a direct form the increments of displacement Δs and of strain $\Delta \epsilon$, at station i+1, as a linear combination of the corresponding values at previous station i, through coefficients which depend on the local secant stiffnesses k and r of the steel and of the bond stress-slip relationships at i and i+1. But since similar relationships hold for all the previous subintervals, it is possible to express Δs_{i+1} and $\Delta \epsilon_{i+1}$ also as a linear combination of the initial values Δs_1, $\Delta \epsilon_1$. That is,

$$\begin{aligned} \Delta s_{i+1} &= \alpha'_i \Delta s_1 + \beta'_i \Delta \epsilon_1 \\ \Delta \epsilon_{i+1} &= \gamma'_i \Delta s_1 + \delta'_i \Delta \epsilon_1 \end{aligned} \tag{4.16}$$

If the coefficients α'_{i-1}, β'_{i-1}, γ'_{i-1}, and δ'_{i-1} have been determined, by analogy to Eq. 4.16,

$$\begin{aligned} \Delta s_i &= \alpha'_{i-1} \Delta s_1 + \beta'_{i-1} \Delta \epsilon_1 \\ \Delta \epsilon_i &= \gamma'_{i-1} \Delta s_1 + \delta'_{i-1} \Delta \epsilon_1 \end{aligned} \tag{4.17}$$

whereas, according to Eqns. 4.14 and 4.15, one also has:

$$\begin{aligned} \Delta s_{i+1} &= \alpha_i \Delta s_i + \beta_i \Delta \epsilon_i \\ \Delta \epsilon_{i+1} &= \gamma_i \Delta s_i + \delta_i \Delta \epsilon_i \end{aligned} \tag{4.17a}$$

Substituting Eqn. 4.17 into 4.17a and comparing with Eqn. 4.16, the required expressions become:

$$\begin{aligned} \alpha'_i &= \alpha_i \alpha'_{i-1} + \beta_i \gamma'_{i-1} \\ \beta'_i &= \alpha_i \beta'_{i-1} + \beta_i \delta'_{i-1} \\ \gamma'_i &= \gamma_i \alpha'_{i-1} + \delta_i \gamma'_{i-1} \\ \delta'_i &= \gamma_i \beta'_{i-1} + \delta_i \delta'_{i-1} \end{aligned} \tag{4.18}$$

which provide the recurrence formulas for constructing the coefficients in Eqn. 4.16. As a particular case for the end point n:

$$\begin{aligned} \Delta s_n &= \alpha'_{n-1}\Delta s_1 + \beta'_{n-1}\Delta\epsilon_1 \\ \Delta\epsilon_n &= \gamma'_{n-1}\Delta s_1 + \delta'_{n-1}\Delta\epsilon_1 \end{aligned} \tag{4.19}$$

So, for example, if the boundary value case is the one which leads to the nonlinear equation 4.10, this can now be written in terms of incremental quantities as:

$$\Delta s_n(\Delta\epsilon) - \Delta\bar{s}_n = 0 \tag{4.20}$$

and, using the first of Eqns. 4.19,

$$\alpha'_{n-1}\Delta s_1 + \beta'_{n-1}\Delta\epsilon_1 - \Delta\bar{s}_n = 0 \tag{4.20a}$$

or, after a simple manipulation,

$$\Delta\epsilon_1 = \frac{\Delta\bar{s}_n - \alpha'_{n-1}\Delta s_1}{\beta'_{n-1}} \tag{4.20b}$$

Appropriate relationships, analogous to Eqns. 4.20, 4.20a, and 4.20b, can be easily written for the other two cases of boundary conditions considered in Section 4.1.

Equation 4.20a is, of course, nonlinear in the unknown $\Delta\epsilon_1$, the nonlinearity being hidden in the coefficients α'_{n-1}, β'_{n-1}, which depend on the distribution of secant stiffnesses of the steel and of the bond stress-slip relationships and, therefore, on the distributions of $\Delta\epsilon$ and Δs along the bar. However, Eqn. 4.20a has a form which makes it very suitable for yielding good starting values for the solution of Eqn. 4.20. In fact, using for the computation of α'_{n-1}, β'_{n-1}, the distribution of secant stiffnesses corresponding to those in the previously converged step, a very good starting value is usually obtained for $\Delta\epsilon_1$ from Eqn. 4.20b. On the same basis, during the stage of the integration procedure considered in Section 4.2, repeated use of Eqn. 4.16 provides good starting values for the solution of Eqn. 4.9.

One starting value is now available for the solution of each of the nonlinear equations involved. The second value, which is needed for the iterative scheme described in Section 4.3, is very simply obtained by multiplying the first value by a number very close to unity.

4.5 AN ALTERNATIVE ITERATIVE SCHEME

So far, Eqn. 4.20b has been considered only for obtaining initial estimates for the solution of Eqn. 4.20, or, which is equivalent, of Eqn. 4.10, in the context of a rather complicated procedure described in the previous sections. But Eqn. 4.20 (or an equivalent one, corresponding to a different case of boundary conditions) can also be used directly in an alternative iterative scheme, which is much simpler, in principle, for the solution of the global problem formulated in Eqn. 4.1. In fact, Eqn. 4.20b can be regarded as a nonlinear equation of the form:

$$x = f(x),$$

which very naturally suggests the solution scheme known as "simple iteration," which employs the recurrence formula:

$$x^{j+1} = f(x^j) \tag{4.21}$$

According to this scheme, a first value of $\Delta\epsilon_1$ can be computed as in the previous section from Eqn. 4.20b on the basis of the distribution of secant stiffnesses used in the previously completed step. Using this first value of $\Delta\epsilon_1$, Δs and $\Delta\epsilon$ are determined at each station from Eqn. 4.16. The corresponding increments ΔN_i and Δq_i are computed using the pertinent constitutive relationships, and new values of the secant stiffnesses k_i and r_i along the bar length are calculated. With the new stiffness distribution, a new $\Delta\epsilon_1$ is computed from Eqn. 4.20b and the procedure is continued until two consecutive values of $\Delta\epsilon_1$ conform to a prescribed tolerance.

This approach, which is very attractive from the point of view of simplicity of formulation and implementation, was used during the first stages of this study. It works correctly, but it is less efficient than the more complicated scheme used thereafter and described in the first part of this chapter. The main reasons for the inferior behavior of this alternative iterative scheme (Eqn. 4.21) are the slower convergence rate near a root and the possibility of nonconvergence in some critical steps, which can be avoided only using very small steps in the incremental procedure.

4.6 COMPUTER PROGRAM

The numerical procedure described in Sections 4.1 to 4.4 has been implemented in a computer program named BOND, which presently runs on a VAX 11/70 computer. The program has been structured in such a way that the material laws for ssteel and of bond stress-slip relationships can be easily modified without interfering with the algorithmic or the input-output structure. The material description is, in fact, implemented in three subroutines whose tasks are, respectively:

(1) Read the proper information which characterizes the constitutive relationships (for bond or steel) and set the necessary initializations.

(2) For a given pair of arguments, which are, respectively, the increment of displacement (slip) for the bond law or of strain for the steel law and an integer number, which refers to the point where the local constitutive relation is being considered, return the value of the corresponding resultant of the tangential bond force, q, or the normal force in the steel bar, N.

(3) Update the proper quantities defining the constitutive laws after convergence has been achieved and a step completed.

The exchange of information among the three subroutines is realized only through labelled common blocks. The exchange of information between the material subroutines and the rest of the program is also realized through labelled common blocks, with the exceptions of the second subroutine, which also has two arguments, as referred to above.

Details like names of the subroutines, names of the labelled common blocks, and names and meanings of the variables present in the common blocks are given in Appendix A. These details should enable a user to modify, or rewrite from scratch, the subroutines describing bond and/or steel. Presently, the models described in Chapters 2 and 3 are implemented. Appendix A also contains detailed information about the input and an example data file for the present version.

Another important feature of the program is its capability of producing outputs in graphic form. Two kinds of graphic outputs are possible: hysteretic loops and distributions along the bar length of steel strain, bar force, bond force, and slip. The graphic capability is considered essential to make the program an effective tool of investigation. This graphic capability has been extensively utilized throughout the present study.

V. COMPARISON OF ANALYTICAL PREDICTIONS OF THE RESPONSE OF ANCHORED BEAM BARS WITH TEST RESULTS

The force-slip relationships for the pulled bar end, obtained using the analytical models for bond and steel and the analytical procedure described in the previous chapters, are compared in Figs. 5.1 to 5.3 with experimental results obtained in some of the Berkeley tests [5]. The following specimens were chosen for comparison because the necessary test data are given in the report.

Test Number 3: Monotonic pull only

Test Number 13: Monotonic pull-push

Test Number 14: Cyclic pull-push

In all tests, #8 ($d_b \approx 25\ mm$) deformed bars were used. The anchorage length was $l_d = 25\,d_b$. The concrete had a compression strength of $f_c' \approx 30\ N/mm^2$ ($\approx$ 4300 psi). The characteristic values for the local bond stress-slip relationships of the different zones along the anchorage length (unconfined concrete in tension, confined concrete, unconfined concrete in compression) were taken from [7]. The assumed numerical values describing the local bond model and the steel model are given in Table 5.1.

As can be seen, experimental and analytical results agree qualitatively well. However, the quantitative agreement is not very good. The calculated maximum loads are about 15% larger (Test 3) or 15% smaller (Tests 13 and 14) , respectively, than the experimental values. This might be due to inevitable scatter of bond tests. According to Ref. [7], the local bond stress for given slip values may deviate up to 15% from the average value, even under ideal test conditions. Therefore, the behavior of the above mentioned specimens was calculated again, but this time the characteristic bond stresses were changed by 10% compared to the average values given in Table 5.1. The main results are plotted in Figs. 5.4 to 5.9.

Figures 5.4 to 5.6 show the normal force-slip relationships for the pulled bar end. In Figs. 5.4, 5.5, and 5.6b,c analytical and experimental results are plotted. (Figure 5.6a shows only the

analytically obtained force-slip relationship, which must be compared with the experimental one plotted in Fig. 5.3a.) With a 10% change, the agreement between analytical and experimental results is much better than in Figs. 5.1 to 5.3 and seems to be acceptable. However, the slope of the reloading branch of the normal force-slip relationship for cycles between relatively large slip values is considerably steeper than observed in the experiments (see Fig. 5.6c). This is caused by the assumed local bond stress slip relationship, which simplifies the real behavior for slip values close to the peak values of slip during cycling (see Chapter 2).

In Figs. 5.7 to 5.9 the distribution of steel strain, normal force, slip and bond force along the anchorage length are plotted for each of the above mentioned specimens for characteristic points of the pertinent load histories (see Figs. 5.4 - 5.6). From an analysis of the comparison between experimental and analytical results offered in the figures, the following observations can be made.

The analytically obtained response agrees qualitatively well and quantitatively reasonably well with the behavior observed in the experiments. However, the agreement is not as close as for the normal force-slip relationship for the pulled bar end. Reasons for this are given below.

After yielding of the bar, because of the small slope of the strain hardening branch of the stress-strain relationship, a small difference between calculated and measured resistance of the anchored bar results in a relatively large difference between calculated and measured steel strain at the loaded bar end. For example, a difference between measured and calculated resistance as small as 10% may result in a difference between calculated and measured maximum steel strain of about 20 mm/m. In the light of this reasoning, the differences between computed and measured maximum steel strains seem to be acceptable.

At the pulled bar end, a concrete cone is fractured by bond forces spreading from the bar lugs into the concrete. This results in a loss of bond and an almost constant steel strain along the corresponding part of the bar. The length of the cone, which depends on many parameters (e.g. spacing of ties, column bars and concrete cover), shows a considerable scatter [5].

In the calculations, the bond over a definite length ($5 d_b$) was assumed to be affected by the fracture of a concrete cone; the influence of the load intensity on the length of this cone was neglected. A comparison between analytical and experimental results shows that the assumed length is acceptable for loads not too much above yield but may be too short for high loads or large values of peak slip.

Therefore, in the latter case, the length of penetration of yield into the joint used in calculations is smaller than the length found in the experiments (Fig. 5.7, Point (2)).

To achieve an even better agreement between analytically and experimentally obtained distributions of steel strain, bond forces, and slip, additional calculations were carried out in which the bond behavior in the outer zones of the anchorage length were varied over a large range. In this way close agreement between analytical and experimental response could be obtained for a certain test specimen. However, the same assumptions did not necessarily give a much better agreement than described above when applied to another specimen. This shows the random behavior of bond.

In spite of the observed differences, it is considered that the obtained accuracy of reproduction of experimental results seems to be sufficient for practical applications. This is so because one has to bear in mind that the inelastic response of anchored main bars depends on the behavior of the mechanical characteristics of steel, namely yield strength and strain hardening, which will scatter considerably in practice. Therefore, it would be illogical to require better accuracy in bond than that offered by these characteristics. However, it is desirable to check whether or not the results of tests by other investigators described in literature can also be reproduced with sufficient accuracy. This work was not carried out as a part of this study. If for some reason a much better agreement between the analytical and experimental response of anchored main beam bars is desired, the following improvements of the proposed analytical models are necessary.

(a) Improvement of the strain hardening branch of the analytical steel model. At present, the slope of this branch is assumed to be constant; in reality the slope varies considerably.

(b) Improvement of the local bond model for the reloading branch at large values of peak slip. At present, a relatively sudden increase of the bond resistance is assumed when approaching the peak slip. In reality, the increase is gradual.

(c) Improvement of the local bond model, valid for the outer zones of the anchorage length (unconfined concrete in tension and compression). The behavior of bond in these zones is yet almost unknown [7]. Therefore, the "improvements" are highly speculative and their accuracy must be proved by a good agreement between analytical and experimental response of a large number of tests.

VI. NUMERICAL STUDIES

6.1 General

In the following section the influence of some important parameters on the behavior of anchored beam bars will be discussed. However, first certain results that are difficult to interpret will be commented upon.

Figure 6.1 shows the calculated response of a reinforcing bar ($d_b = 25\,mm \approx \#8$) embedded in well confined concrete ($f_c' = 50\ N/mm^2 \approx 7200$ psi) having a short anchorage length $l_d = 5\ d_b$. It is loaded at one end only and subjected to reversed slip with increasing amplitude (Fig. 6.1a). The local bond law is assumed, for reasons of simplicity, to be the same for all points along the bar. The yield stress f_y of the bar was assumed to be 300 N/mm^2 (43 ksi).

The shape of the analytically obtained normal force-slip relationship of point 1 of the anchored bar (Fig. 6.1b) agrees qualitatively well with test results [5]. Also, the distribution of steel strain, slip, normal force, and bond force along the anchorage length at the values of peak slip of the first cycle (Figs. 6.1e,f) agree well with expectations. However, the distribution of slip along the anchorage length in the second cycle appear to be wrong, because the unloaded end is pulled out more than the loaded end (see lower left graph of Figs. 6.1g and 6.1h). Furthermore, the distribution of steel strains seems to be wrong as well (see upper left graphs in Figs. 6.1g and 6.1h). Notwithstanding the above, the calculated response of the anchored bar is correct and can be explained as follows.

During cycling the whole bar is slipping. The slip of the unloaded bar end can be considered as the movement of a rigid body. The deformation δ of the bar caused by the normal force is the difference between the slip at a certain point of the bar and the slip of the free bar end. The distribution of δ along the anchorage length is plotted in Fig. 6.2 for several load stages.

In the first cycle (path OAB, Fig. 6.1b), the bar yields in tension and compression (Fig. 6.1d). After unloading (path BB_1), permanent steel strains remain (Fig. 6.1d). This results in

permanent bar deformations, δ, along the embedment length (Fig. 6.2, load point B_1). The steel strains and bar deformations are not changed much when a small normal force is built up at B_2 (Fig. 6.1b) due to frictional bond resistance. Between B_2 and B_3 the bar is pushed back as a rigid body with frozen strains and stresses (Fig. 6.1b). At B_3 the normal force starts to increase again (Fig. 6.1b) because an increasing bond resistance is built up starting from the bar end. However, because the bond is severely damaged by the previous cycle (path OAB in Fig. 6.1c), the resistance of the anchored bar is much smaller than in the first cycle (path B_3CD, Fig. 6.1b), and the strain along the part of the bar that had previously yielded in compression remains negative (Fig. 6.1d). Therefore, the bar deformations, δ, seem to show a wrong distribution along the anchorage length (Fig. 6.2, load point C). However, compared to the unloaded state B_1, positive deformations occur along the entire length of the anchored bar with a normal distribution (see Fig. 6.2, line $(\delta_C - \delta_{B_1})$), but they are not large enough to overcome the permanent negative deformations.

Summarizing, a strange looking but analytically correct distribution of steel strain and slip along the anchorage length can occur when the bar is yielded in a cycle and the bond resistance in the subsequent half cycle is too small to build up a sufficiently large normal force to overcome the permanent deformations. Several numerical examples show that those distributions can also occur at a point away from the loaded bar end.

In some of the tests presented in [5], a distribution of steel strains and slip along the anchorage length measured at certain load points was similar to the one described above.

6.2 INFLUENCE OF DIFFERENT PARAMETERS ON RESPONSE OF ANCHORED BEAM BARS

6.2.1 MODEL FOR STRESS-STRAIN RELATIONSHIP OF REINFORCING STEEL

As described in Chapter 3, a nonlinear model and a bilinear model for the stress-strain relationship of reinforcing steel (see Fig. 3.6) are provided as options in the computer program. While the bilinear model is much simpler, the nonlinear model reproduces the real behavior of

reinforcing steel during cyclic loading more accurately.

Figure 6.3 shows the influence of the steel model on the calculated response of a reinforcing bar ($d_b = 25\ mm$) embedded in well confined concrete ($f_c' = 30\ N/mm^2$) having an anchorage length of $l_d = 15\ d_b$. It is loaded at one end only and subjected to reversed slip with increasing amplitude (Fig. 6.3a). The local bond law was assumed, for reasons of simplicity, to be the same for all points along the anchorage length. In one run the bilinear steel model and in the other the nonlinear steel model was used. The parameters describing the steel models are given in the lower right graph of Fig. 6.1a. All other parameters were kept constant.

As can be seen from Fig. 6.3b, the overall response (normal force-slip relationship for point 1) is not much influenced by the different steel models. A relatively small difference exists only for the reloading branches. This behavior can be clarified with the aid of Fig. 6.3c. In this figure, the normal force-strain relationship of point 1 (loaded bar end) is plotted. It can be seen that only the reloading branches of the normal force-strain relationship, obtained with the bilinear and nonlinear models, differ from each other, while the strains at maximum load are almost identical.

Additional numerical studies were carried out, varying the following parameters.

-anchorage length: $l_d = 5\ d_b$ to $25\ d_b$;

-loading: at one bar end only as well as at both ends (pull-push loading with forces of the same magnitude);

-steel strain at peak values of slip ($\epsilon \approx 10\ mm/m$ to $60\ mm/m$);

-bond behavior along the embedment length: same local bond laws for all points as well as different local bond laws in the outer parts of the anchorage length.

From the results of these calculations, it can be concluded:

(1) The influence of the steel model (bilinear or nonlinear with asymptotic constant slope for the strain hardening branch) on the response of an anchored bar is relatively small. Differences exist only between the reloading parts of the normal force-slip relationship.

(2) The necessary computer time is about 2 to 3 times longer when using the nonlinear model than for the bilinear model.

(3) The analytically dissipated energy is slightly smaller for the nonlinear model than for the bilinear model.

(4) Normally the bilinear model should be used. Only if an accurate appraisal of the amount of energy dissipated by the anchored bar is of main interest, use of the bilinear model and the larger computation time can be justified.

6.2.2 SEVERITY OF HYSTERETIC REQUIREMENTS

The steel strains imposed by earthquakes on a main beam bar just outside a joint may be as small as the strain at yield if the seismic input is small or plastic hinges occur away from the joint, or they may reach under extreme circumstances up to 100 mm/m in a major earthquake. In the studies reported herein, a maximum strain of 40 mm/m was considered. The response of anchored beam bars will greatly depend on the hysteretic requirements. Therefore, their influence was investigated using the following model, which represents a beam bar anchored in an interior joint.

bar diameter:	$d_b = 25\ mm$ (#8 bar)
anchorage length:	$25\ d_b$
loading:	push-pull loading with forces of equal magnitude
local bond laws:	see Table 5.1, valid for $f_c' = 30\ N/mm^2$ ($\approx$ 4300 psi)
steel law:	bilinear steel model with
	$f_y = 450\ N/mm^2$ ($\approx$ 65 ksi)
	$E_o = 2.05 \cdot 10^5\ N/mm^2$ ($\approx$ 29700 ksi)
	b $= E_1/E_o = 0.017$

The following hysteretic requirements were chosen:

Run	No. of Cycles	Peak Steel ϵ	Add'l No. of Cycles	New Peak ϵ
1	6	$\epsilon = \pm\epsilon_y$		
2	3	$\epsilon = \pm 5$ *mm/m*	3	$\epsilon = \pm 10$ *mm/m*
3	3	$\epsilon = \pm 10$ *mm/m*	3	$\epsilon = +=20$ *mm/m*
4	3	$\epsilon = \pm 15$ *mm/m*	3	$\epsilon = \pm 30$ *mm/m*
5	3	$\epsilon = \pm 20$ *mm/m*	3	$\epsilon = \pm 40$ *mm/m*

Since the computer program does not accept steel strains at the loaded bar ends as input, but only slip values, the latter were chosen in such a way that the steel strains given above were reached under monotonic loading. Bond is damaged by cyclic loading. Therefore, the peak steel strains reached after the first cycle may be smaller than the values aimed at.

In Fig. 6.4a to Fig. 6.4e the normal force-slip relationship of the specified runs are plotted. For comparison, the response of the anchored bar under monotonic loading is also shown. As expected, stiffness and strength of the anchorage are increasingly reduced with increasing hysteretic requirements. Furthermore, the ratio between the energy dissipated by the bar anchored in the joint and the energy that would be dissipated by a bar that is rigidly anchored (no slip) and subjected to the same strain histories decreases with increasing hysteretic requirements. Even cycling between slip values corresponding to peak steel strains $\epsilon = \pm\epsilon_y$ leads to a considerable reduction of the maximum resistance and an increase in the deformability at maximum loads compared to monotonic loading (Fig. 6.4a). This is mainly caused by the reduction of bond resistance at the compressed bar end (see Fig. 6.4f) due to the formation of a small concrete cone during previous loading in tension. In the present example, cycling between slip

values corresponding to peak steel strain $\epsilon = \pm 10\ mm/m$ and $\epsilon = \pm 20\ mm/m$ leads to severe deterioration of bond so that the maximum resistance of the anchored bar at slip values larger than the peak values during previous cycles is only about 45 percent of the maximum resistance under monotonic loading (Fig. 6.4c). The maximum resistance of the anchored bar after cycling between slip values corresponding to steel strains $\epsilon = \pm 20\ mm/m$ and $\epsilon = \pm 40\ mm/m$ is even more reduced and amounts to only about 15 percent of the strength under monotonic loading (Fig. 6.4e).

6.2.3 CHARACTERISTICS OF STEEL

In this and the following sections, the model described in Section 6.2.2 was used, with the hysteretic requirements of Run 4 ($\epsilon_{max} = \pm 15\ mm/m$ and $\pm 30\ mm/m$ see Section 6.2.2). The investigated parameter was varied as described in the following; all other values were kept constant.

6.2.3.1 YIELD STRESS

Figure 6.5 shows the influence of yield stress on the response of anchored beam bars. The yield stress was varied between $f_y = 300\ N/mm^2$ ($\approx$ 43 ksi) and 600 N/mm^2 ($\approx$ 87 ksi) to cover the possible extreme values that can be found in practice. The behavior under monotonic loading is summarized in Fig. 6.5a. For a slip s_1 smaller than that to produce yielding of the bar with the highest yield strength (and even to slip values $s_1 \leqslant 4\ mm$), the anchorage force increases with increasing yield strength. The slip at which the maximum resistance is reached increases considerably with decreasing yield stress. However, the strength of the anchorage is almost independent of f_y. Note that in the calculations steel strength and ultimate steel strain were not limited, so that all bars could reach the stress at peak anchorage resistance, which is about 630 N/mm^2. If in an actual test the steel strength is smaller than this value, the bar would rupture.

The deterioration of the resistance of anchorages caused by cyclic loading well into the plastic region increases significantly with increasing yield stress. For the given conditions

(anchorage length $l_d = 25\ d_b$), the deterioration due to load cycles is small for bars with a yield stress $f_y = 300\ N/mm^2$ (Fig. 6.5b). The observed deterioration is mainly caused by the formation of a concrete cone at both ends of the anchored bar. On the contrary, when high strength bars are cycled after being strained monotonically up to $\epsilon = 10\,mm/m$, the bond deterioration is very large (Fig. 6.5d). Note that the bar with $f_y = 600\ N/mm^2$ was cycled 6 times between slip values corresponding to steel strains $\epsilon = \pm 10\ mm/m$, because these were the largest steel strains that could be reached under monotonic loading. In the other examples ($f_y = 300$ and $450\ N/mm^2$), 3 cycles between slip values corresponding to steel strains $\epsilon = \pm 15\ mm/m$ were performed followed by 3 cycles with steel strains $\epsilon = \pm 30\ mm/m$. Note that the residual strength after cycling is slightly larger for the bar with $f_y = 600\ N/mm^2$ (Fig. 6.5d) than for the bar with $f_y = 450\ N/mm^2$ (Fig. 6.5c) because of the lower hysteretic requirements ($\epsilon = \pm 10\ mm/m$ instead of $\epsilon = \pm 30\ mm/m$) for the bar with the highest yield stress.

It is important to note that anchored bars with a low yield stress show a superior behavior during cyclic loading well into the strain hardening region. This is due to the following causes. The load necessary to strain a bar to a given strain value $\epsilon > \epsilon_y$ decreases with decreasing yield stress. That means that under otherwise constant conditions the slip corresponding to a certain strain will also decrease with decreasing f_y. Because in the examples studied, cycling was performed between constant slip values, the developed bond of bars with a low yield stress was smaller than the bond of high strength bars and thus the less bond damage occurred during cyclic excitations. It should be noted that in practice the lug pattern of high strength bars is usually superior to that of low strength bars to increase their bond behavior. This influence was neglected in the calculations. Furthermore, the slope of the strain hardening branch of reinforcing bars with a low yield stress is usually higher than for high strength bars. Therefore, in practice the influence of the yield stress on the response of anchored bars under cyclic loading well into the strain hardening region will be smaller than shown above.

It should be checked by additional calculations whether the influence of the yield stress is

negligible if the anchorage length is proportional to f_y, as usually specified in codes.

6.2.3.2 SLOPE OF STRAIN HARDENING BRANCH

Figure 6.6 shows the influence of the slope E_1 of the strain hardening branch on the response of an anchored bar. The slope E_1 was varied between 0.85% and 3.4% of the elastic slope E_o. The assumed values of E_1 cover the complete range encountered in practice.

Under monotonic loading, the strength of an anchorage is independent of the slope, E_1, of the strain hardening branch. However, the slip at which the maximum bond resistance is reached increases with decreasing values for E_1 (Fig. 6.6a). Cyclic loading well into the strain hardening region produces increasingly more deterioration of the anchorage resistance with increasing values for E_1 (compare Fig. 6.6b with Fig. 6.6c).

The influence of the slope of the strain hardening branch of the stress-strain relationship of reinforcing bars on the behavior of anchorages under monotonic and cyclic loading is similar to the influence of the yield stress; however, it is less pronounced. This behavior can be rationalized in an analogous manner.

Summarizing, it can be stated that under otherwise constant conditions the lower the yield strength (strain) and/or the slope of the strain hardening branch of the stress-strain relationship of the reinforcing bars, the better the performance of anchorages subjected to cyclic loadings which induce strains well beyond yielding of the bars.

6.2.4 ANCHORAGE LENGTH

As expected, under monotonic loading, the strength of anchorages increases with increasing embedment length (Fig. 6.7a). While for $l_d = 15\ d_b$ the bar is pulled out before reaching yield, bars with $l_d = 25\ d_b$ reach a peak strain value of $\epsilon \approx 40\ mm/m$. The response of anchorages with lengths of $l_d = 35\ d_b$ and $45\ d_b$ is almost identical in the plotted slip range. The steel strain at a slip $s_1 = 20\ mm$ is $\epsilon_{max} \approx 70\ mm/m$, which means that the bars would be close to fracture.

The analytical steel model does not limit the maximum steel stress but assumes infinite length of the strain hardening branch. The advantage of this assumption is that equilibrium is possible under any condition, and the program does not become unstable. However, because of this, rupture of a bar cannot be predicted by the program.

The hysteretic loops of anchorages with $l_d = 25\ d_b$ are significantly pinched (Fig. 6.7b), which is caused by bond damage along the entire embedment length. This can be seen from Fig. 6.8a, which shows the distribution of slip along the anchorage length. The peak slip value at the tensioned bar end is $s_1 = 5\ mm$. According to [7], the concrete keys between lugs begin to shear off at local slip values $s_1 \approx 1\ mm$ for the assumed concrete strength. While under monotonic loading the slip values along the inner part of the anchorage length are just below this critical value, the distribution of slip values after cyclic loading clearly indicates a shear failure in the concrete keys between lugs along the entire embedment length. On the contrary, anchorages with a length of 35 d_b show almost stable hysteretic loops (Fig. 6.7c), and the concrete keys along the inner part of the anchorage length between x $\approx$ 8 d_b and x $\approx$ 30 d_b are undamaged (Fig. 6.8b). An even superior performance shows anchorages with a length $l_d = 45\ d_b$ (Figs. 6.7d and 6.8c).

VII. PRACTICAL IMPLICATIONS OF RESULTS

In this chapter the results discussed in Chapter 6 are evaluated regarding the practical implications of anchorage requirements of deformed reinforcing bars in well confined interior joints. First, the length required to anchor main beam bars of a certain diameter with a given deformation pattern is discussed. This length depends on:

(1) The mechanical characteristics of concrete and steel (mainly concrete strength and yield stress and strain hardening characteristics of the reinforcing bars) as well as on the amount of confinement.

(2) The loading conditions. The shortest anchorage length is appropriate for monotonic loadings, which can include sustained or repeated loadings in the service load range. The required anchorage length increases with increasing hysteretic requirements, i.e. with severity and number of deformation reversals.

(3) Acceptable performance (slip). The performance criteria during cyclic excitations depend on the allowable degree of bond damage along the embedment length.

The hysteretic requirements depend on the problem at hand. For example, they will be different for structures designed to resist impact loading than for structures designed to resist earthquakes of different magnitudes. These requirementss can be defined by specifying the time history of strain of a bar at the beginning of the anchorage length.

In [19] the response (performance) of ductile moment-resisting reinforced concrete frames subjected to ground motions induced by recent major earthquakes was analyzed. According to this study, a large number of cycles with steel strains below, or not much above, yield strain are to be expected in a major earthquake. However, only a few cycles (up to 3) with very large strains (up to 20 to 40 mm/m) are likely. Therefore, in the numerical examples discussed in Chapter 6 three cycles between slip values that have been determined from the monotonic loading envelope for a steel strain at the beginning of the anchorage $\epsilon = \pm$ 15 mm/m, followed by another three cycles between slip values corresponding to a maximum steel strain $\epsilon = \pm$ 30 mm/m under monotonic loading, were performed. While the cycles between

slip values corresponding to $\epsilon = \pm$ 15 mm/m should represent the influence of all cycles with relatively low peak steel strains, the cycles between slip values corresponding to $\epsilon = \pm$ 30 mm/m should model the largest requirements to be expected from response to earthquake ground motion. It is believed that the chosen requirements adequately and conservatively model the actual requirements for major earthquakes to be expected.

The bond behavior is significantly influenced by concrete strength and is of random nature. Building codes (e.g. [20,21]) require that concrete be proportioned and produced in such a way that the frequency of strength tests below the specified value is minimized; usually the specified value is identical with the 5%-fractile of concrete strength. To take the random nature of bond into account, the required anchorage length could be evaluated using one of the two following assumptions.

Assumption	Bond Behavior	Compressive Strength
1	Fractile of test results	Strength specified in code
2	Average of test results	Strength specified in code

Assumption 1 seems to be too conservative, because there is only a very low probability for the simultaneous occurrence of a low concrete strength and a relatively bad bond behavior. Therefore, Assumption 2 was used in the numerical examples. The assumed local bond laws are only valid for well confined joints. The necessary amount of confinement is given in [7].

According to the results presented in Chapter 6, under otherwise constant conditions, the necessary anchorage length increases with increasing yield stress. The yield stress specified in building codes refers to the minimum or characteristic yield stress; the actual yield stress may be much larger. In seismic resistant design of ductile structures, an upper limit for the yield stress is specified as well. According to [21], the actual yield stress may not exceed the specified value by more than 15 percent. Assuming this ratio, the yield stress of Grade 40 or

60 bar may not exceed f_y = 317 or 475 N/mm^2, respectively. The Uniform Building Code [22] requires that the actual yield stress of steel shall not exceed the specified value by more than 18,000psi (124 N/mm^2). Assuming this value, the yield stress of a Grade 40 or 60 bar may not exceed f_y = 400 N/mm^2 or 538 N/mm^2, respectively.

There is no consensus regarding the allowable degree of bond damage along the anchorage length or regarding performance criteria during cyclic loading. For such an evaluation, one should take the following facts into account.

(1) In the pull-out tests [5] with deformed bars of Grade 60 steel, cracks indicating the formation of a concrete cone appeared at steel stresses $\sigma_s \approx$ 40 to 50 ksi ($\approx$ 280-350 N/mm^2). This means that damage of bond in the end regions of the anchorage length can hardly be avoided in practice.

(2) Bending, shear or splitting cracks can be effectively repaired by injecting epoxy resin. There is some disagreement in literature whether this method is effective in restoring bond. According to some sources (e.g. [23]), the bond behavior of specimens injected with epoxy resin was almost identical to the behavior of comparable virgin ones. However, only small slip values were induced before the injection. When large slip values were induced before injection, the bond behavior was significantly inferior compared to the virgin loading [24]. Therefore, it must be concluded that bond cannot be effectively restored if the concrete keys between lugs have been pulverized due to crushing and shearing off.

(3) In dynamic analyses the influence of slip of anchored bars on the response of reinforced concrete structures is usually neglected. This is only correct if the fixed-end rotation caused by slip is relatively small and the hysteretic loops are stable, which is only possible when a long embedment length is employed.

Under due consideration of the above points, it is proposed to anchor main beam bars in such a way that (1) the inevitable bond damage during cyclic loading is limited to the end regions of the embedment length and is mainly caused by the formation of concrete cones, (2)

the hysteretic loops of the anchored bar remain essentially stable, and (3) the strength of the anchorage would continue to increase for slip values larger than the peak values during previous cycles.

If these conditions are fulfilled, it seems possible to restore the bond in the end region by replacing the concrete forming a cone so that strength and stiffness of the anchorage do not differ much from the values before an earthquake. Furthermore, the influence of slip on the global response of the structure during cyclic loading should be very small.

A more precise definition of hysteretic requirements and of performance criteria is desirable but cannot be given at the present time.

Evaluating the results of the numerical studies given in Chapter 6 in the above manner, one gets the following length l_d required to anchor deformed bars in well confined interior joints:

Grade 40 Steel: $l_d \approx 25\text{–}30\ d_b$

Grade 60 Steel: $l_d \approx 35\text{–}40\ d_b$

The smaller of the above given values ($l_d = 25\ d_b$ or $35\ d_b$ for Grade 40 or Grade 60 steel, respectively) are valid for reinforcing bars complying with [21] (actual yield stress exceeds the specified value by not more than 15 percent). The bigger value ($l_d = 30\ d_b$ or $40\ d_b$ for Grade 40 or Grade 60 steel, respectively) should be used for reinforcing bars complying with the Uniform Building Code [22], because the maximum yield stress is less restricted in [22] than in [21]. These values are valid for a specified concrete strength $f_c' = 30\ N/mm^2$ ($\approx$ 4300 psi). The influence of concrete strength on the response of anchored bars was not investigated in the numerical studies. However, it is reasonable to assume that the required anchorage length varies approximately as $\sqrt{30/f_c'}$ (f_c' in N/mm^2). Although in Chapter 6 #8 bars ($d_b \approx 25$ mm) were assumed, it seems reasonable to extend the results to different bar diameters, at least in the range from #6 to #10 bars ($d_b \approx 19$ to 32 mm).

The given anchorage lengths agree well with the values proposed in [25], which were

found in a completely different manner by evaluating the results of tests on interior joints. However, the proposals should be considered as tentative and should be checked by additional numerical studies.

The width of columns at interior joints required to sufficiently anchor beam bars is very large. In practice, columns are often smaller than dictated by the above requirements. In this case, the following possibilities are available.

(a) Use of small size bars having the smallest f_y and strain hardening characteristics available in the market.

(b) Detailing of the beam reinforcement in such a way that the possible plastic hinges would occur in the girders away from the column faces so that the steel at the beginning of the anchorage will remain elastic. In this manner severe bond damage within the joint can be avoided. The effectiveness of this method has been confirmed experimentally [26,27] and is in agreement with the results of the presented numerical studies.

(c) Taking into account the influence of slip of anchored beam bars on the dynamic response of the structure in the analysis. In order to do this with acceptable computational effort, simplified and reliable analytical models for normal force-slip or steel strain-slip relationships of anchored bars are necessary. Studies are in progress to formulate such models as a function of the relevant parameters. This approach allows the prediction of the dynamic response of structures due to ground motions more accurately, accounting for the effects of bond-slip and, therefore, permits the designer to judge if the effects of slippage at the joint can be tolerated or not. However, it has a major drawback. After the event of a strong earthquake, the bond along the total anchorage length may be severely damaged and cannot be repaired by conventional methods. This may mean that the structure may suffer significant damage even during strong winds and/or moderate earthquakes due to fixed end rotations of the beams caused by slip of the anchored bars. This risk might not be acceptable to the owner. It should be noted that large slippage of the continuous beam bars at interior joints does not necessarily imply failure of anchorage and, therefore,

collapse of the structure, provided that the beam bars are not cut off close to the column faces. The danger is that this slippage reduces so much the lateral stiffness of the structure that it may become unserviceable.

VIII. CONCLUSIONS AND RECOMMENDATIONS

8.1 CONCLUSIONS REGARDING THE ANALYTICAL MODEL FOR ANCHORED BARS

The analytical model for an anchored beam bar, described in Chapter 4, based on the analytical model for the local bond stress-slip relationship (Chapter 2) and the analytical model for the steel stress-strain relationship (Chapter 3) was used to predict the response of anchored bars. The analytically determined responses were compared with experimental results obtained in some of the Berkeley tests [5] (Chapter 5). From these comparisons, the following conclusions can be drawn.

(1) The proposed mathematical models allow the prediction of the response of deformed reinforcing bars anchored in well confined concrete under generalized excitations with sufficient accuracy for practical applications.

(2) In the analytically predicted response, only the slope of the reloading branch of the normal force-slip relationship for cycles between relatively large slip values is considerably steeper than observed in experiments. This is caused by the assumed local bond stress-slip relationship which simplifies the real behavior close to the peak slip value of previous cycles.

8.2 CONCLUSIONS REGARDING THE APPLICATION OF THE ANALYTICAL MODEL

The analytical model of an anchored beam bar was used to investigate the influence of various parameters on the response of reinforcing bars embedded in well-confined interior joints (Chapter 6). From the results obtained in this study, the following main observations can be made.

(1) The simplified assumption of a bilinear analytical model for the stress-strain relationship of reinforcing steel, rather than the use of a realistic nonlinear relationship, does not significantly influence the response of anchored bars under cyclic excitations.

(2) Under otherwise constant conditions, the amount of bond damage increases with increasing hysteretic requirements (intensity of strain and number of cycles) and decreasing anchorage length. Even cycles between peak steel strains just reaching yield strain may lead to the formation of a concrete cone at the tensioned bar end and the corresponding loss of bond over a short length, which depends on the detailing of the confining reinforcement.

(3) The performance of anchorages can be significantly improved by choosing bars with low yield stress and/or a low slope of the stress-strain relationship in the strain hardening range.

8.3 CONCLUSIONS REGARDING PRACTICAL IMPLICATIONS OF RESULTS

The results of the numerical studies were used to assess the practical implications for the anchorage of deformed bars in well-confined interior joints of ductile moment-resistant frames (Chapter 7). From this assessment, the following proposals are made:

(1) To minimize damage of bond along the anchorage length and the influence of slip on the dynamic response of structures due to ground motions during major earthquakes, the anchorage length should be:

$l_d = 25\ d_b - 30\ d_b$ (Grade 40 Steel)

$l_d = 35\ d_b - 40\ d_b$ (Grade 60 Steel)

The above given values are valid for a specified concrete strength $f_c' = 30\ N/mm^2$ ($\approx$ 4300 psi) and for #6 to #10 bars ($d_b \approx 19$–$32\ mm$). For a different concrete strength the given anchorage length should be multiplied with the factor $(30/f_c')^{0.5}$, where f_c' is the actual specified concrete strength in N/mm^2.

(2) If the widths of columns at interior joints is smaller than the proposed anchorage length, the formation of plastic hinges in the girders near the column faces should be avoided by detailing the beam reinforcement in an appropriate manner. Another possibility is to take into account the influence of slip of beam bars on the dynamic response of reinforced

concrete structures subjected to strong ground motions.

8.4 RECOMMENDATIONS FOR FUTURE WORK

While the analytical studies reported herein have clarified some aspects of the behavior of beam bars anchored in interior joints when they are subjected to monotonic and cyclic loading, some areas have not yet been fully explored and should be the subject of future studies. Some of the needed studies are recommended below.

(1) A reasonably good agreement between analytical and experimental results has been shown for #8 bars ($d_b = 25\ mm$, $f_y = 475\ N/mm^2$), embedded in well confined concrete ($f_c' = 30\ N/mm^2$) with a straight anchorage length $l_d = 25\ d_b$. **It should be checked whether the response of anchored bars under different conditions (different bar diameter, yield stress, concrete strength, or anchorage length) can also be predicted with reasonable accuracy.**

(2) The shape of the monotonic envelope of the local bond stress-slip relationship depends significantly on the deformation pattern of the bar (clear distance between lugs and related rib area). The local bond law is further influenced by concrete strength and bar diameter. **More numerical studies are needed to evaluate the influence of these and other relevant parameters on the behavior of anchored beam bars under monotonic and cyclic loading.**

(3) The present numerical studies deal only with anchorages in interior joints. **The response of beam bars anchored at exterior joints by hooks with or without a preceding straight length must be investigated.**

(4) The required anchorage length depends significantly on hysteretic requirements and on performance criteria during cyclic excitations. **More precise definitions of such requirements and performance criteria than given in the report are needed.**

(5) If the actual anchorage length is shorter than the above proposed values, significant pull-out of the main beam bars may occur, thereby causing beams to experience significant fixed-end rotations. **The influence of this effect on the dynamic response of structures**

should be examined. To reduce the necessary amount of computation, simple and reliable models for the normal force-slip relationship of the anchored bar are needed. Studies are in progress to formulate such models as a function of the relevant parameters.

IX. REFERENCES

1. Popov, E. P., "Mechanical Characteristics and Bond of Reinforcing Steel Under Seismic Conditions," *Proceedings,* Workshop on Earthquake-Resistant Reinforced Concrete Building Construction, University of California, Berkeley, July 11-15, Vol. II, pp. 658-682.

2. Takeda, T., Sozen, M., and Nielsen, N. N., "Reinforced Concrete Response to Simulated Earthquakes," *Journal of the Structural Division,* ASCE, Vol. 96, No. 12, Dec. 1970.

3. Ismail, M. A. and Jirsa, J. O., "Behavior of Enclosed Bars Under Low Cycle Overloads Producing Inelastic Strains," *Journal of the American Concrete Institute,* Vol. 69, No. 7, July 1972.

4. Ma, S. Y., Bertero, V. V., and Popov, E. P., "Experimental and Analytical Studies on the Hysteretic Behavior of Reinforced Concrete Rectangular and T-Beams," *Report No. EERC 76-2,* Earthquake Engineering Research Center, University of California, Berkeley, 1976.

5. Viwathanatepa, S., Popov, E. P., and Bertero, V. V., "Effects of Generalized Loadings on Bond of Reinforcing Bars Embedded in Confined Concrete Blocks," *Report No. EERC 79-22,* Earthquake Engineering Research Center, University of California, Berkeley, 1979.

6. Tassios, T. P., "Properties of Bond Between Concrete and Steel Under Load Cycles Idealizing Seismic Actions," *Bulletin d'Information No. 131* of the Comite Euro-International du Beton, Paris, April 1979.

7. Eligehausen, R., Bertero, V. V., and Popov, E. P., "Local Bond Stress-Slip Relationships of Deformed Bars Under Generalized Excitations, Tests and Analytical Model," UCB report in preparation.

8. Ciampi, V., Eligehausen, R., Bertero, V. V., and Popov, E. P., "Analytical Model for Deformed Bar Bond under Generalized Excitatons," *Proceedings,* IABSE Colloquium on Advanced Mechanics of Reinforced Concrete, Delft, June 1981.

9. Rehm, G. and Eligehausen, R., "Influence of High Cycle Repeated Loads on the Bond Behavior of Ribbed Reinforcing Bars," *ACI Journal,* American Concrete Institute, February 1979.

10. Capecchi, D., Ciampi, V., and Vestroni, F., "Numerical Studies on the Behavior of a Reinforced Concrete Beam Element under Repeated Loadings," *Bulletin d'Information No. 132* of the Comite Euro-International du Beton, Paris, April 1979.

11. Giuffre, A. and Pinto, P. E., "Reinforced Concrete Behavior Under Strong Repeated Loadings," *G. Genio Civile,* No. 5, 1970 (in Italian).

12. Menegotto, M. and Pinto, P. E., "Method of Analysis for Cyclically Loaded Reinforced Concrete Plane Frames Including Changes in Geometry and Nonelastic Behavior of Elements Under Combined Normal Force and Bending," *Proceedings,* IABSE Symposium on the Resistance and Ultimate Deformability of Structures Acted on by Well-Defined Repeated Loads, Lisbon, 1973.

13. Jennings, P. C., "Response of Simply Yielding Structures to Earthquake Excitation," *Report No. 6360,* California Institute of Technology, Pasadena, California, June 1963.

14. Matzen, V. C. and McNiven, H. D., "Investigation of the Inelastic Characteristics of a Single-Story Steel Structure Using System Identification and Shaking Table Experiments," *Report No. EERC 76-20,* Earthquake Engineering Research Center, University of California, Berkeley, August 1976.

15. Ramberg, W. and Osgood, W., "Description of Stress-Strain Curves by Three Parameters," *Technical Note No. 902,* NACA, July 1943.

16. Dafalias, Y. K. and Popov, E. P., "A Model of Nonlinearly Hardening Materials for Complex Loadings," *Acta Mechanica, 21,* pp. 173-192, 1975.

17. Stanton, J. F. and McNiven, H. D., "The Development of a Mathematical Model to Predict the Flexural Response of Reinforced Concrete Beams to Cyclic Loads, Using System Identification," *Report No. EERC 79-02,* Earthquake Engineering Research Center, University of California, Berkeley, January 1979.

18. Bjorck, A. and Dahlquist, G., "**Numerical Methods,**" Prentice Hall, 1974.

19. Zagajeski, S. W. and Bertero, V. V., "Computer-Aided Optimum Seismic Design of Ductile Reinforced Concrete Moment-Resisting Frames," *Report No. UCB/EERC-77/16,* Earthquake Engineering Research Center, University of California, Berkeley, December 1977.

20. ACI Standard 318-77, "Building Code Requirements for Reinforced Concrete," 1977 Edition.

21. "Seismic Design of Concrete Structures," Preliminary Draft of an Appendix to the CEB-FIP Model Code, Bulletin d-Information No. 133, Comite Euro-International du Beton, Paris, April 1980.

22. *Uniform Building Code,* International Conference of Building Officials, Whittier, California, 1979.

23. Chung, H. W., "Epoxy Repair of Bond in Reinforced Concrete Members," *ACI Journal,* American Concrete Institute, Jan-Feb. 1981.

24. Viwathanatepa, S., Popov, E. P., and Bertero, V. V., "Seismic Behavior of Reinforced Concrete Interior Beam-Column Subassemblages," *Report No. UCB/EERC-79/14,* Earthquake Engineering Research Center, University of California, Berkeley, June 1979.

25. Park, R., "Accomplishments and Research and Development Needs in New Zealand," *Proceedings,* Workshop on Earthquake-Resistant Reinforced Concrete Building Construction, University of California, Berkeley, Vol. II, July 1977.

26. Galunic, B., Bertero, V. V., and Popov, E. P., "An Approach for Improving Seismic Behavior of Reinforced Concrete Interior Joints," *Report No. UCB/EERC-77/30,* Earthquake Engineering Research Center, University of California, Berkeley, December 1977.

27. Paulay, T., Park, R., and Birss, G. R., "Elastic Beam-Column Joints for Ductile Frames," *Proceedings,* Seventh World Conference on Earthquake Engineering, Volume 6, Istanbul, Turkey, September 1980.

APPENDIX A - COMPUTER PROGRAM "BOND"

The organization of the computer program BOND has been briefly described in Section 4.6. This appendix contains details useful to a user who would like to modify the material laws, instructions for the preparation of input data files for the present version of the program, and a list of an input data file for an example problem.

A.1 Modification of Material Laws by the User

The computer program BOND has been organized in such a way that the existing material laws for steel and bond can be easily modified, or even completely reformulated, by a user without interfering with the algorithm or the input-output structure of the *base program.* The material description is, in fact, implemented in two groups of three subprograms for local bond and steel, respectively. The transmittal of information to and from the base program occurs mainly by means of labelled common blocks.

A.1.1 Labelled COMMON Blocks

The labelled COMMON blocks used in the two groups of three subprograms are following:[1]

(a) COMMON /POINT/ NP,IP

where NP is the number of points of the spatial discretization and IP is an integer not to be used in the present version;

(b) COMMON /KS/ RK(51),S(51)[1]

where vectors RK and S list the local secant stiffnesses for bond and steel laws, respectively, at different points of the spatial discretization;

(c) COMMON /INCREM/ DEPS(51),DU(51),DN(51),DQ(51)[1]

[1] The dimension for the vectors appearing in the COMMON blocks corresponds to the maximum number of points of the spatial discretization allowed for in the present version of the program.

where vectors DEPS, DU, DN, and DQ list, respectively, the current increments of strain $\Delta\epsilon$, slip Δu, normal steel force ΔN, and bond force per unit length Δq at the nodes;

(d) COMMON /FN2/ RN(S1),EPS(51)[1]

where vectors RN and EPS contain, respectively, current values of normal steel force N and corresponding strain ϵ;

(e) COMMON /FQ2/ Q(51),U(51)[1]

where vectors Q and U contain current values of bond force q and corresponding slip u.

A.1.2 Subprograms for Steel

The three subprograms required are two subroutines and one function. Exchange of information with the base program is realized, with the exception of the function, which has also two arguments, only through the labelled COMMON blocks previously listed. Exchange of information among the three subprograms will usually require one additional COMMON block for which the label /FN1/ is suggested. The subprograms may include additional COMMON blocks and may call other subprograms in order to perform the assigned tasks. These tasks are specified as follows:

(a) SUBROUTINE INPFN

Purpose of the subroutine is to read proper information characterizing the constitutive relationship for steel and set necessary initializations. The subroutine requires labelled COMMON blocks /POINT/, /KS/, and /FN2/. Necessary initializations are:

-set vectors RN and EPS to zero

-set local secant stiffness vector RK to its initial value

(b) FUNCTION FN(DEPP,I)

Purpose of the function is to return for a given pair of arguments, DEPP and I, which are, respectively, the increment of strain $\Delta\epsilon$ and the number of the point where the local constitutive relationship is being considered, the value of the corresponding normal steel

force N. The function requires labelled COMMON block /FN2/.

(c) SUBROUTINE UPFN

Purpose of this subroutine is to update, for all the points of the spatial discretization, all the proper quantities which define the constitutive law for steel, and to prepare for the next step. In fact, this subroutine is called by the base program only after convergence has been achieved and a step completed. The subroutine requires labelled COMMON blocks /POINT/, /INCREM/, and /FN2/. Necessary updating includes:

-set the updated value of the strain vector EPS equal to the previous one plus the current increment DEPS;

-set accordingly the updated value of the normal force vector RN.

A.1.3 Subprograms for Local Bond

The three subprograms required are two subroutines and one function. Exchange of information with the base program is realized, with the exception of the function, which has also two arguments, only through the labelled COMMON blocks previously listed. Exchange of information among the three subprograms will usually require one additional COMMON block for which the label /FQ1/ is suggested. The subprograms may include additional COMMON blocks and may call other subprograms in order to perform the assigned tasks. These tasks are specified as follows:

(a) SUBROUTINE INPFQ

Purpose of the subroutine is to read proper information characterizing the constitutive relationship for local bond and set necessary initializations. The subroutine requires labelled COMMON blocks /POINT/, /KS/, and /FQ2/. Necessary initializations are:

-set vectors Q and U to zero;

-set local secant stiffness vector S to its initial value.

(b) FUNCTION FQ(DU,I)

Purpose of the function is to return for a given pair of arguments DU and I, which are, respectively, the increment of slip Δu and the node number where the local constitutive relationship is being considered, the value of the corresponding bond force per unit length q. The function requires labelled COMMON block /FQ2/.

(c) SUBROUTINE UPFQ

Purpose of this subroutine is to update, for all the points of the spatial discretization, all the proper quantities which define the constitutive law for local bond, and to prepare for the next step. In fact, this subroutine is called by the base program only after convergence has been achieved and a step completed. The subroutine requires labelled COMMON blocks /POINT/, /INCREM/, and /FQ2/. Necessary updating includes:

-set the updated value of the slip vector U equal to the previous one plus the current increment DU;

-set accordingly the updated value of the bond force vector Q.

Note that in the existing version of the local bond model this subroutine calls at each point of the spatial discretization another subroutine, called DAMAGE, which first computes updated damage factors and then, based on those, "reduced envelopes" and "frictional resistance" for the next step.

A.2 Input Data for the Present Version of the Program

General Procedure Data

(a) Read NP, ICASE, NCYC (3I5)

-NP number of points defining the spatial discretization (maximum value 51)

-ICASE integer referring to the boundary condition case (1, 2, or 3, according to the list considered in Section 4.1 and Fig. 4.2)

-NCYC number of loading points defining the loading history (maximum value 50)

(b) Read X(I), I=1,NP (5F10.0)

-X vector containing the x coordinates of the NP points defining the spatial discretization (as many lines as needed to specify NP coordinates) [mm]

(c) Read KCYC(I), I=1,NCYC (10I5)

-KCYC vector which specifies the number of loading increments in which the loading between any two points, i-1, i, of the loading history (defined subsequently by the vectors BC1, BCN) has to be subdivided; it is used to set the steps of the numerical procedure

(d) Read BC1(I), I=1,NCYC (5F10.0)

-BC1 vector containing the assigned displacement (slip) [mm] at end point 1 of the bar, for each of the NCYC points defining the loading history

(e) *Only* for boundary condition case 1; to be skipped otherwise.

Read BCN(I), I=1,NCYC (5F10.0)

-BCN vector containing the assigned displacements (slip), [mm] at end point NP of the bar, for each of the NCYC points defining the loading history

(f) Read NITER, NITER1 (2I5)

-NITER maximum number of iterations for the main iteration loop (suggested values between 10 and 30). If convergence is not achieved after NITER iterations, the step length (loading increment) is automatically halved.

-NITER1 same as NITER, but for the secondary iteration loops (suggested values between 30 and 50)

(g) Read TOL, TOL1, TOLDUM (3F10.0)

-TOL tolerance parameter for convergence in the main iteration loop (suggested values: 10^{-6} - 10^{-7} for boundary condition cases 1 and 3, 10^{-11} - 10^{-13} for case 2)

-TOL tolerance parameter for convergence in the secondary iteration loop (suggested values: 10^{-6} - 10^{-7})

-TOLDUM tolerance parameter for the maximum automatic subdivision of the original step of the incremental procedure (If this tolerance is set, for example, to 10^{-2}, procedure stops and a message is printed when the automatic subdivision leads to a step smaller than 1/100 of the original one. Suggested values for this parameter are between 10^{-1} and 10^{-3}.)

Steel Data

These data are read from present version of subroutine INPFN.

(a) Read RK0,ALN,RNY,R0,A1,A2 (6F10.0)

-RK0 initial slope of the force-strain relationship for steel [N]

-ALN strain-hardening ratio $b = E_1/E_o$ (see Fig. 3.1)

-RNY normal force at yield [N]

-R0,A1,A2 parameters defining the nonlinear steel model, as in Eqn. 3.3. If R0 is set equal to 0, the bilinear model is used.

Bond Data

These data are read from present version of subroutine INPFQ.

(a) Read NGR (I4)

-NGR number of groups of different bond laws. For each group the corresponding parameters will be given in (b); a point-group correspondence will be assigned in (c).

(b) *To be repeated* for each (index J) of the NGR groups:

Read V1P(J),V2P(J),V3P(J),G1P(J),G3P(J) (5F10.0)

Read V1M(J),V2M(J),V3M(J),G1M(J),G3M(J) (5F10.0)

Read B(J),SS0(J),ALP(J),ALM(J) (4F10.0)

The first two groups of five data are the five parameters defining the two monotonic envelopes, for positive and negative slip values, respectively (Section 2.4). In particular, V1P,V2P,V3P are s_1, s_2, s_3 and G1P,G3P are the bond forces, $q_1 = \pi d_b \tau_1$ and $q_3 = \pi d_b \tau_3$ (compare Section 2.2.2), used to characterize the positive envelope. V1M,V2M,V3M,G1M,G3M characterize, in turn, the envelope in the negative region, but they also have to be given positive values.

The last set of four data contains, respectively:

-the exponent β in the expression of the initial part of the monotonic envelope (Section 2.2.2), assumed to be the same for both positive and negative envelopes;

-the ratio of the stiff slope of the unloading branch to the maximum between the two secant moduli G1P/V1P and G1M/V1M;

-the amplification factors for computing energy dissipation, b^+ and b^-, as explained in Section 2.4.

(c) Read NN(I), I=1,NP (20I4)

-NN integer vector which assigns to each point I of the spatial discretization, the corresponding number of the bond law group

(d) Read B1,B2,B3,B4,B5 (5F10.0)

Damage parameters for computing reduced envelopes. They are:

-B1 fraction of energy dissipated by friction alone to be taken into account for computing the total dissipated energy E which appears in the expression of the damage parameter d (compare Section 2.2.3 and Fig. 2.3); $B_1 = 0.5$

-B2,B3 first and second exponent appearing in the expression of the damage parameter d (Fig. 2.3); to be given the values 1.2 and 1.1, respectively

-B4,B5 to be given the values 1. and 0., respectively. These parameters refer to a previous more complicated expression for the damage d, which is not used in the present version.

(e) Read F1,F2,F3,F4 (4F10.0)

Damage parameters for computing frictional resistance:

-F1,F2 parameters defining the linear part ($\tau_f/\tau_3 = F1 + F2 \cdot s_{max}/s_3$) of the curve fitted through experimental data and presented in Fig. 2.4 (compare also Section 2.2.4). Values are, respectively, 0.1 and 1.8.

-F3,F4 first and second exponent appearing in the expression of d_f as a function of the energy dissipated by friction alone (Section 2.2.4). This expression is analogous to the one given for d in Fig. 2.3. Values to be given are 1.2 and 0.67, respectively.

General Output Specification Data

(a) Read KSTEP,KSTEP1,IEL,IEL1 (4I4)

These parameters may be used to produce an extended printout of all the iteration computations when numerical problems are expected in certain stages or have been experienced in a previously aborted run. The printout is given between step KSTEP and KSTEP1 and for all the discretization points between IEL and IEL1. Usually these integers will be chosen so as to produce no printout (for example, 999,999,999,999).

(b) Read FILNAM (A8)

-FILNAM name of the file where results are stored. Results are written on the file as unformatted data in the following sequence:

-At the beginning of the file and after reading the input data:

WRITE(1) NP,NCYC,(KCYC(I),I=1,NCYC)

WRITE(1) (X(J),J=1,NP).

-After completing each step of the incremental procedure:

WRITE(1) (EPS(I),I=1,NP)

WRITE(1) (U(I),I=1,NP)

WRITE(1) (RN(i),I=1,NP)

WRITE(1) (Q(I),I=1,NP)

Results stored may be used, and usually are, for subsequent graphics.

A.3 Example Data File

The example data file presented here refers to the case of a monotonic pull-push test (Case 3), with imposed slip (at the pulled left end, Point x=0) up to 15 mm, to be reached in 75 load increments. Other parameters characterizing the numerical test are:

-bar diameter: $d_b = 25\ mm$

-anchorage length: $l_d = 15\ d_b = 375\,mm$, divided into 28 intervals (29 points)

-steel characteristics: $E_o = 1.0 \cdot 10^8\ N/mm^2$, $E_1/E_o = 0.017$, $N_y = 2.21 \cdot 10^5\ N/mm^2$ ($f_y = 450\ N/mm^2$), bilinear -bond characteristics and distribution: as in Table 5.1 (29 discretization points and 7 different bond law groups)

The input data file which follows is given in a free format form, with fields separated by commas.

```
29,3,1
0.,12.5,25.,37.5,50.
62.5,75.,87.5,100.,112.5
125.,137.5,150.,162.5,187.5
```

212.5,225.,237.5,250.,262.5

275.,287.5,300.,312.5,325.

337.5,350.,362.5,375.

75

-15.

30,50

1.e-7,1.e-6,1.e-3

1.0e+8,0.017,2.21e+5,0.,18.5,0.15e-3

7

1.,3.,10.5,1570.,589.

0.3,0.3,1.,393.,0.1

0.4,8.8,1.,114.

1.,3.,10.5,1444.,540.

0.475,0.975,3.375,559.,98.2

0.4,9.5,1.,11.

1.,3.,10.5,1185.,442

0.825,2.325,8.125,893.,295.

0.4,12.,1.,3.5

1.,3.,10.5,1060.,393.

1.,3.,10.5,1060.,393.

0.4,13.,1.,1.

0.825,2.325,8.125,893.,295.

1.,3.,10.5,1185.,442.

0.4,12.,3.5,1.

0.475,0.975,3.375,559.,98.

1.,3.,10.5,1444.,540.

0.4,9.5,11.,1.

0.3,0.3,1.0,393.,0.1

1.,3.,10.5,1570.,589.

0.4,8.8,114.,1.

1,1,1,1,2,2,3,3,4,4,4,4,4,4,4,4,4,4,4,4,

4,5,5,6,6,7,7,7,7

0.5,1.2,1.1,1.0,0.

0.1,1.8,1.2,0.67

999,999,999,999

ga15m

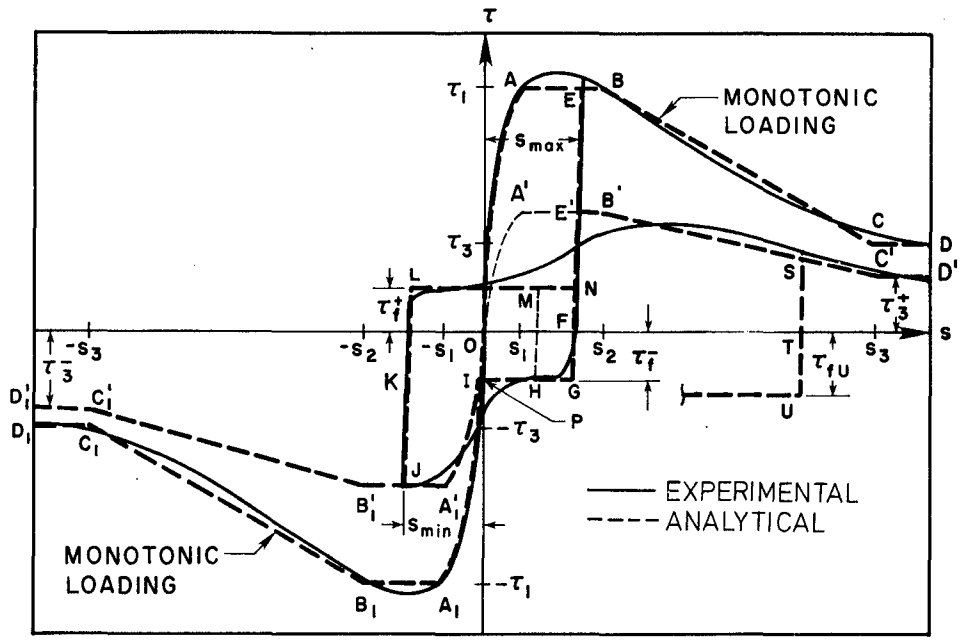

FIG. 2.1 - PROPOSED ANALYTICAL MODEL FOR LOCAL BOND STRESS-SLIP RELATIONSHIP

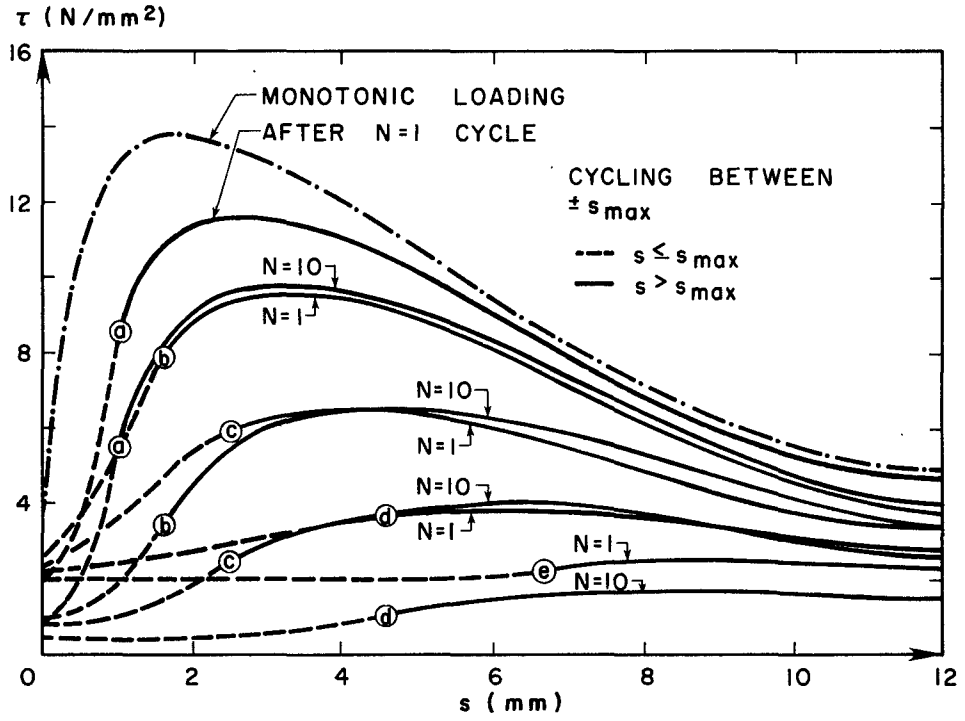

FIG. 2.2 - EFFECTS OF NUMBER OF CYCLES AND OF THE PEAK VALUES OF SLIP s_{max} AT WHICH THE CYCLING IS PERFORMED ON THE ENSUING BOND STRESS-SLIP RELATIONSHIP FOR $s > s_{max}$

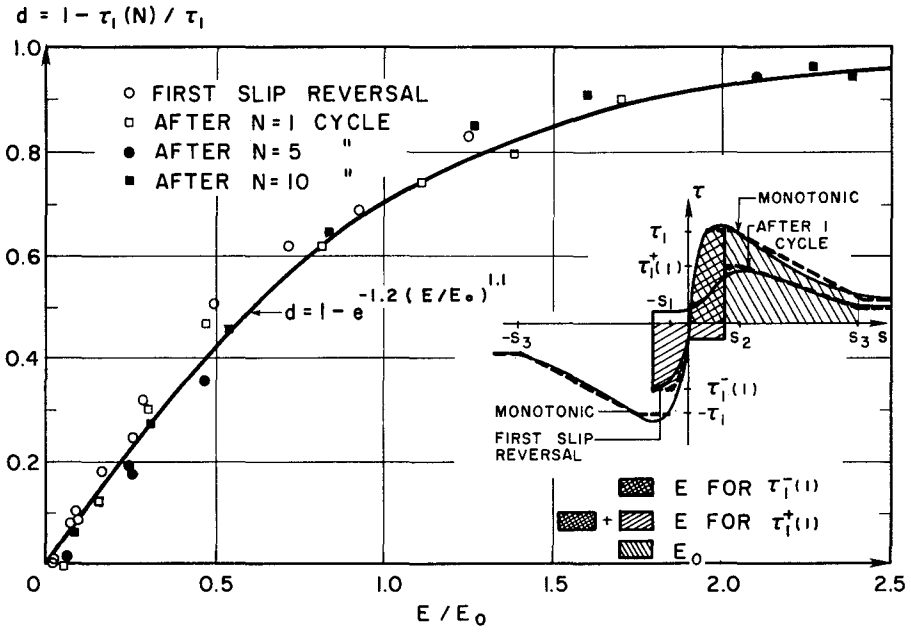

FIG. 2.3 - DAMAGE PARAMETER d AS A FUNCTION OF THE DIMENSIONLESS ENERGY DISSIPATION

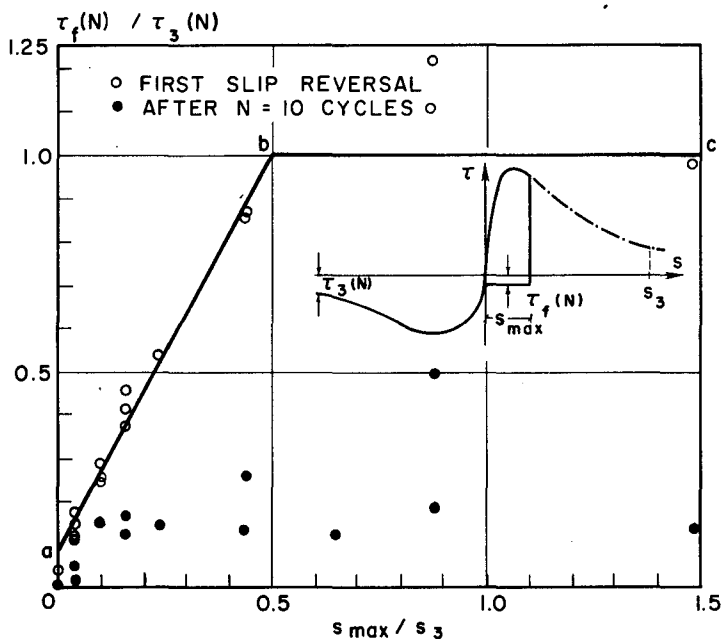

FIG. 2.4 - RELATIONSHIP BETWEEN THE FRICTIONAL BOND RESISTANCE $\tau_f(N)$ AND THE CORRESPONDING ULTIMATE FRICTIONAL BOND RESISTANCE $\tau_3(N)$

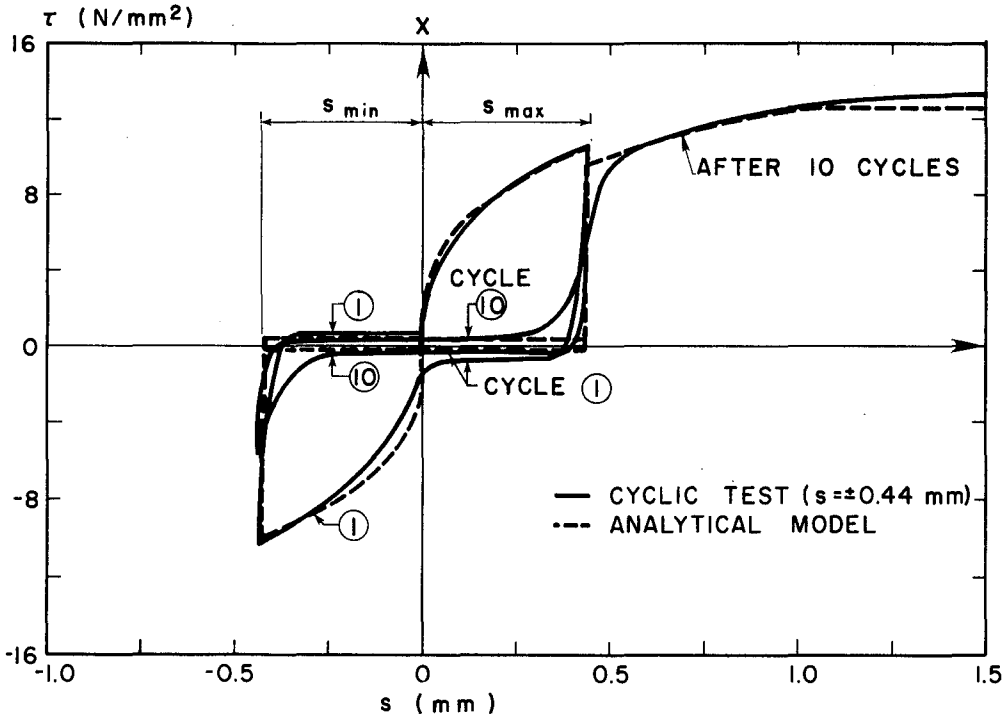

(a) - CYCLING BETWEEN s = ±0.44 mm

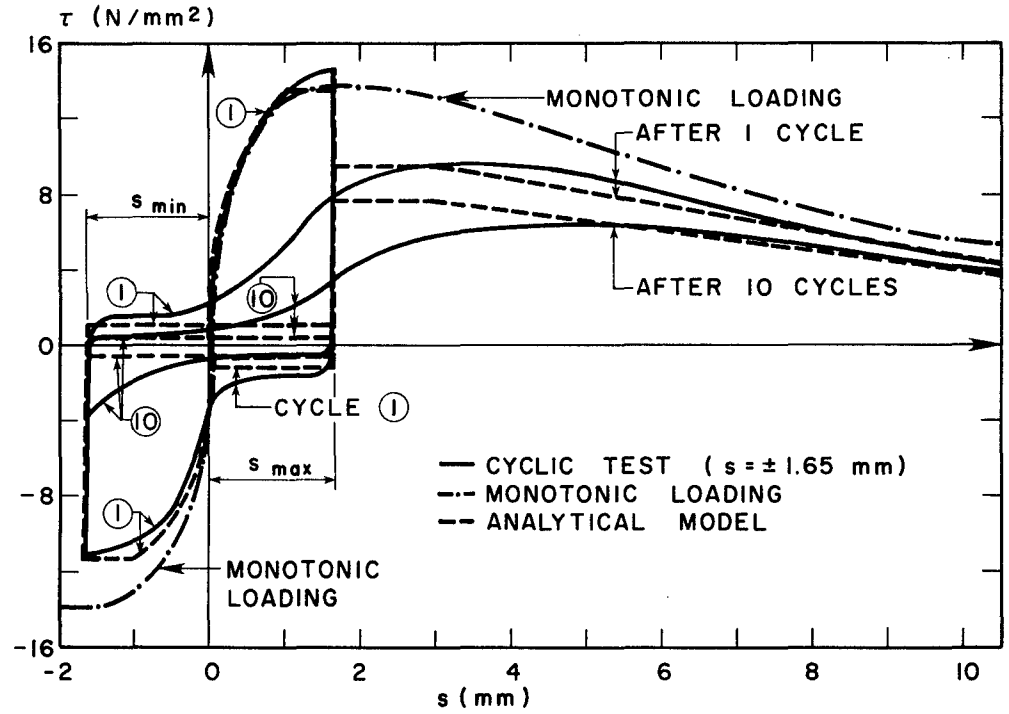

(b) - CYCLING BETWEEN s = ±1.65 mm

FIG. 2.5 - COMPARISON OF EXPERIMENTAL AND ANALYTICAL RESULTS ON LOCAL BOND STRESS-SLIP RELATIONSHIP

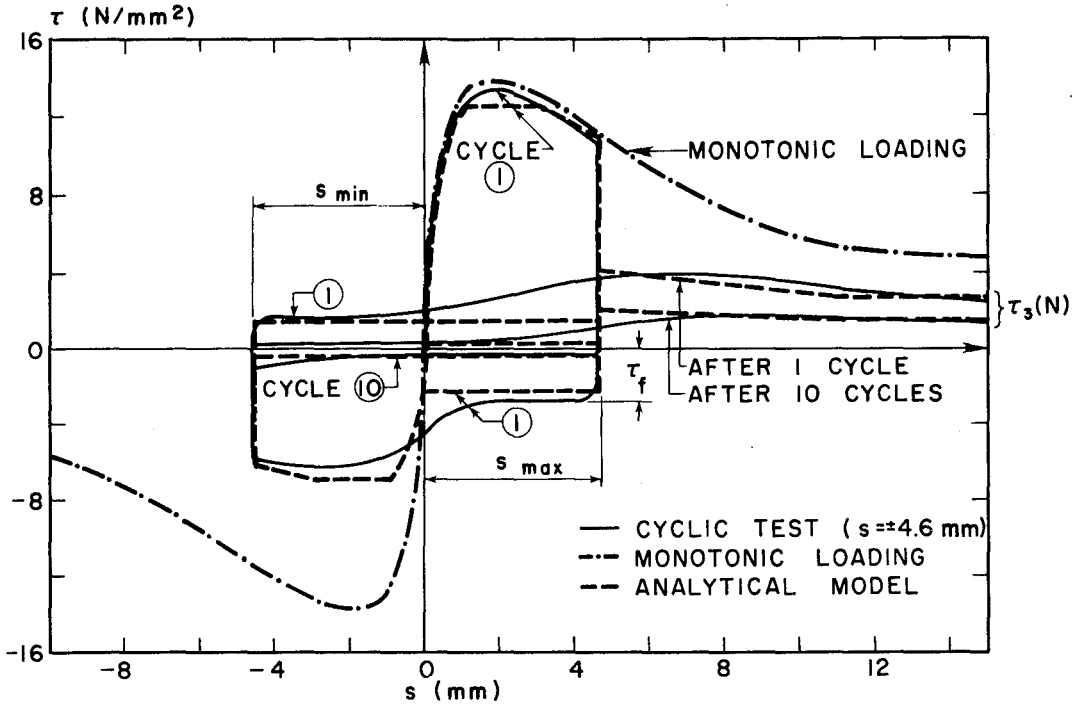

(c) - CYCLING BETWEEN s = ±4.6 mm

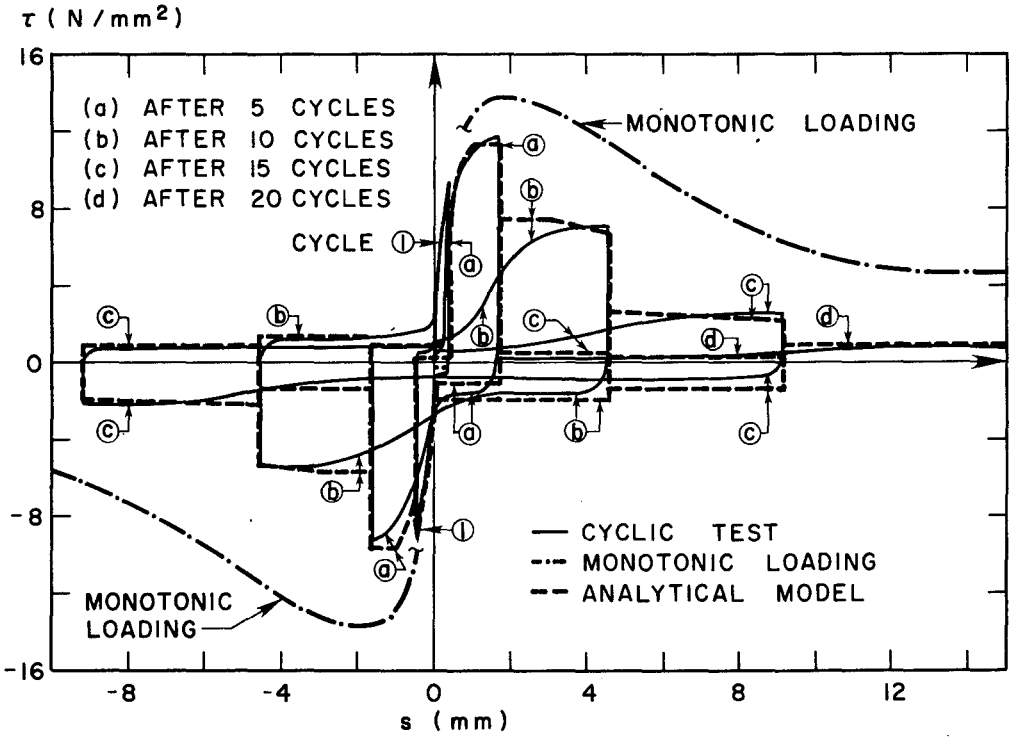

(d) - CYCLING UNDER DIFFERENT INCREASING s_{max}

FIG. 2.5 - COMPARISON OF EXPERIMENTAL AND ANALYTICAL RESULTS ON LOCAL BOND STRESS-SLIP RELATIONSHIP

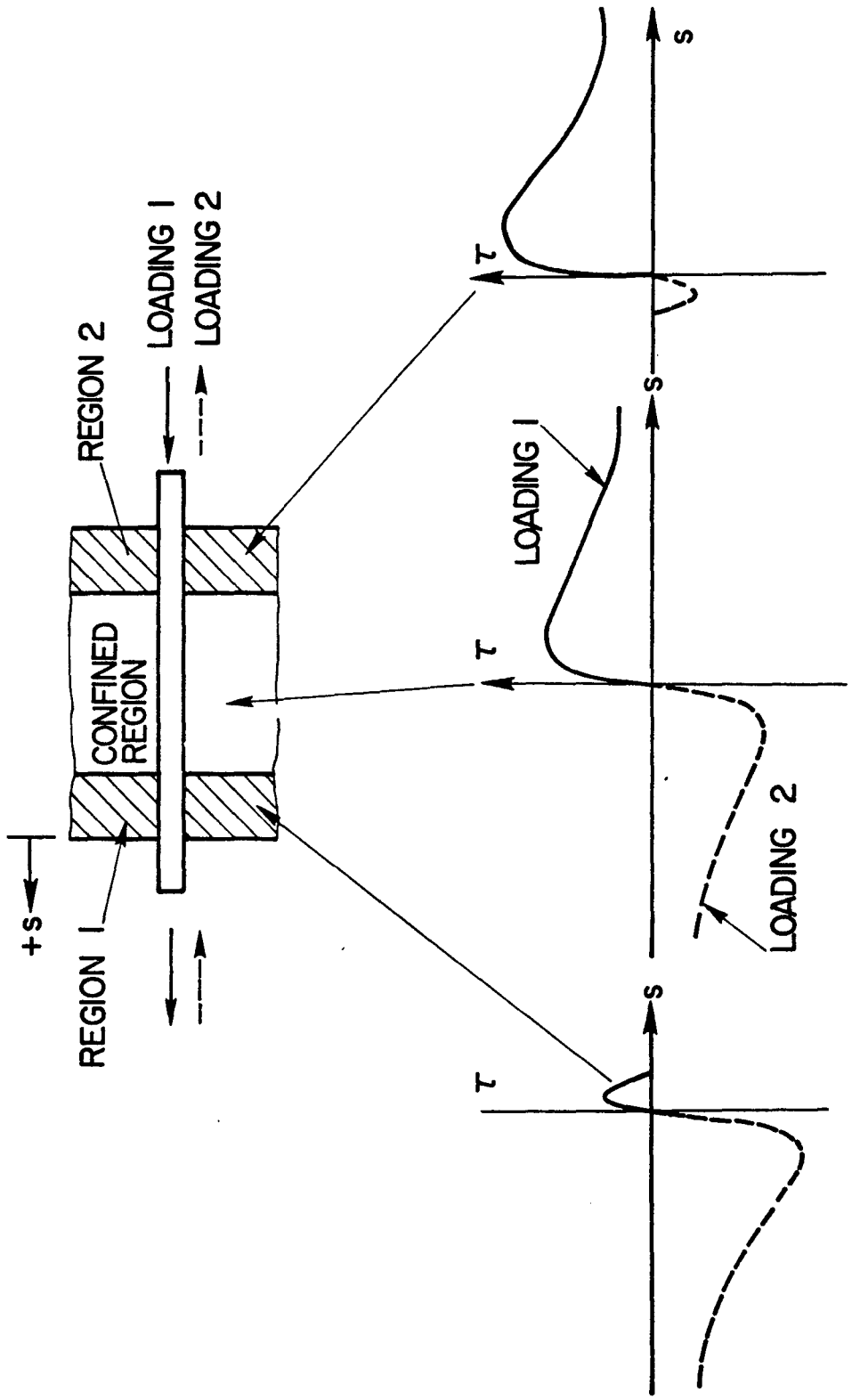

FIG. 2.6 - DIFFERENT BOND REGIONS IN AN INTERIOR JOINT (AFTER [5])

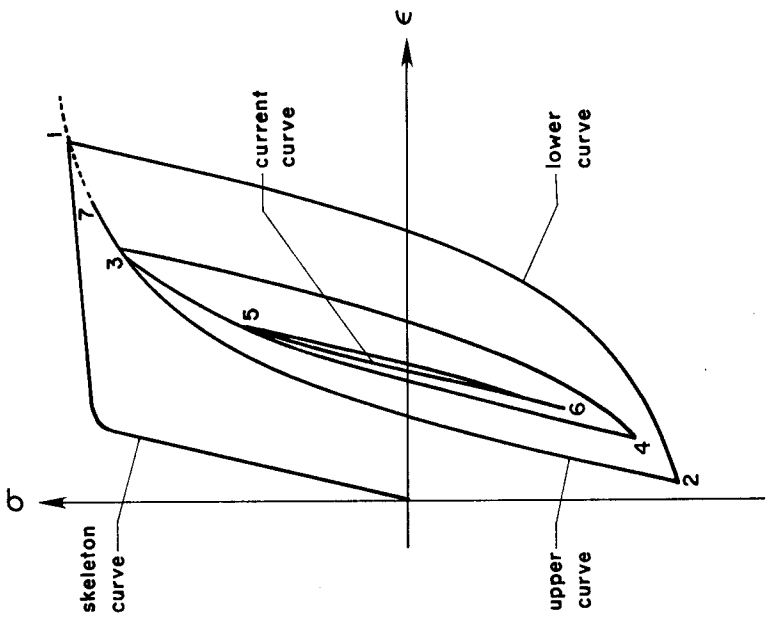

FIG. 3.2 - EXAMPLE FOR CYCLIC LOADING, EXACT CURVE

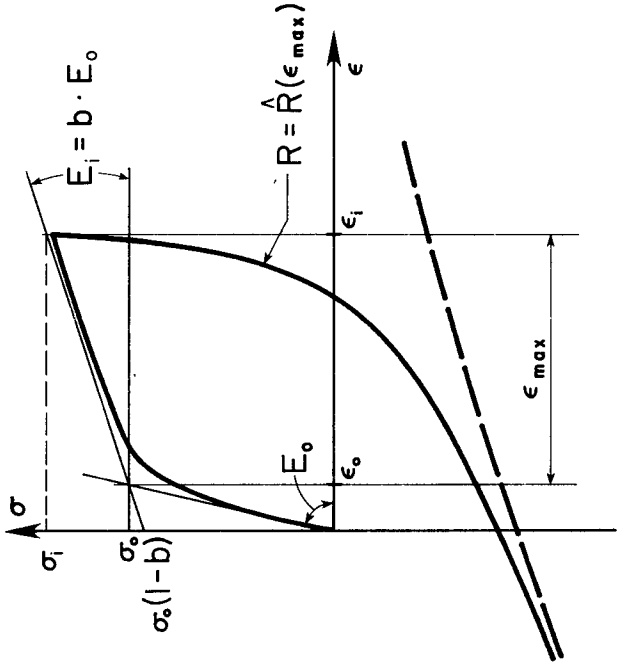

FIG. 3.1 - PARAMETERS DEFINING THE ANALYTICAL STEEL MODEL

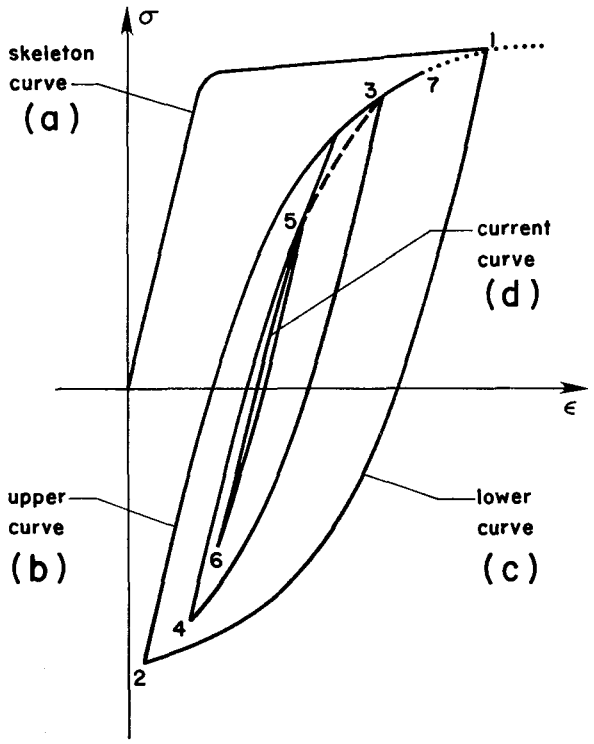

FIG. 3.3 - EXAMPLE FOR CYCLIC LOADING, COMPARISON BETWEEN EXACT CURVE AND CURRENT MODEL

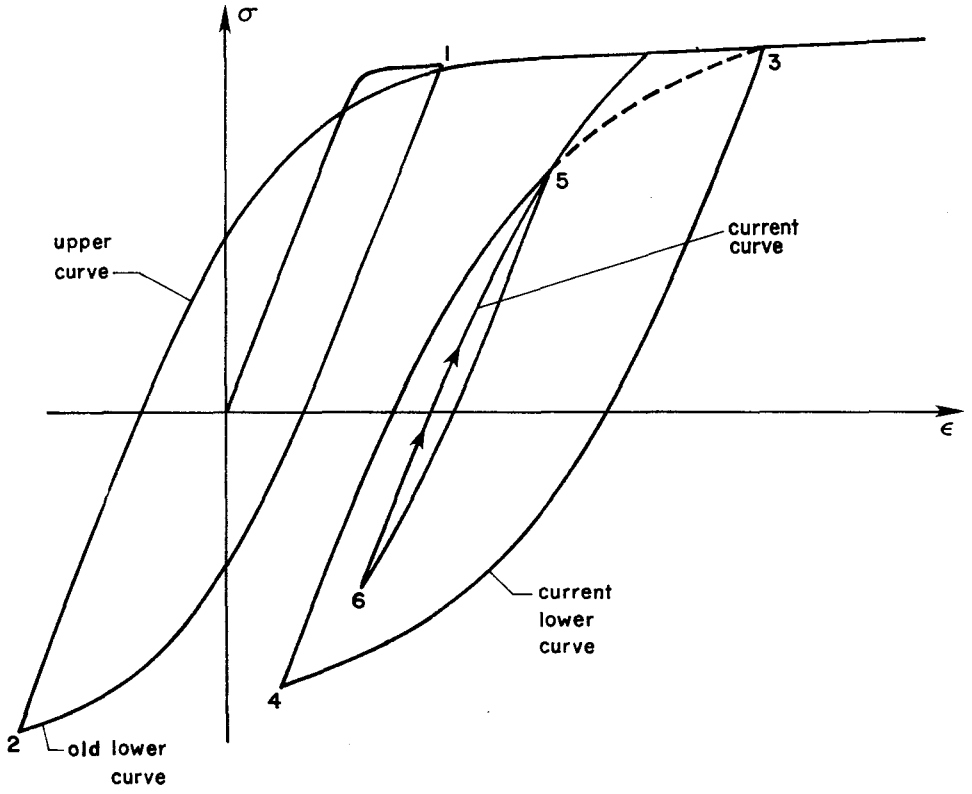

FIG. 3.4 - EXAMPLE FOR CYCLIC LOADING, COMPARISON BETWEEN EXACT CURVE AND CURRENT MODEL

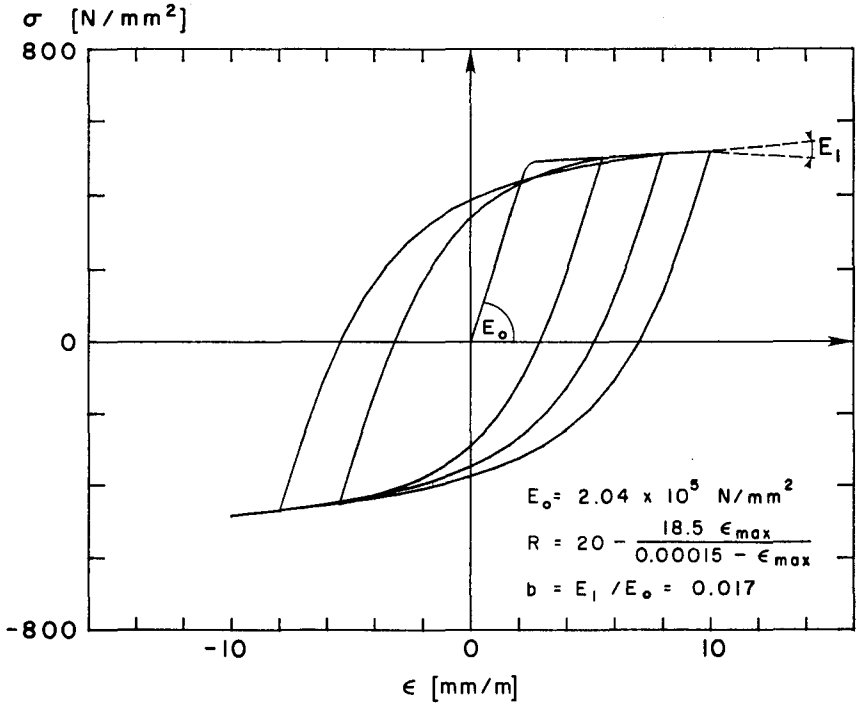

(a) ANALYTICAL

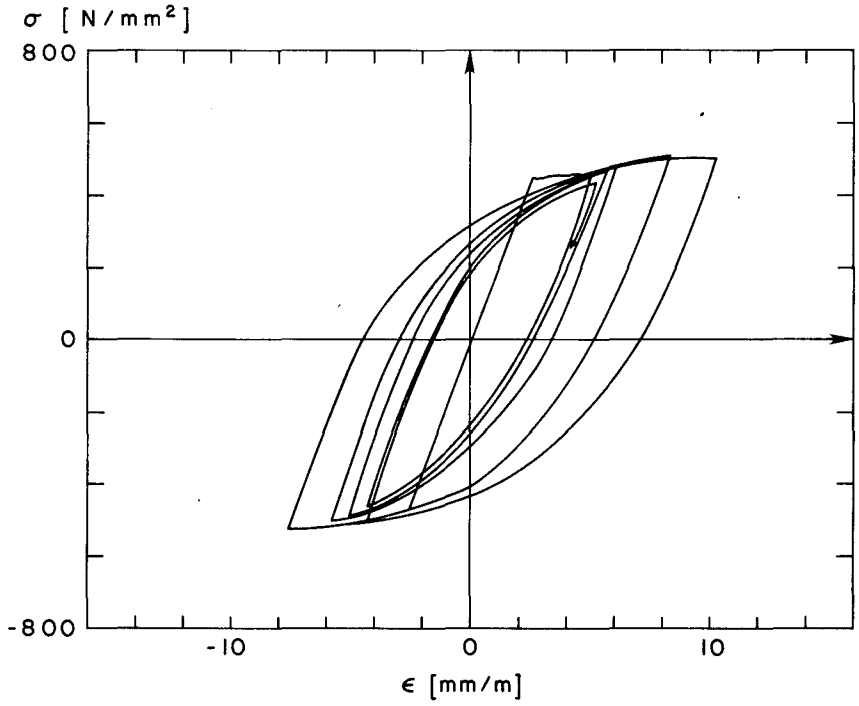

(b) EXPERIMENTAL

FIG. 3.5 - COMPARISON BETWEEN EXPERIMENTAL AND ANALYTICAL RESULTS FOR STRESS-STRAIN RELATIONSHIP OF A REINFORCING BAR, TEST TAKEN FROM REF. [5]

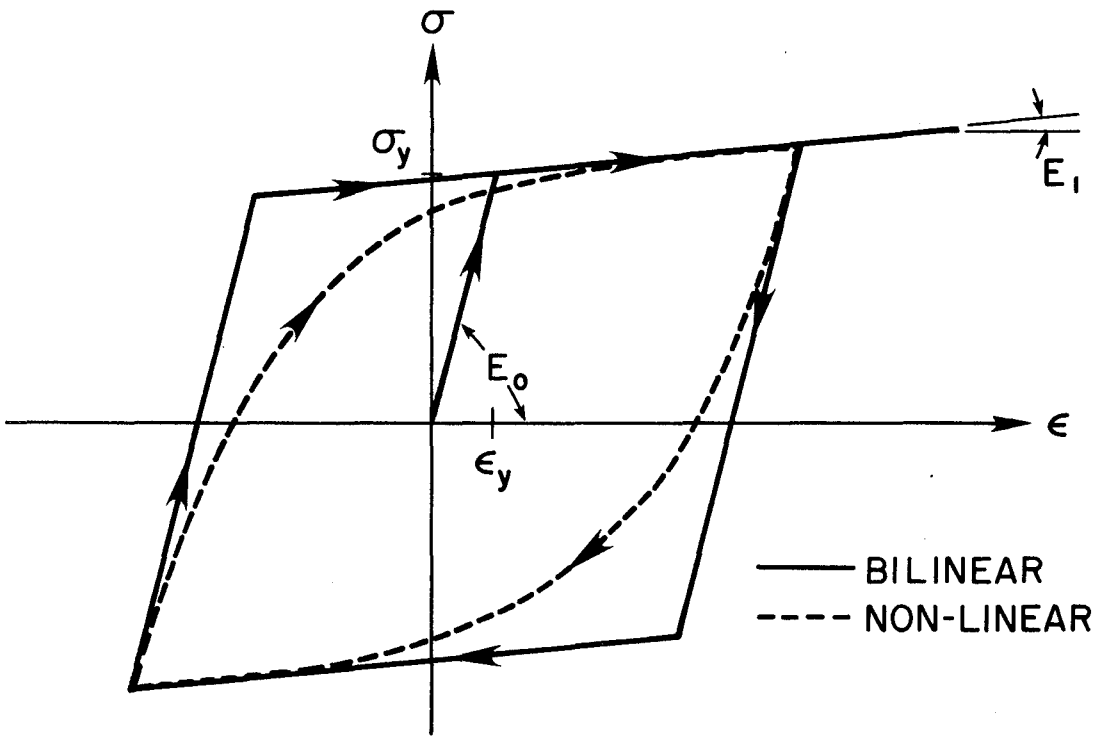

FIG. 3.6 - BILINEAR AND NONLINEAR STEEL MODEL

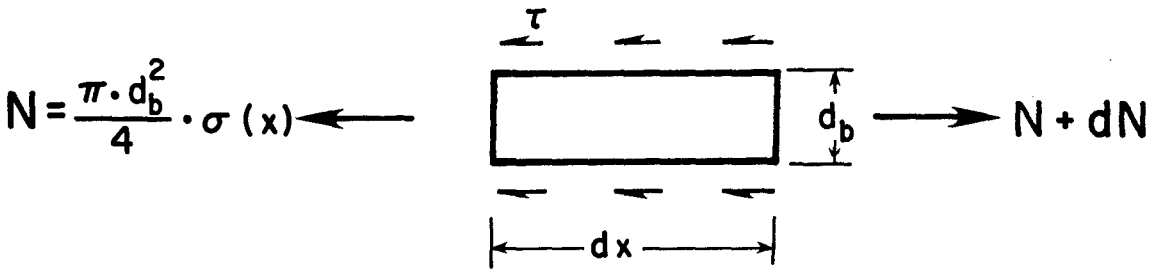

$$\frac{dN(x)}{dx} - \pi \cdot d_b \cdot \tau(x) = 0$$

$$\sigma(x) = \sigma[\epsilon(x)],\ \tau(x) = \tau[s(x)]$$

$\sigma(\epsilon)$ = Constitutive Law for Steel

$\tau(s)$ = " " " Bond

FIG. 4.1 - DIFFERENTIAL EQUATION OF BOND

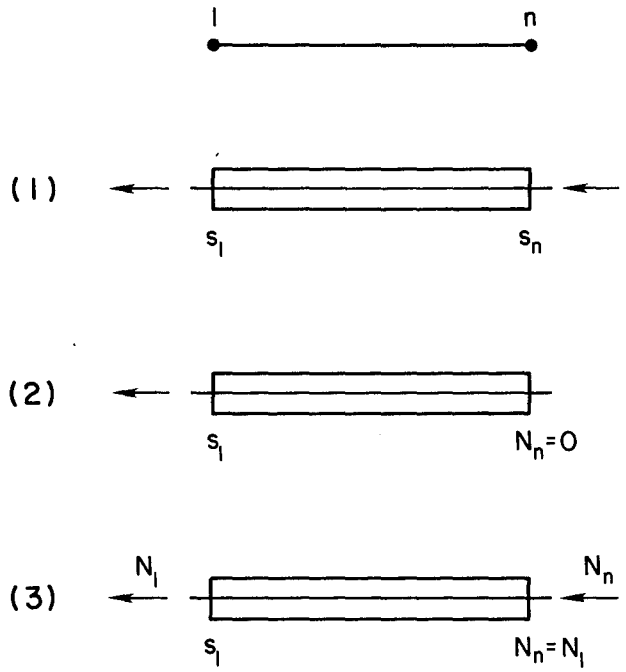

FIG. 4.2 - BOUNDARY CONDITIONS CONSIDERED IN THE PROGRAM.

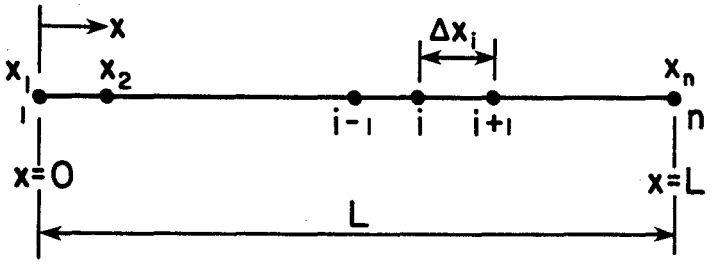

FIG. 4.3 - SUBDIVISION OF BAR

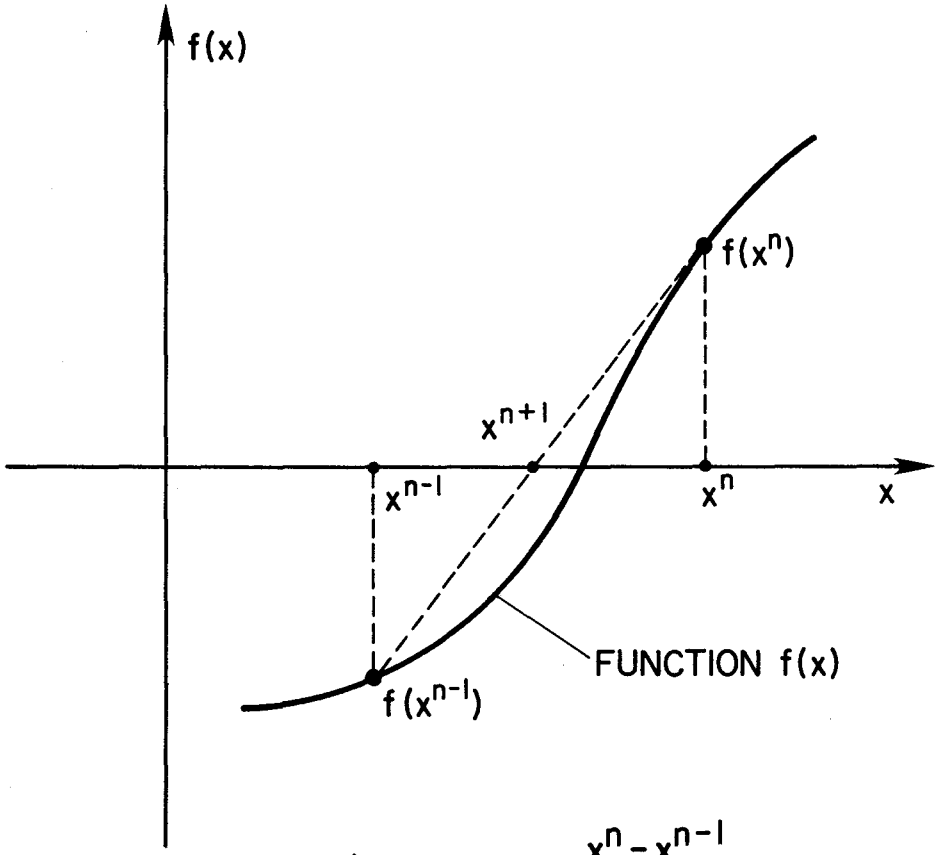

$$x^{n+1} = x^n - f(x^n)\,\frac{x^n - x^{n-1}}{f(x^n) - f(x^{n-1})}$$

FIG. 4.4 - SECANT METHOD

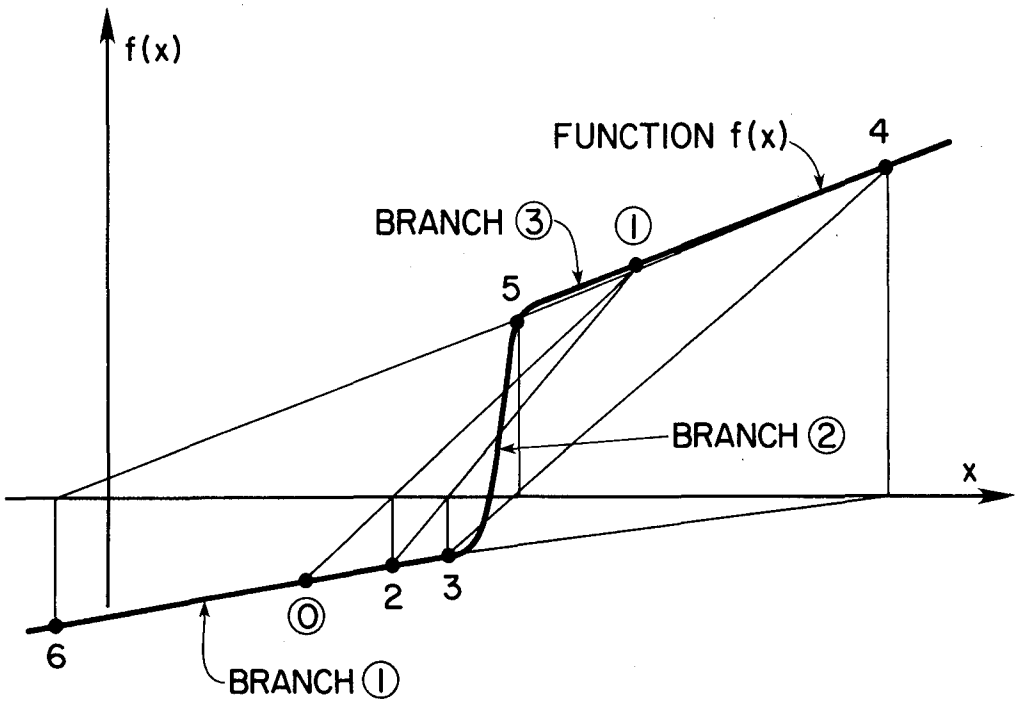

(a) - SECANT METHOD

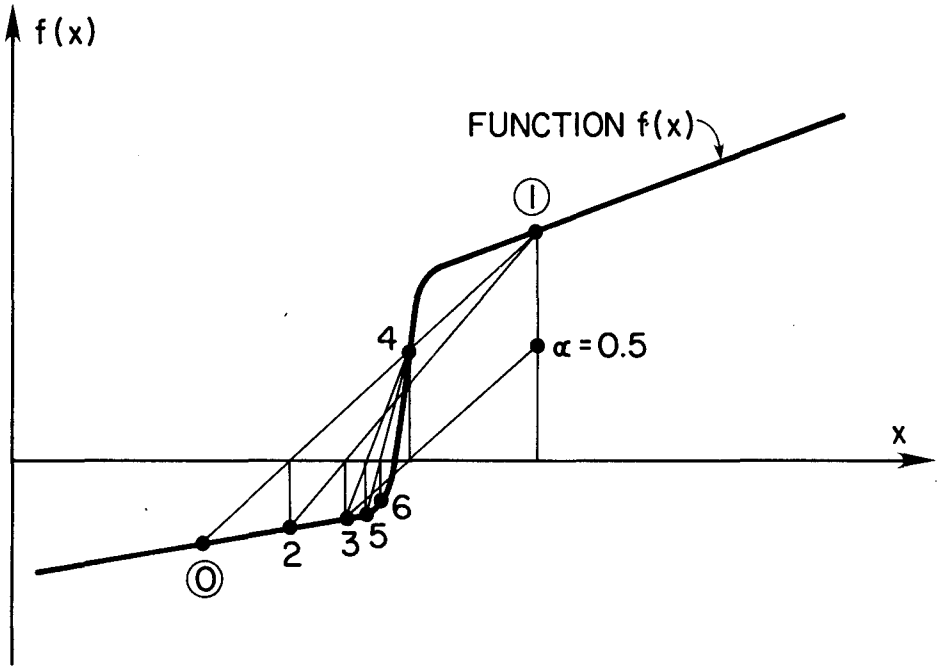

(b) - ILLINOIS ALGORITHM

FIG. 4.5 - ITERATION SCHEME

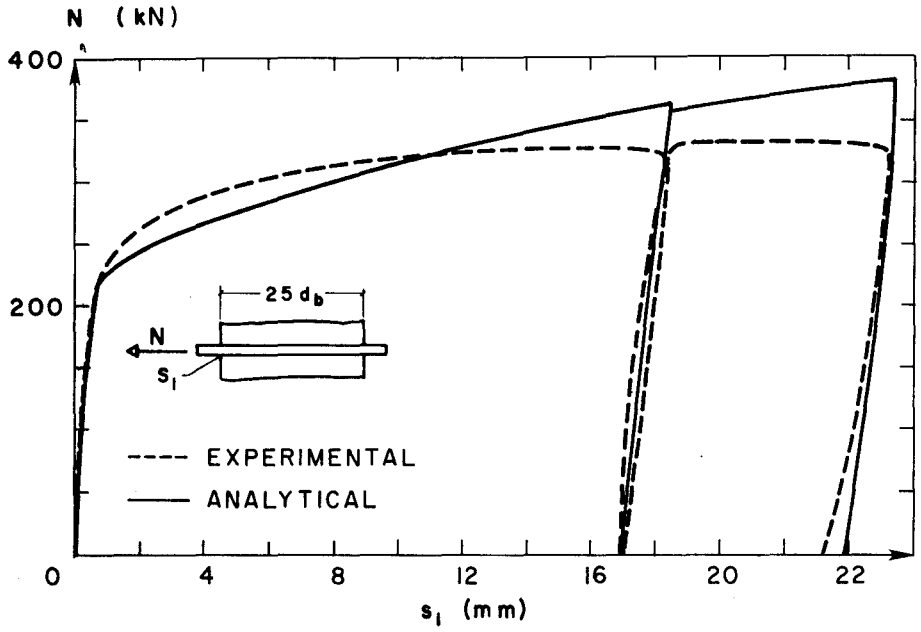

FIG. 5.1 - COMPARISON BETWEEN EXPERIMENTAL AND ANALYTICAL RESULTS, TEST 3 OF REF. [5], AVERAGE BOND BEHAVIOR ASSUMED

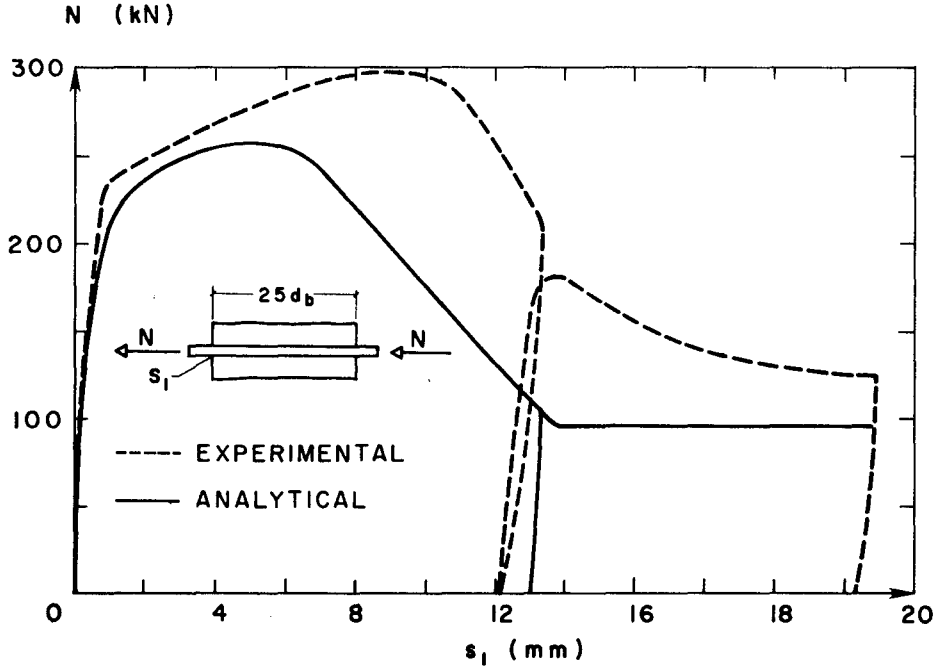

FIG. 5.2 - COMPARISON BETWEEN EXPERIMENTAL AND ANALYTICAL RESULTS, TEST 13 OF REF. [5], AVERAGE BOND BEHAVIOR ASSUMED

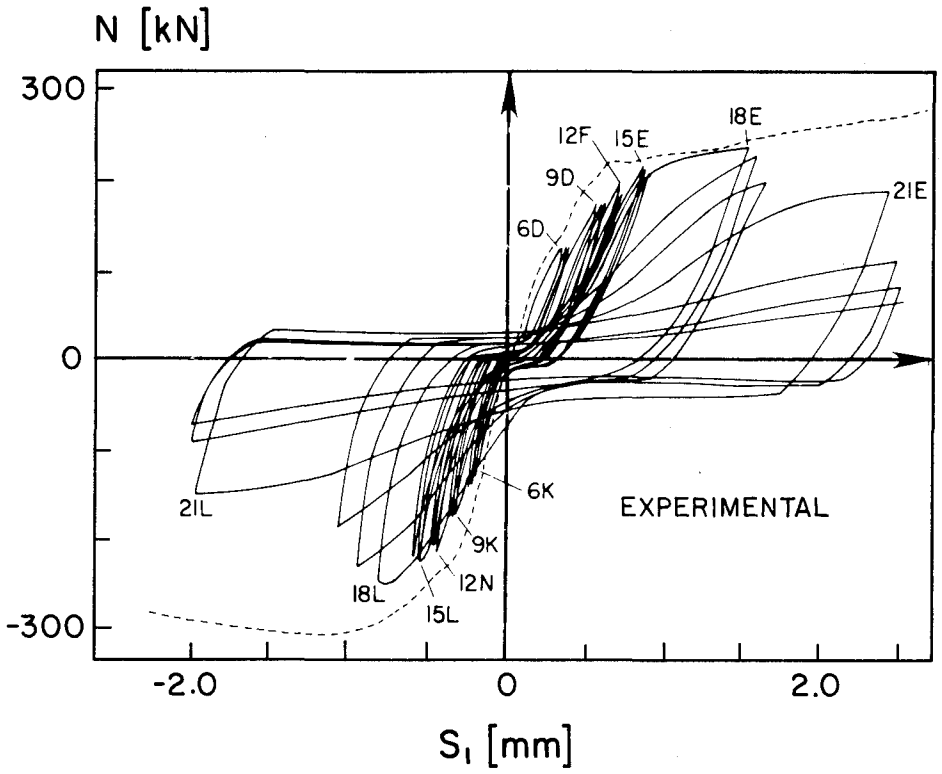

(a) EXPERIMENTAL

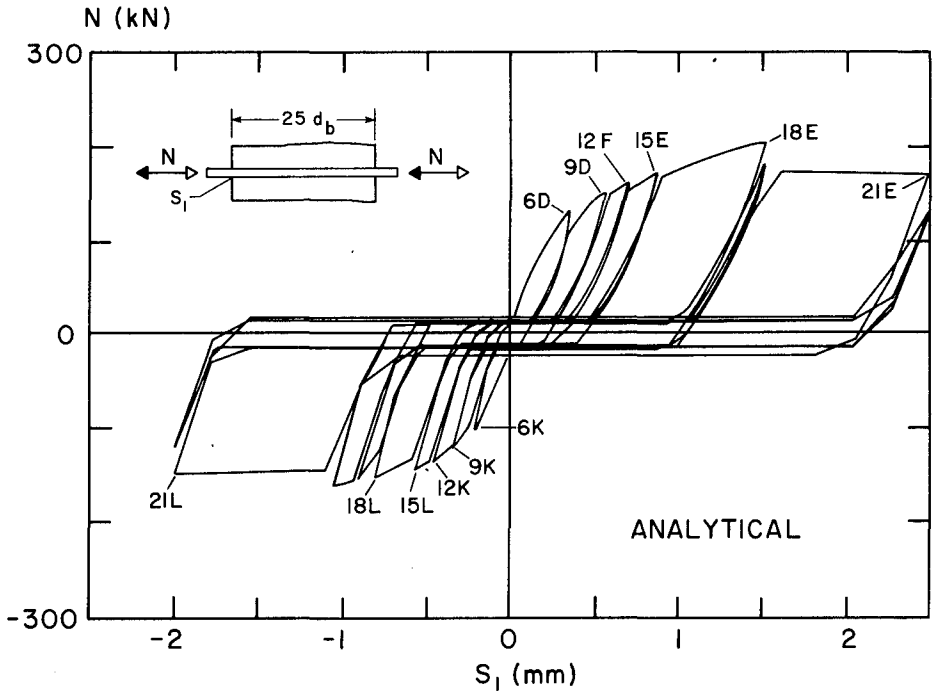

(b) ANALYTICAL, AVERAGE BOND BEHAVIOR ASSUMED

FIG. 5.3 - COMPARISON BETWEEN EXPERIMENTAL AND ANALYTICAL RESULTS, TEST 14 OF REF. [5]

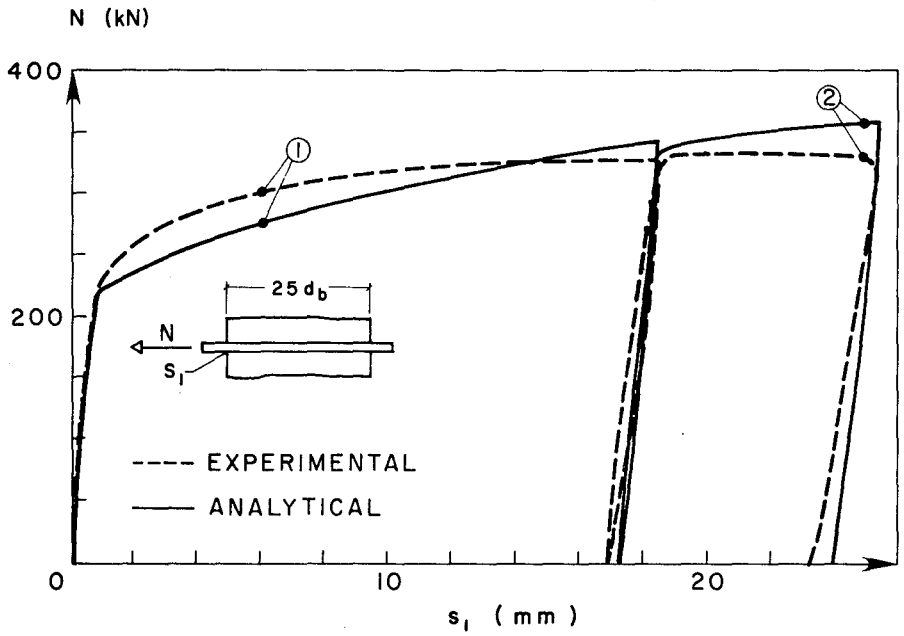

FIG. 5.4 - COMPARISON BETWEEN EXPERIMENTAL AND ANALYTICAL RESULTS, TEST 3 OF REF. [5], BOND RESISTANCE DECREASED BY 10% COMPARED TO AVERAGE BEHAVIOR

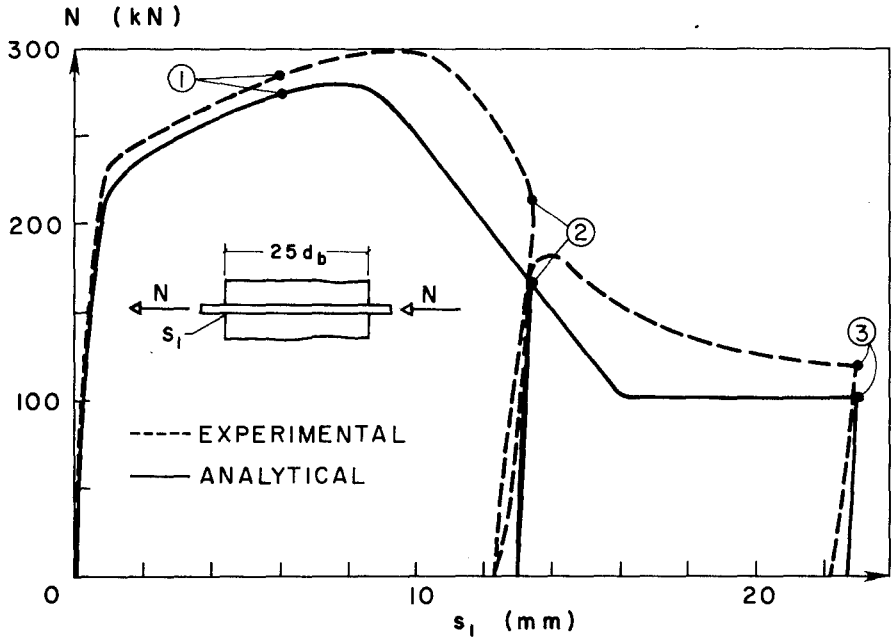

FIG. 5.5 - COMPARISON BETWEEN EXPERIMENTAL AND ANALYTICAL RESULTS, TEST 13 OF REF. [5], BOND RESISTANCE INCREASED BY 10% COMPARED TO AVERAGE BEHAVIOR

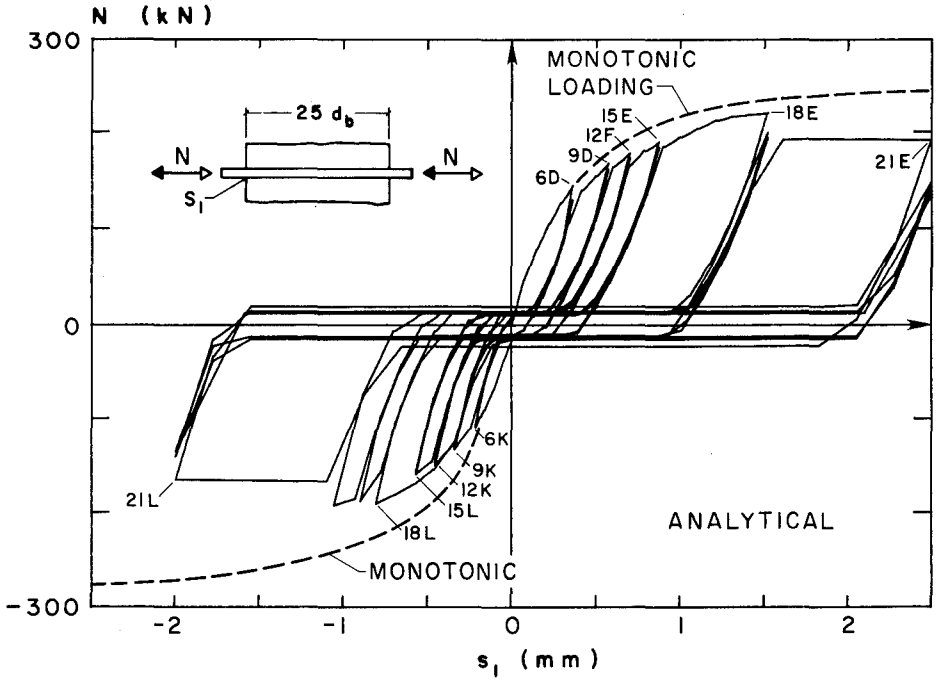

(a) CYCLES 1 TO 21

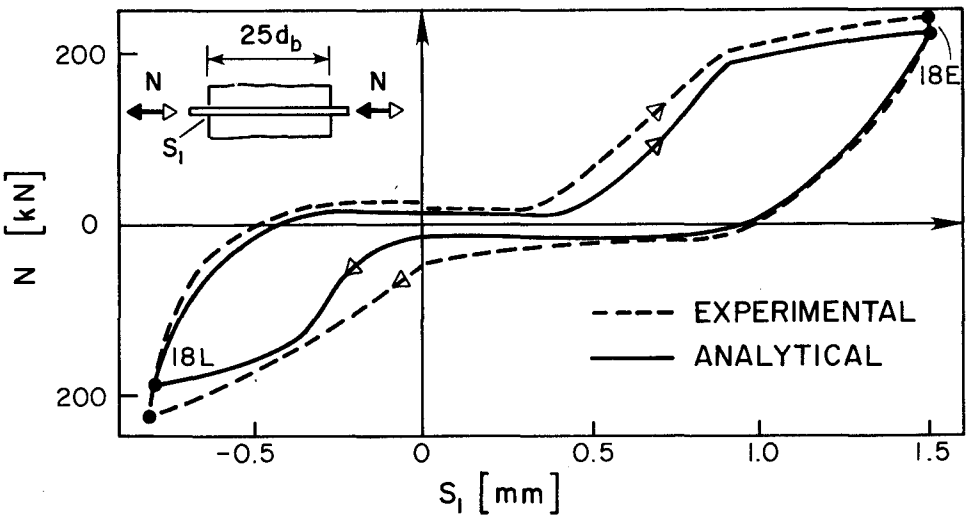

(b) CYCLE 18

FIG. 5.6 - ANALYTICAL RESPONSE OF TEST 14 OF REF. [5], BOND RESISTANCE INCREASED BY 10% COMPARED TO AVERAGE BEHAVIOR, EXPERIMENTAL RESPONSE OF CYCLES 1 TO 21, SEE FIG. 5.3a.

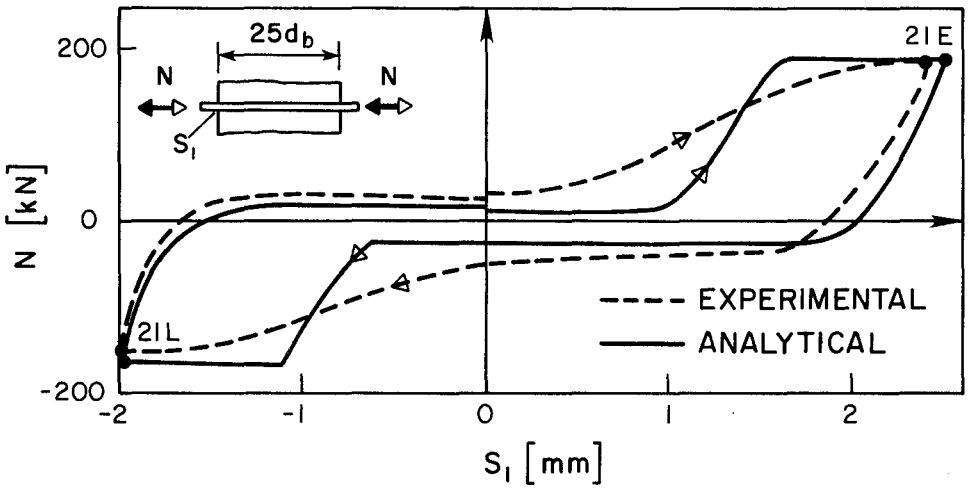

(c) CYCLE 21

FIG. 5.6 - ANALYTICAL RESPONSE OF TEXT 14 of REF. [5], BOND RESISTANCE INCREASED BY 10% COMPARED TO AVERAGE BEHAVIOR.

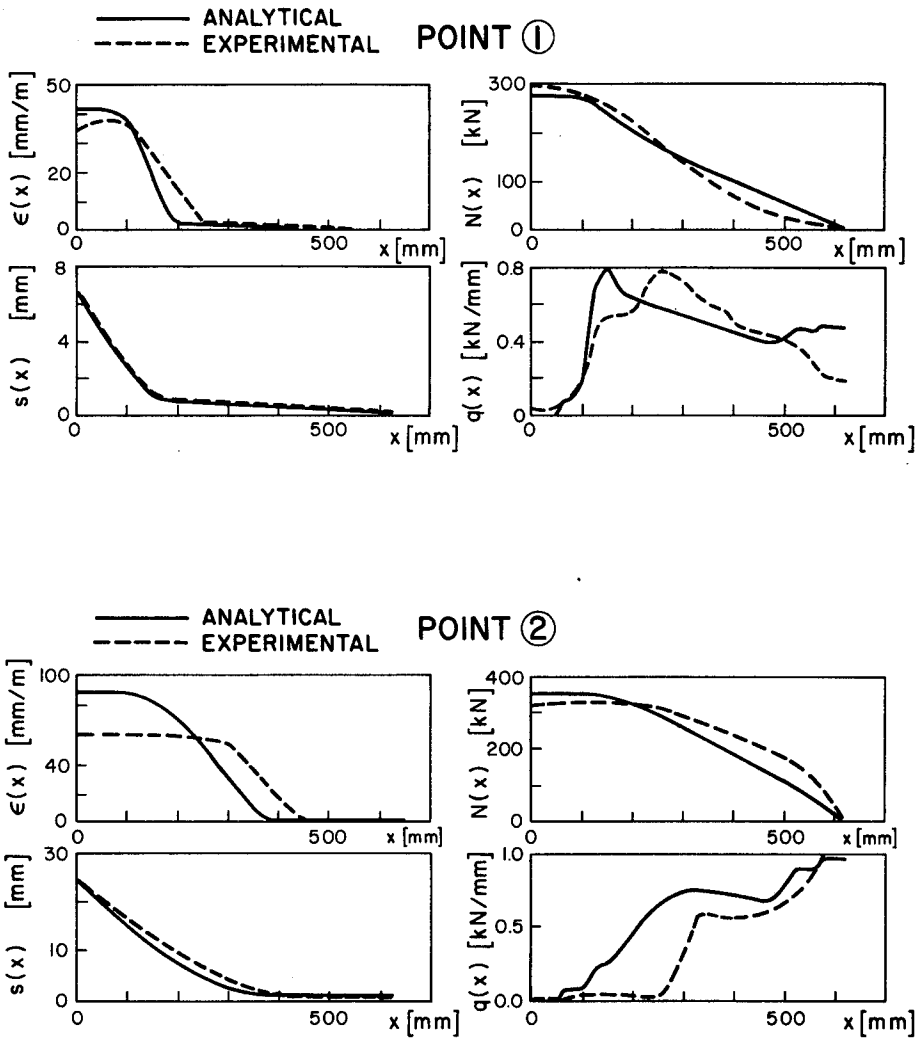

FIG. 5.7 - DISTRIBUTION OF STEEL STRAIN $\varepsilon(x)$, SLIP $s(x)$, NORMAL FORCE $N(x)$, AND BOND FORCE $q(x)$ ALONG THE ANCHORAGE LENGTH, ANALYTICAL AND EXPERIMENTAL RESULTS FOR TWO CHARACTERISTIC LOAD STAGES (SEE FIG. 5.4) OF SPECIMEN 3 OF REF. [5].

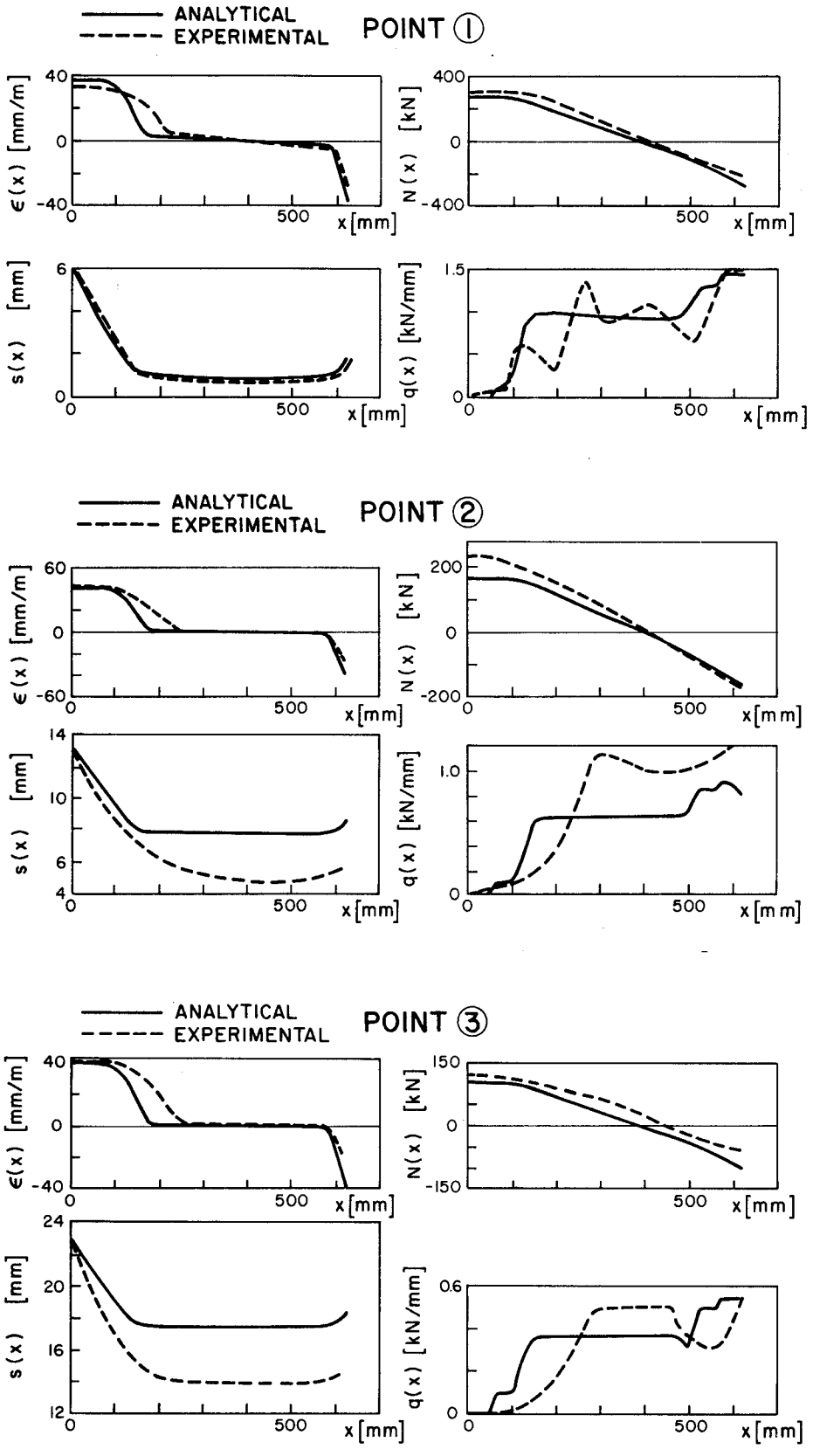

FIG. 5.8 - DISTRIBUTION OF STEEL STRAIN $\varepsilon(x)$, SLIP $s(x)$, NORMAL FORCE $N(x)$, AND BOND FORCE $q(x)$ ALONG THE ANCHORAGE LENGTH, ANALYTICAL AND EXPERIMENTAL RESULTS FOR THREE CHARACTERISTIC LOAD STAGES (SEE FIG. 5.5) OF SPECIMEN 13 OF REF. [5].

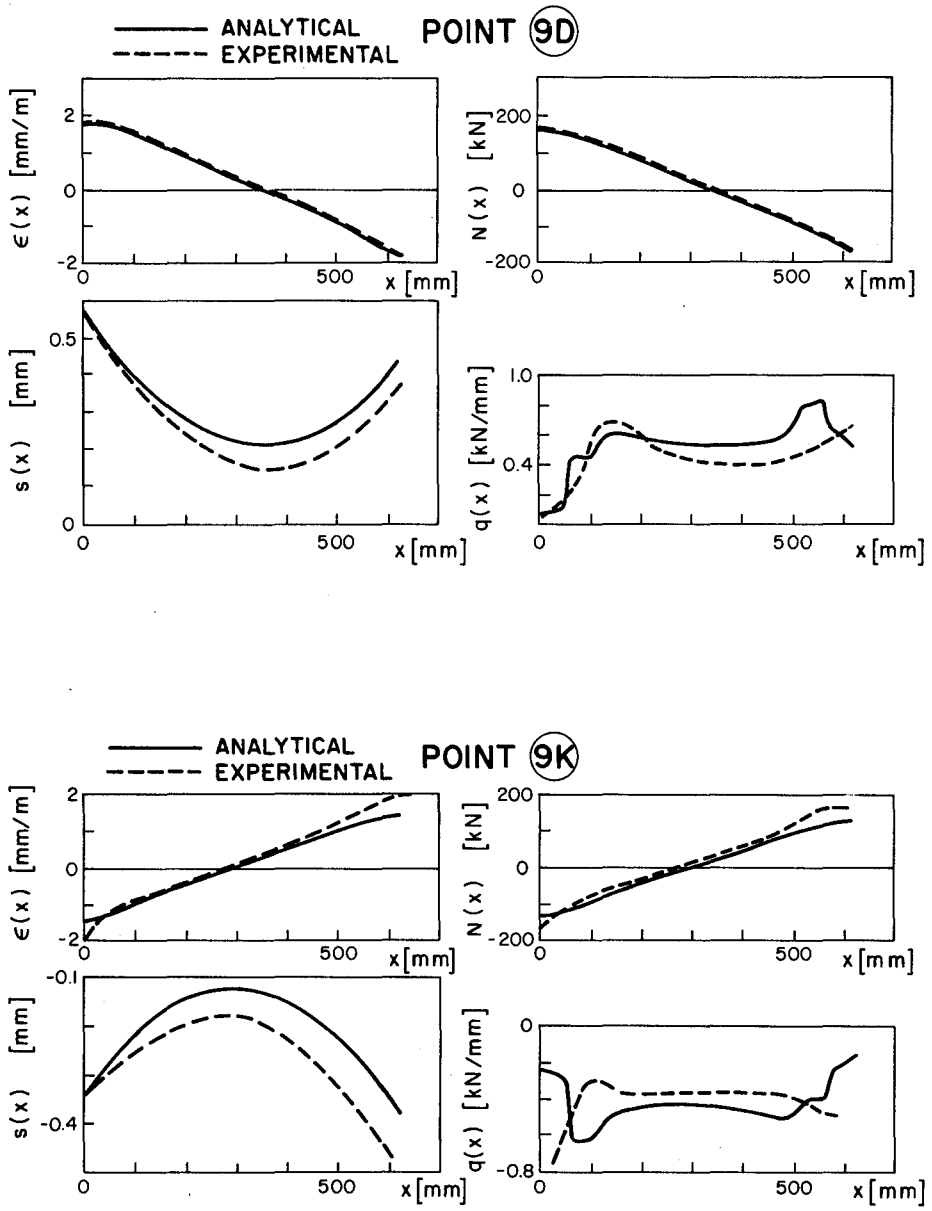

(a) POINT 9D AND 9K

FIG. 5.9 - DISTRIBUTION OF STEEL STRAIN $\varepsilon(x)$, SLIP $s(x)$, NORMAL FORCE $N(x)$, AND BOND FORCE $q(x)$ ALONG THE ANCHORAGE LENGTH, ANALYTICAL AND EXPERIMENTAL RESULTS FOR 6 CHARACTERISTIC LOAD STAGES (SEE FIG. 5.6) OF SPECIMEN 14 OF REF. [5].

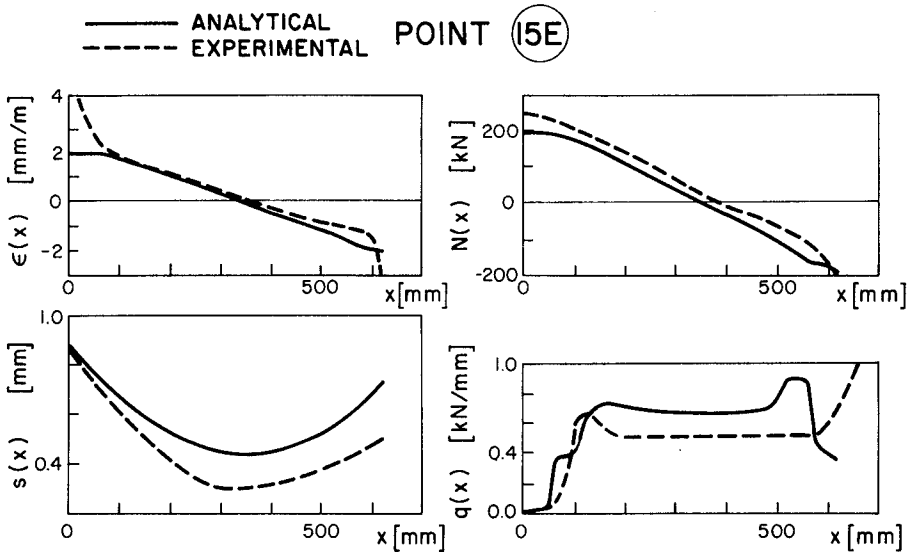

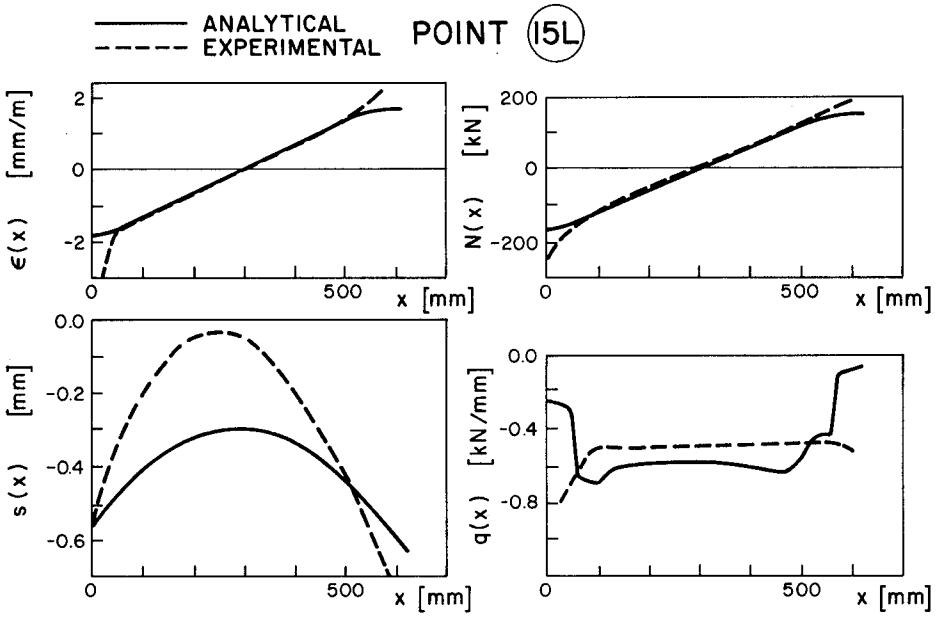

(b) POINT 15E AND 15L

FIG. 5.9 - DISTRIBUTION OF STEEL STRAIN $\varepsilon(x)$, SLIP $S(x)$, NORMAL FORCE $N(x)$, AND BOND FORCE $q(x)$ ALONG THE ANCHORAGE LENGTH, ANALYTICAL AND EXPERIMENTAL RESULTS FOR 6 CHARACTERISTIC LOAD STAGES (SEE FIG. 5.6) OF SPECIMEN 14 OF REF. [5].

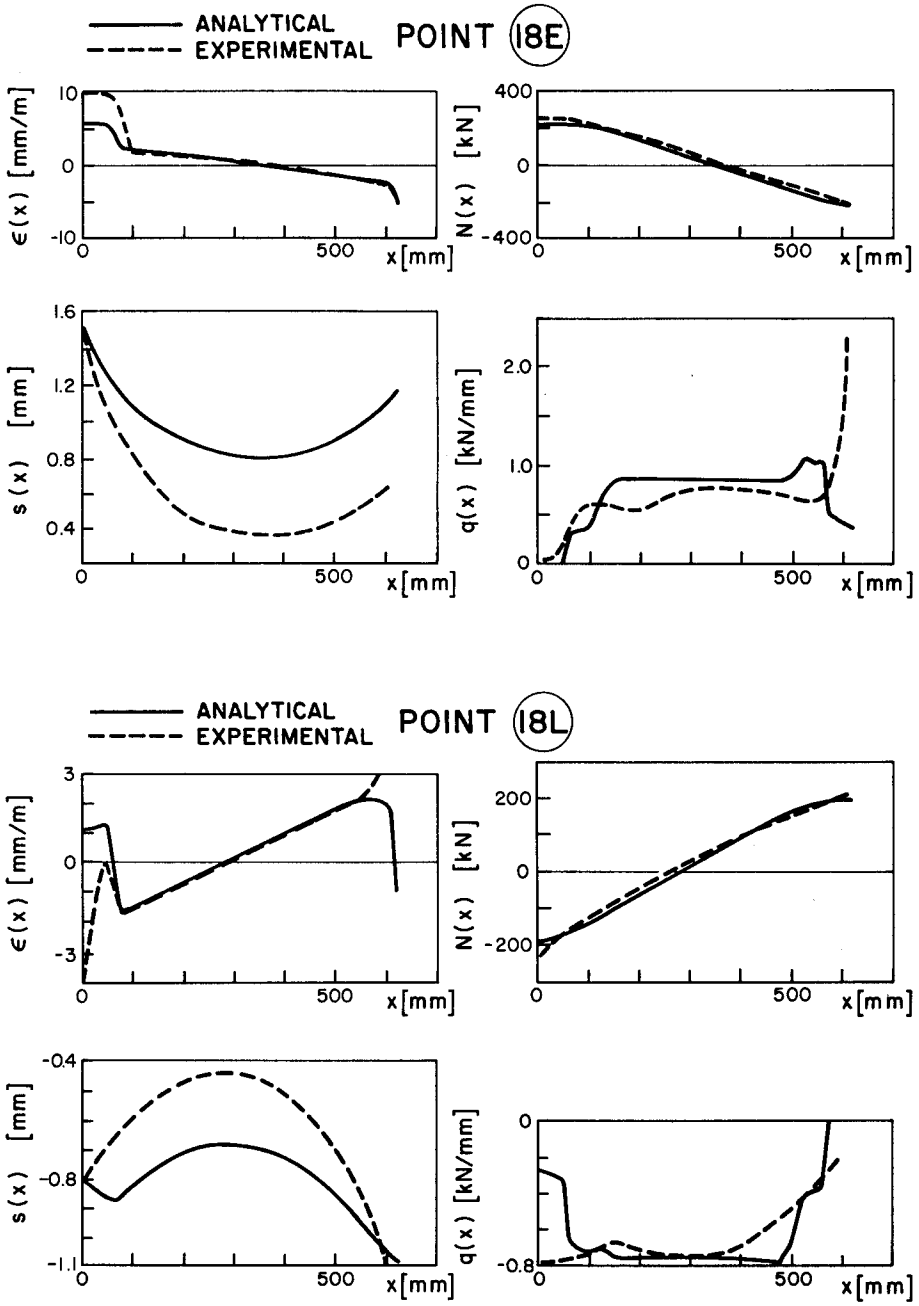

(c) POINT 18E AND 18L

FIG. 5.9 - DISTRIBUTION OF STEEL STRAIN $\varepsilon(x)$, SLIP $s(x)$, NORMAL FORCE $N(x)$, AND BOND FORCE $q(x)$ ALONG THE ANCHORAGE LENGTH, ANALYTICAL AND EXPERIMENTAL RESULTS FOR 6 CHARACTERISTIC LOAD STAGES (SEE FIG. 5.6) OF SPECIMEN 14 OF REF. [5].

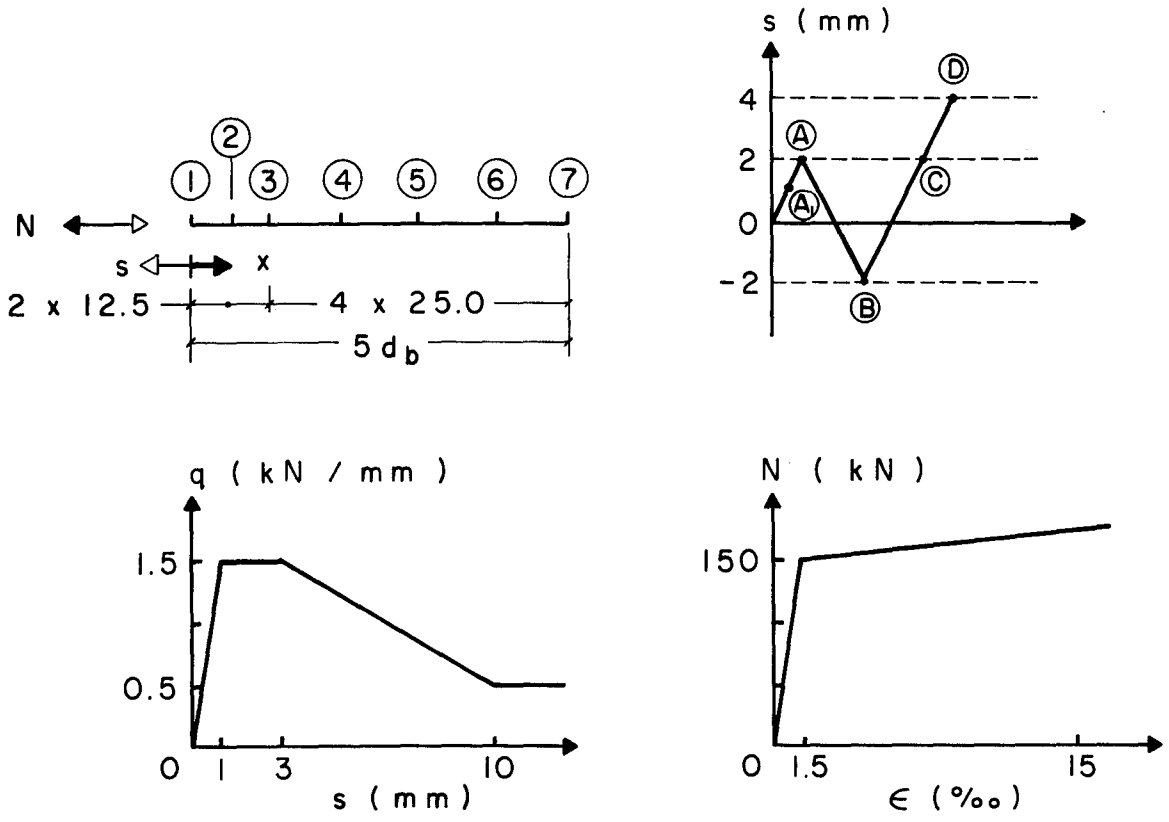

FIG. 6.1a - BAR SUBDIVISION, LOAD HISTORY, LOCAL BOND LAW AND STEEL LAW

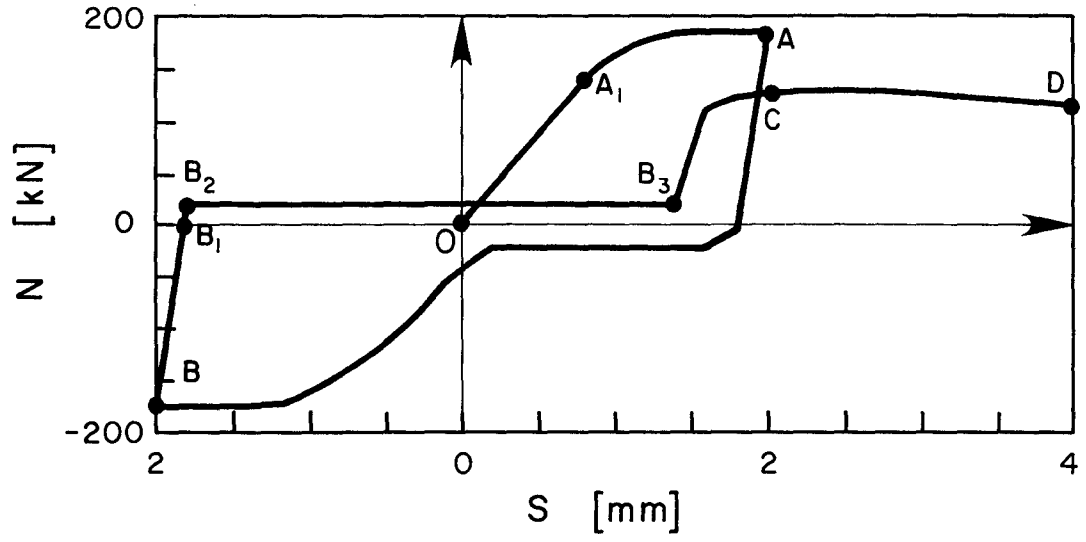

FIG. 6.1b - NORMAL FORCE-SLIP RELATIONSHIP FOR POINT 1

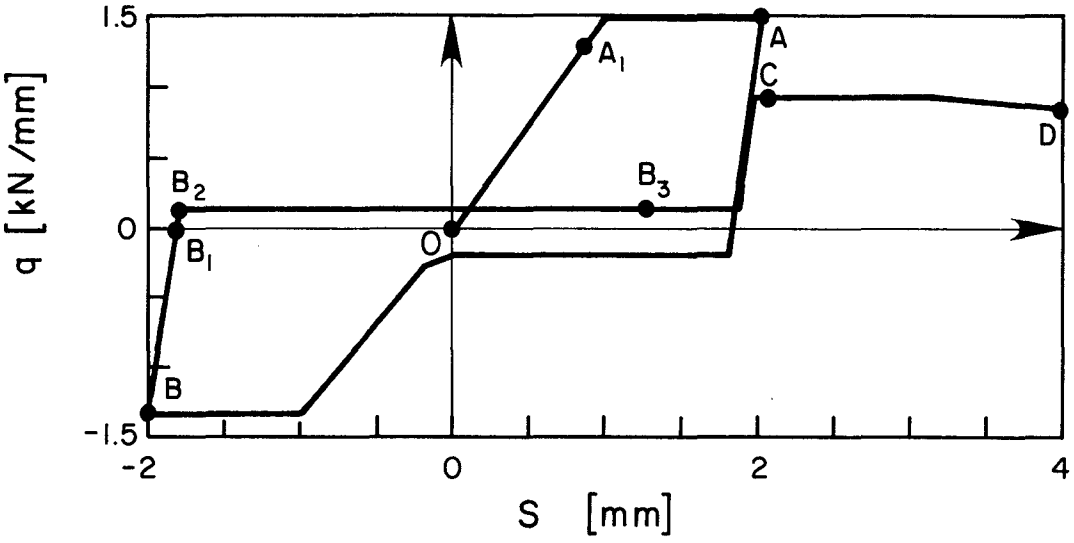

FIG. 6.1c - BOND FORCE-SLIP RELATIONSHIP FOR POINT 1

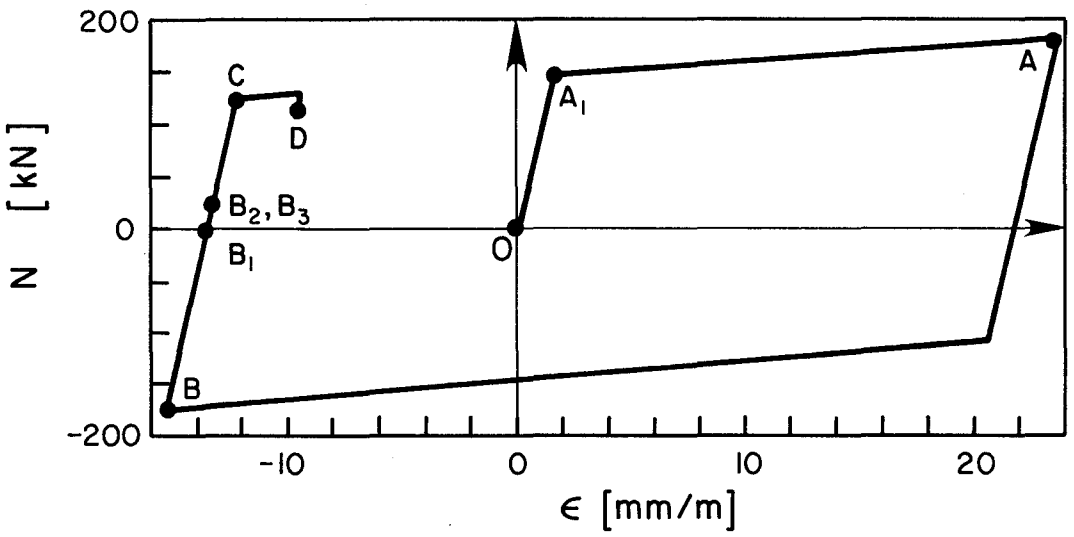

FIG. 6.1d - NORMAL FORCE-STRAIN RELATIONSHIP FOR POINT 1

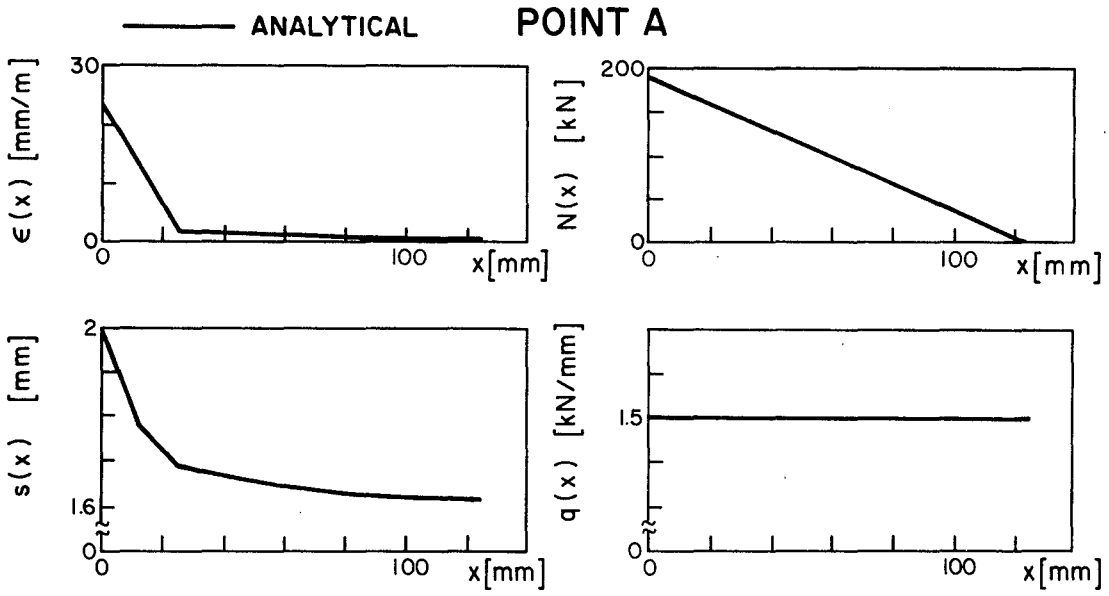

FIG. 6.1e - DISTRIBUTION OF STEEL STRAIN $\varepsilon(x)$, SLIP $s(x)$, NORMAL FORCE $N(x)$ AND BOND FORCE $q(c)$ ALONG THE ANCHORAGE LENGTH AT LOAD POINT A.

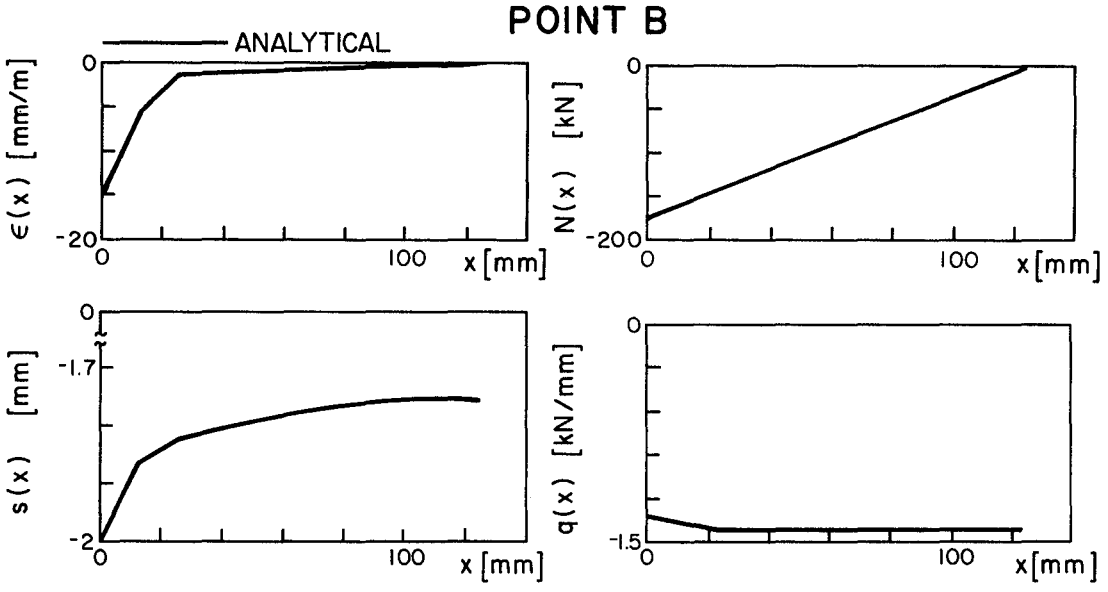

FIG. 6.1f - DISTRIBUTION OF STEEL STRAIN $\varepsilon(x)$, SLIP $s(x)$, NORMAL FORCE $N(x)$ AND BOND FORCE $q(x)$ ALONG THE ANCHORAGE LENGTH AT LOAD POINT B.

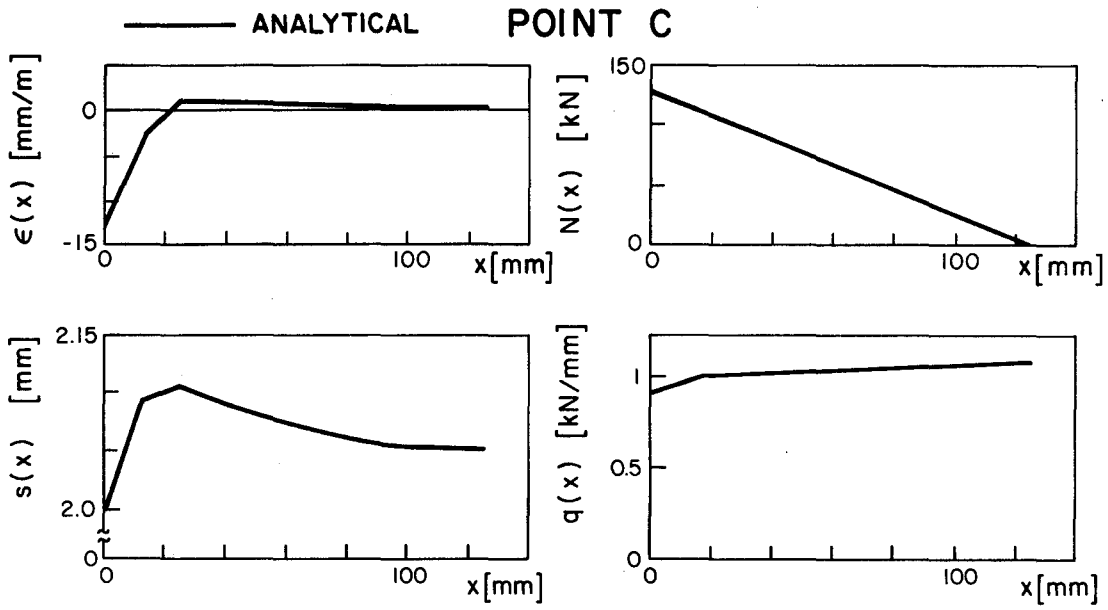

FIG. 6.1g - DISTRIBUTION OF STEEL STRAIN $\varepsilon(x)$, SLIP $s(x)$, NORMAL FORCE $N(x)$ AND BOND FORCE $q(x)$ ALONG THE ANCHORAGE LENGTH AT LOAD POINT C.

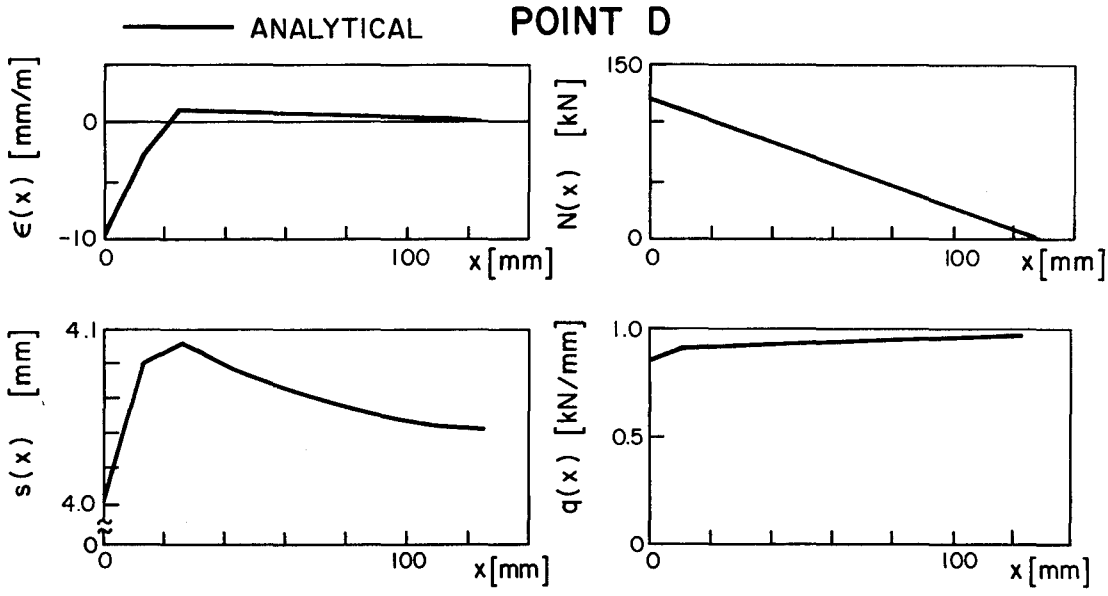

FIG. 6.1h - DISTRIBUTION OF STEEL STRAIN $\varepsilon(x)$, SLIP $s(x)$, NORMAL FORCE $N(x)$ AND BOND FORCE $q(x)$ ALONG THE ANCHORAGE LENGTH OF LOAD POINT D.

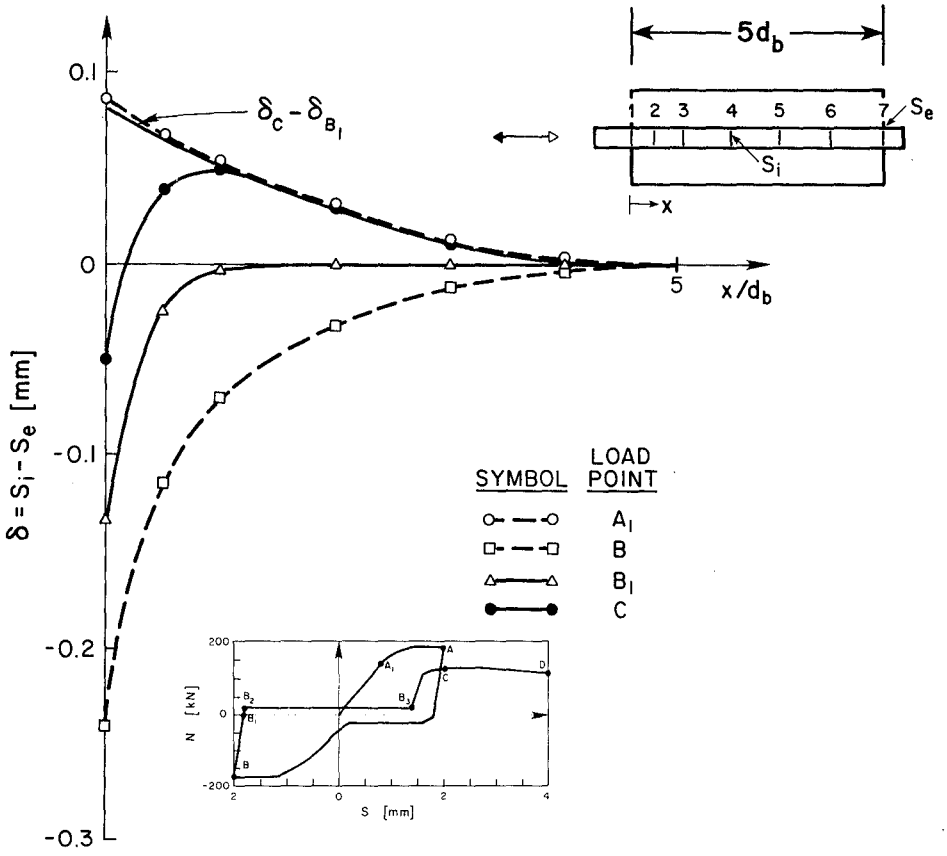

FIG. 6.2 - DISTRIBUTION OF BAR DEFORMATION $\delta = s_i - s_e$ ALONG THE ANCHORAGE LENGTH

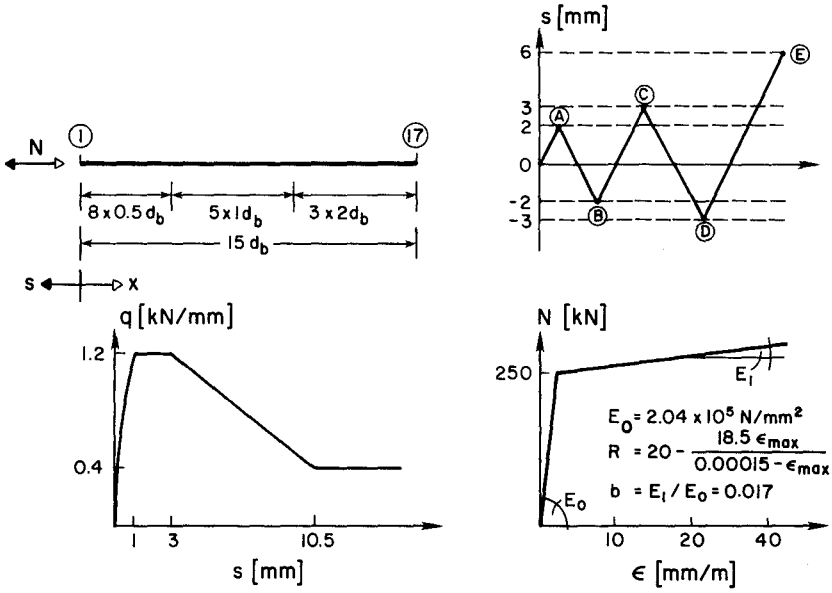

(a) -BAR SUBDIVISIONS, LOAD HISTORY, LOCAL BOND LAW AND STEEL LAW

FIG 6.3 - INFLUENCE OF STEEL MODEL ON THE RESPONSE OF AN ANCHORED BEAM BAR UNDER CYCLIC LOADING

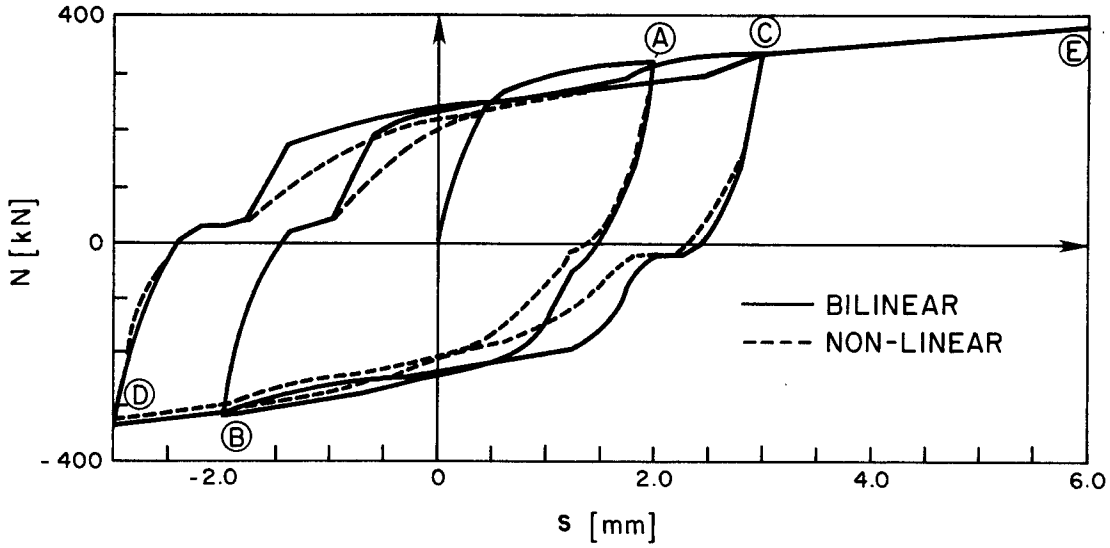

(b) - NORMAL FORCE-SLIP RELATIONSHIP FOR POINT 1.

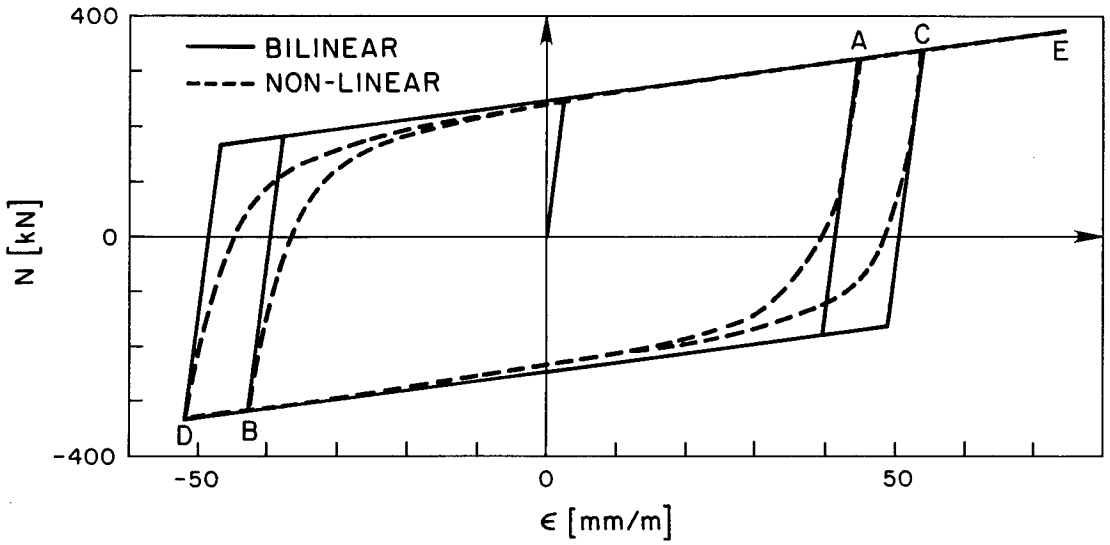

(c) - NORMAL FORCE-STRAIN RELATIONSHIP FOR POINT 1.

FIG 6.3 - INFLUENCE OF STEEL MODEL ON THE RESPONSE OF AN ANCHORED BEAM BAR UNDER CYCLIC LOADING.

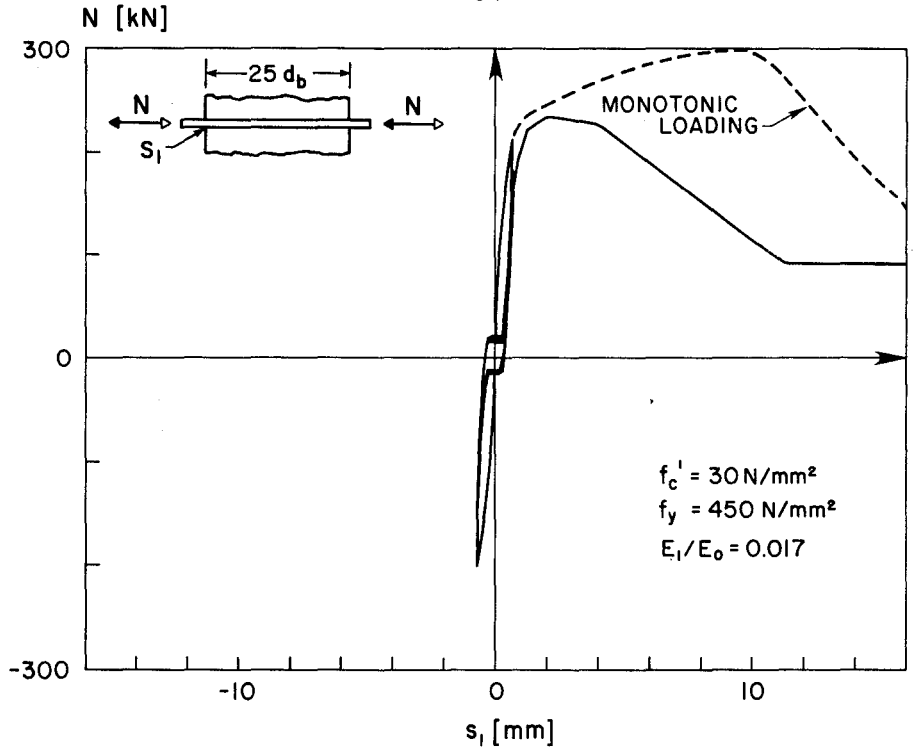

(a) CYCLING BETWEEN SLIP VALUES CORRESPONDING TO PEAK STEEL STRAINS $\varepsilon = \pm\varepsilon_y$

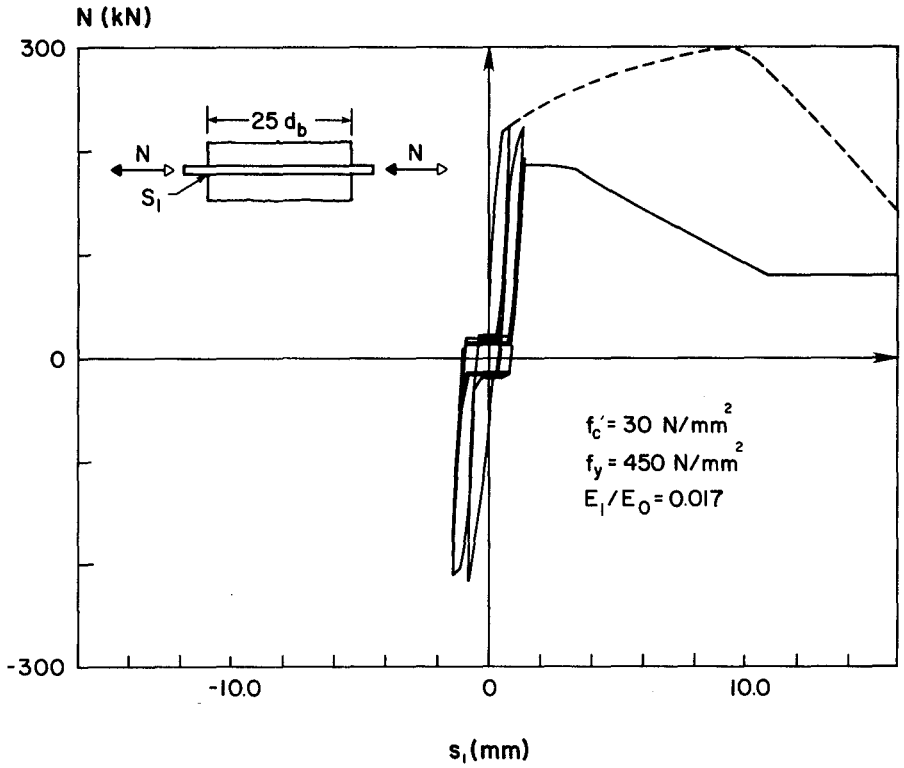

(b) CYCLING BETWEEN SLIP VALUES CORRESPONDING TO PEAK STEEL STRAINS $\varepsilon = \pm 5$ mm/m AND $\varepsilon = \pm 10$ mm/m

FIG. 6.4 - INFLUENCE OF HYSTERETIC REQUIREMENTS ON THE RESPONSE OF AN ANCHORED BEAM BAR UNDER CYCLIC LOADINGS

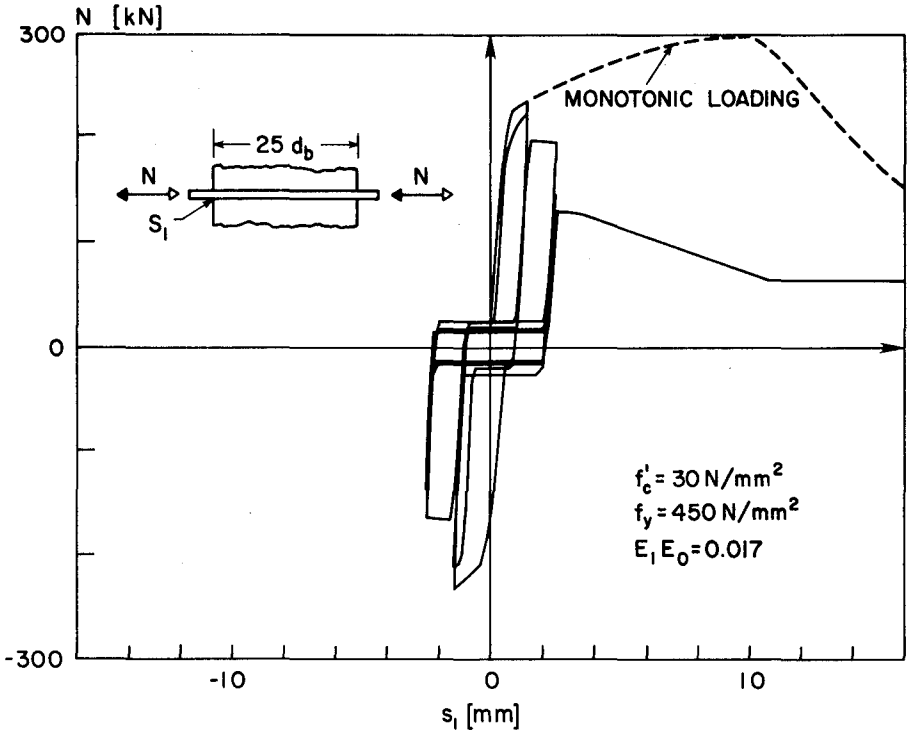

(c) CYCLING BETWEEN SLIP VALUES CORRESPONDING TO PEAK STEEL STRAINS $\varepsilon = \pm 10$ mm/m AND $\varepsilon = \pm 20$ mm/m

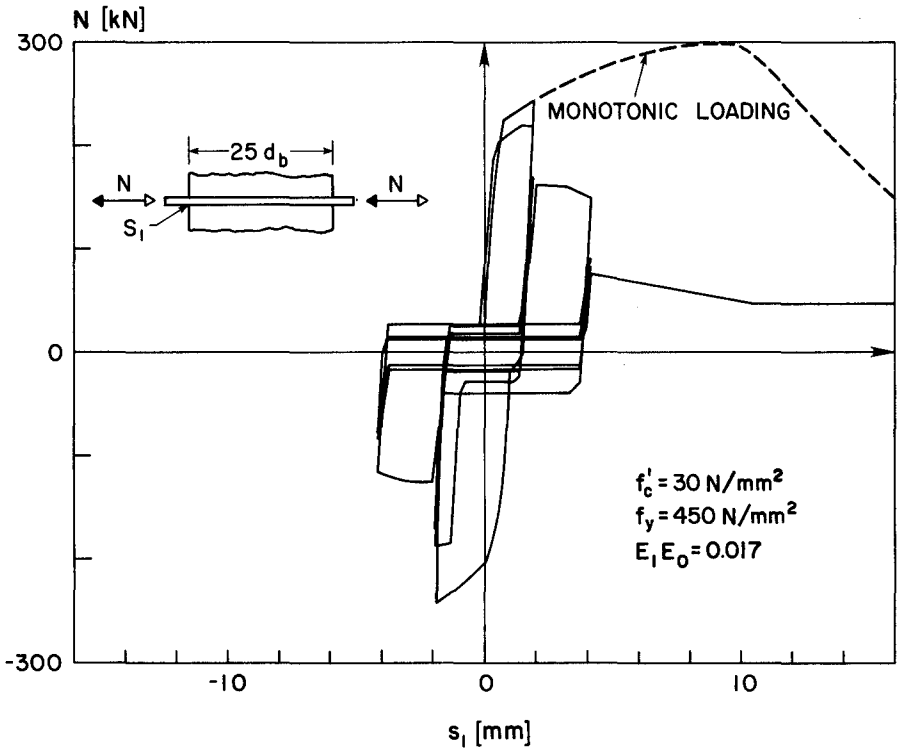

(d) CYCLING BETWEEN SLIP VALUES CORRESPONDING TO PEAK STEEL STRAINS $\varepsilon = \pm 15$ mm/m AND $\varepsilon = \pm 30$ mm/m

FIG. 6.4 - INFLUENCE OF HYSTERETIC REQUIREMENTS ON THE RESPONSE OF AN ANCHORED BEAM BAR UNDER CYCLIC LOADINGS

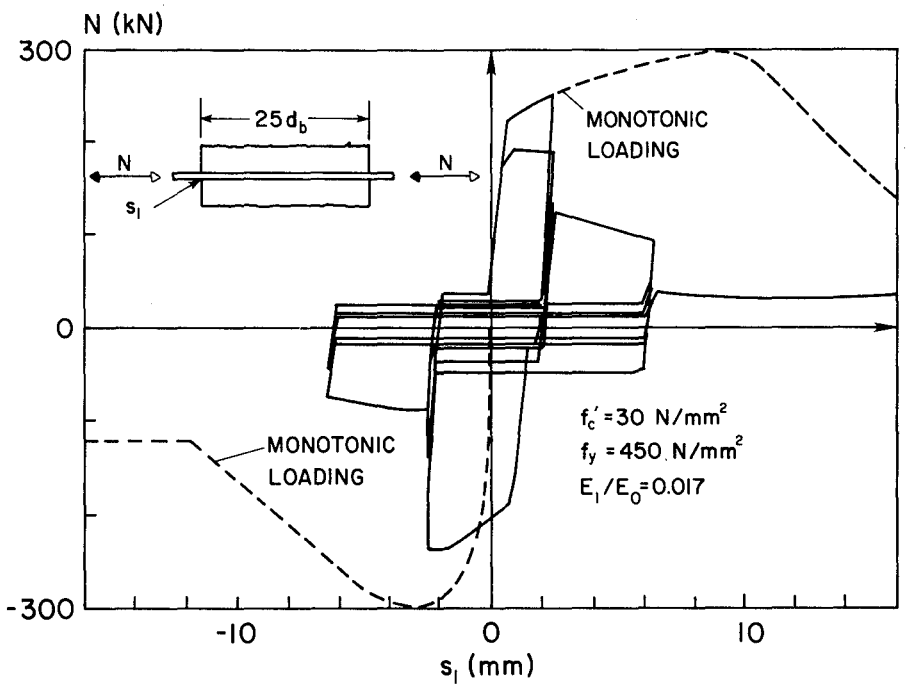

(e) CYCLING BETWEEN SLIP VALUES CORRESPONDING TO PEAK STEEL STRAINS $\varepsilon = \pm 20$ mm/m AND $\varepsilon = \pm 40$ mm/m

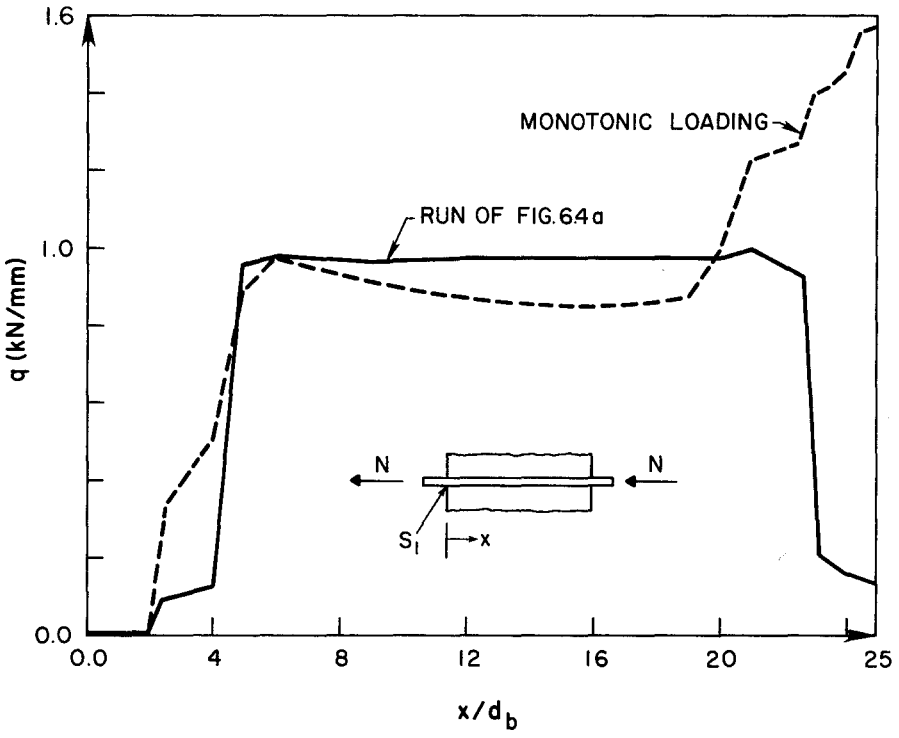

(f) DISTRIBUTION OF BOND FORCES ALONG THE ANCHORAGE LENGTH AT A PEAK SLIP VALUE $s_1 = 4.0$ mm

FIG. 6.4 - INFLUENCE OF HYSTERETIC REQUIREMENTS ON THE RESPONSE OF AN ANCHORED BEAM BAR UNDER CYCLIC LOADINGS

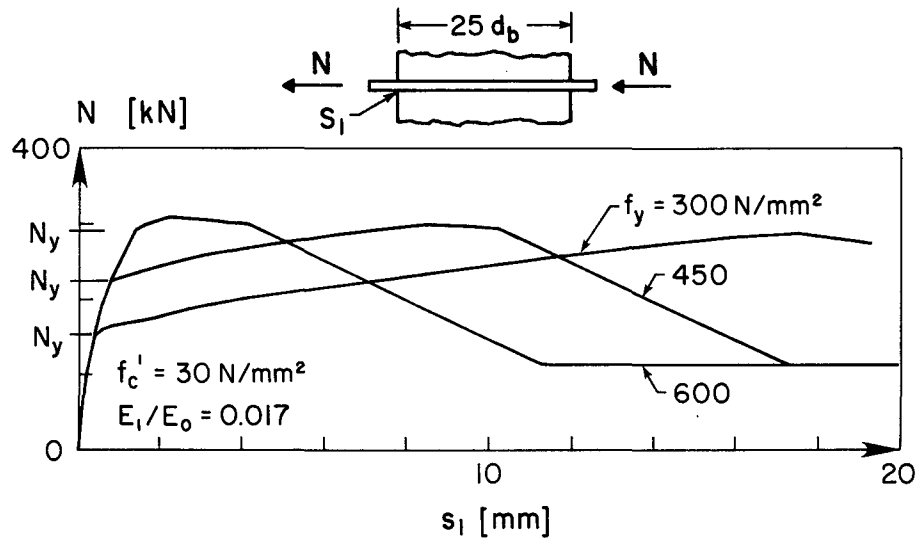

(a) MONOTONIC LOADING

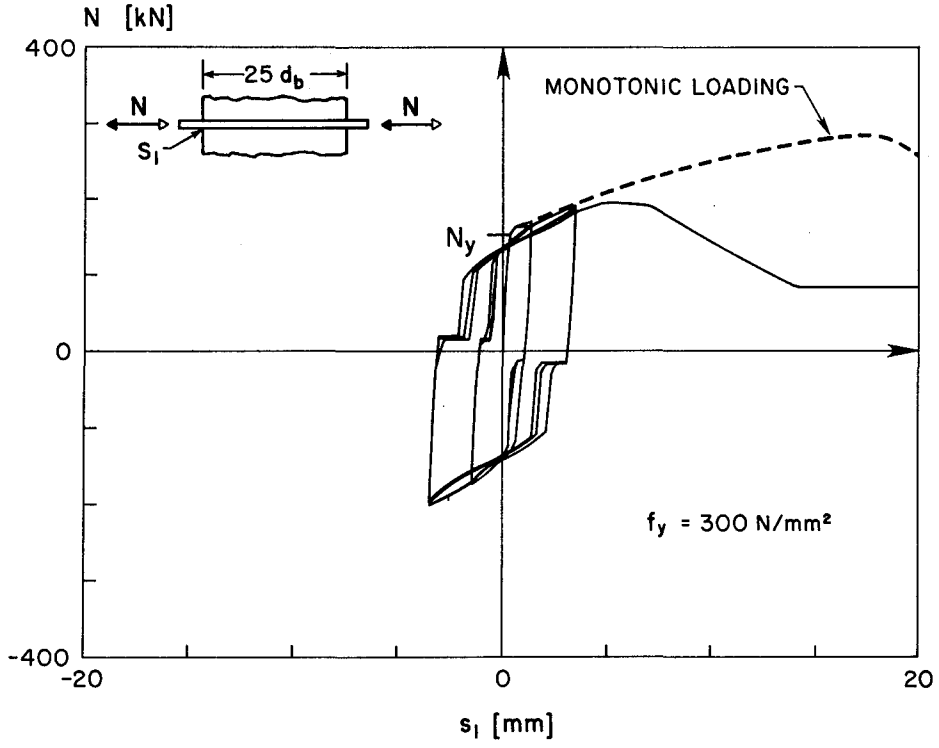

(b) CYCLIC LOADING, f_y = 300 N/mm^2

FIG. 6.5 - INFLUENCE OF YIELD STRESS ON THE RESPONSE OF AN ANCHORED BEAM BAR

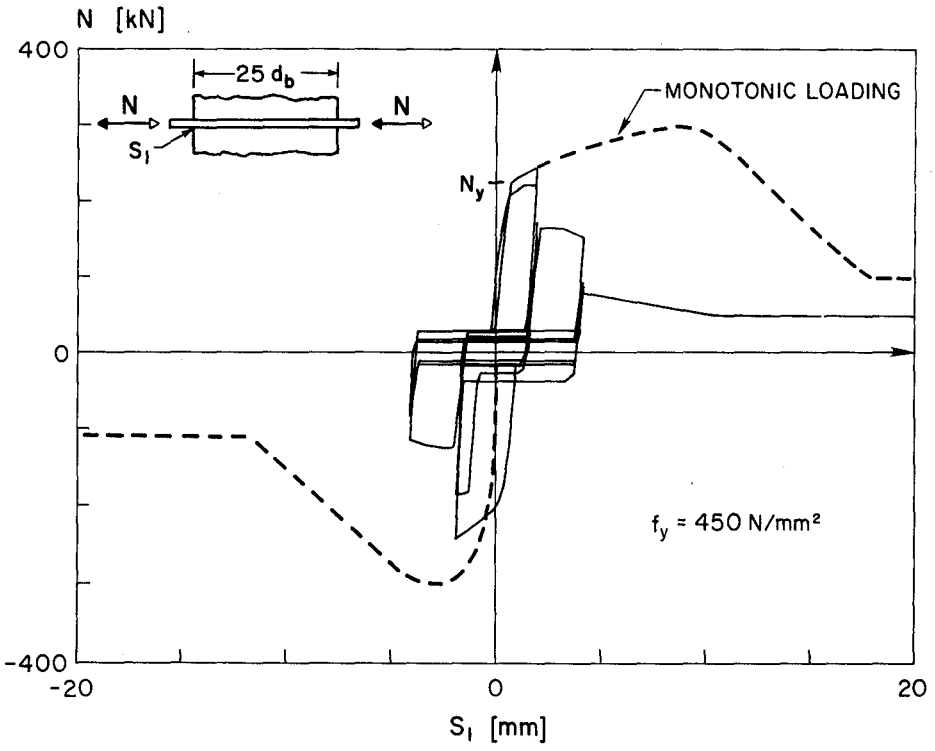

(c) CYCLIC LOADING, f_y = 450 N/mm^2

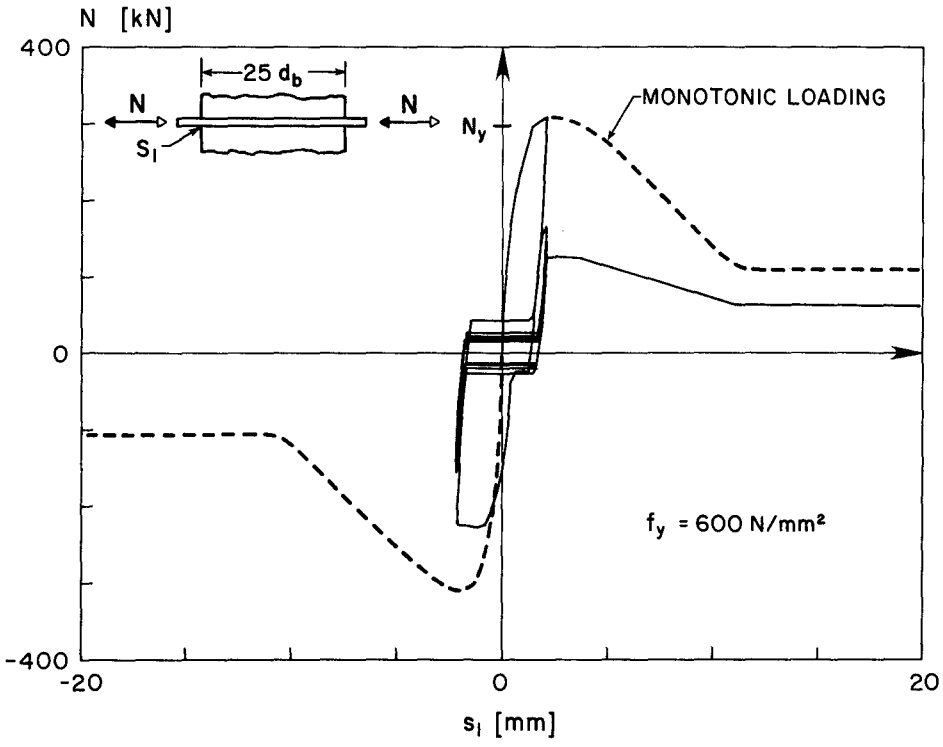

(d) CYCLIC LOADING, f_y = 600 N/mm^2

FIG. 6.5 - INFLUENCE OF YIELD STRESS ON THE RESPONSE OF AN ANCHORED BEAM BAR

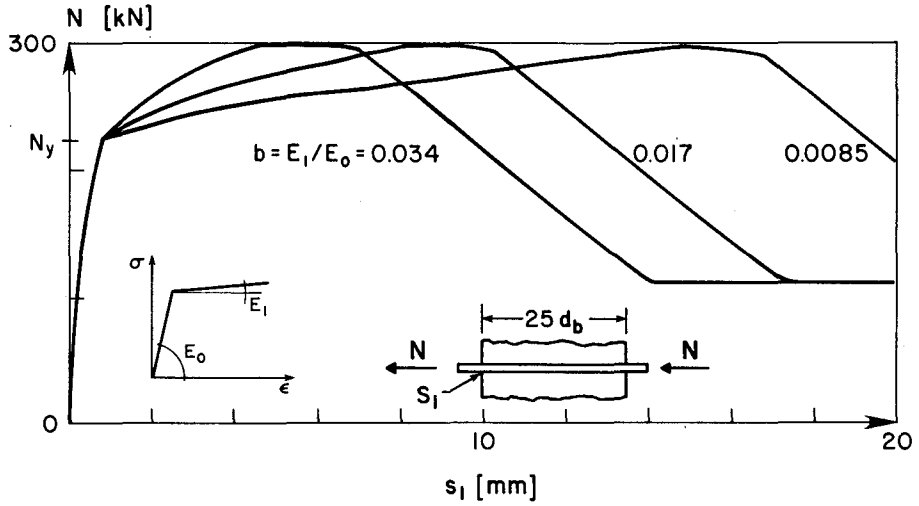

(a) MONOTONIC LOADING

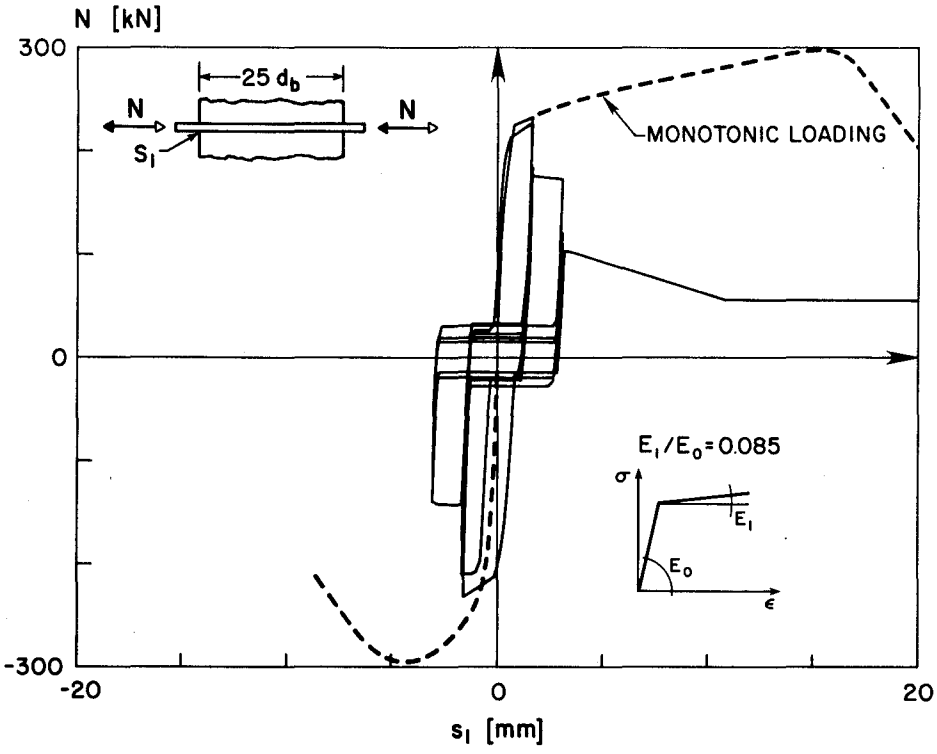

(b) CYCLIC LOADING, $E_1/E_0 = 0.085$

FIG. 6.6 - INFLUENCE OF SLOPE OF STRAIN HARDENING BRANCH ON THE RESPONSE OF AN ANCHORED BEAM BAR

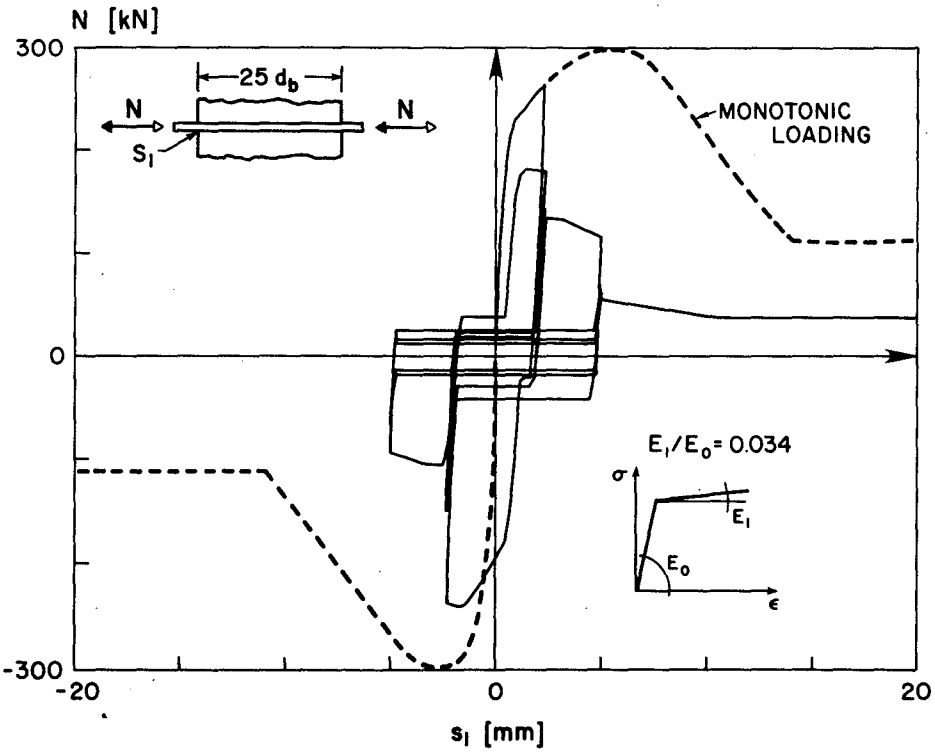

(c) CYCLIC LOADING, E_1/E_0 = 0.034

FIG 6.6 - INFLUENCE OF SLOPE OF STRAIN HARDENING BRANCH ON THE RESPONSE OF AN ANCHORED BEAM BAR.

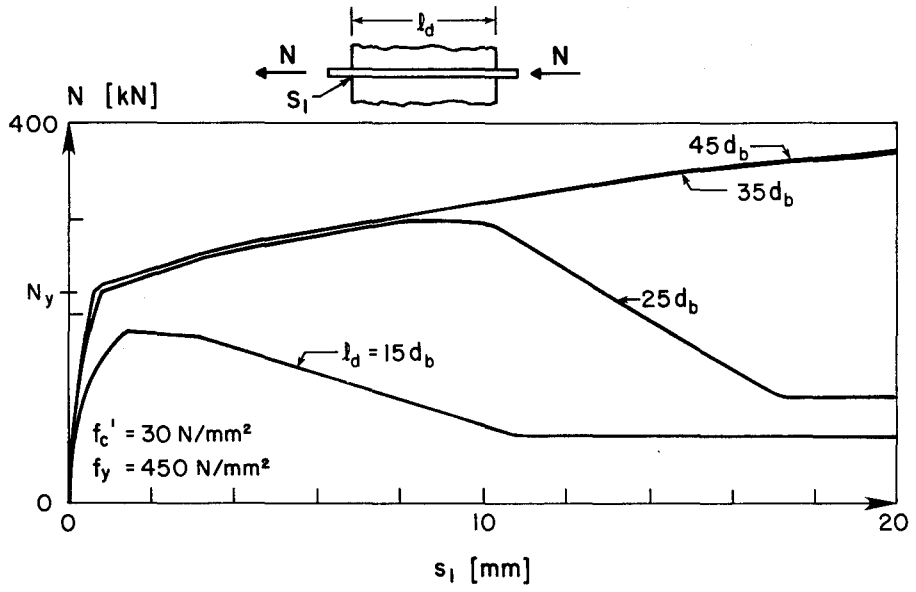

(a) MONOTONIC LOADING

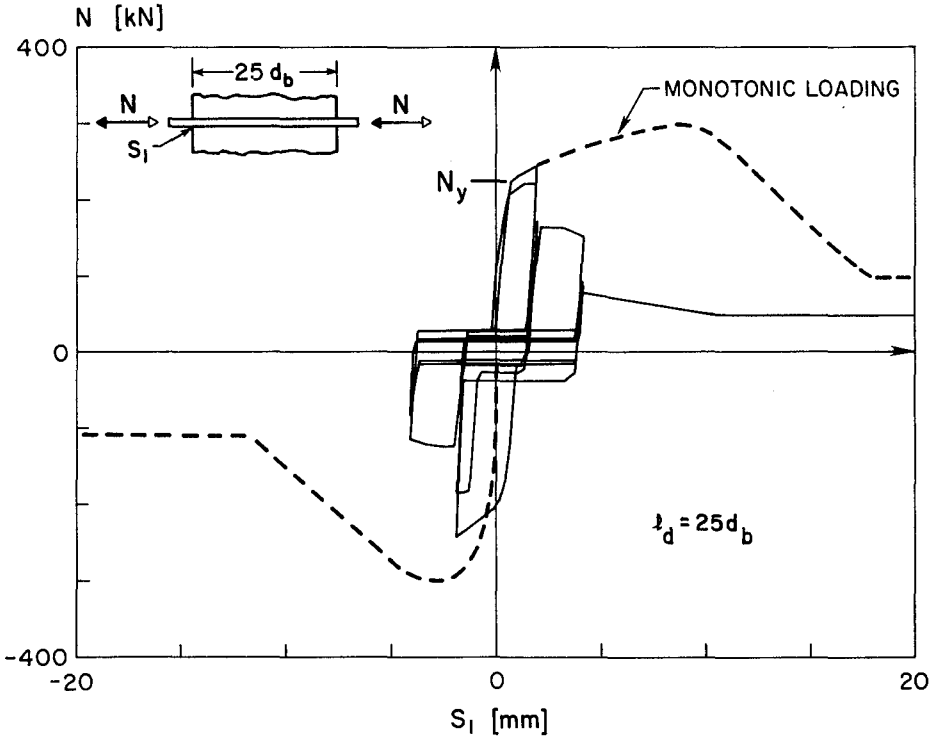

(b) - CYCLIC LOADING, $\ell_d = 25d_b$

FIG. 6.7 - INFLUENCE OF EMBEDMENT LENGTH ON THE RESPONSE OF AN ANCHORED BEAM BAR

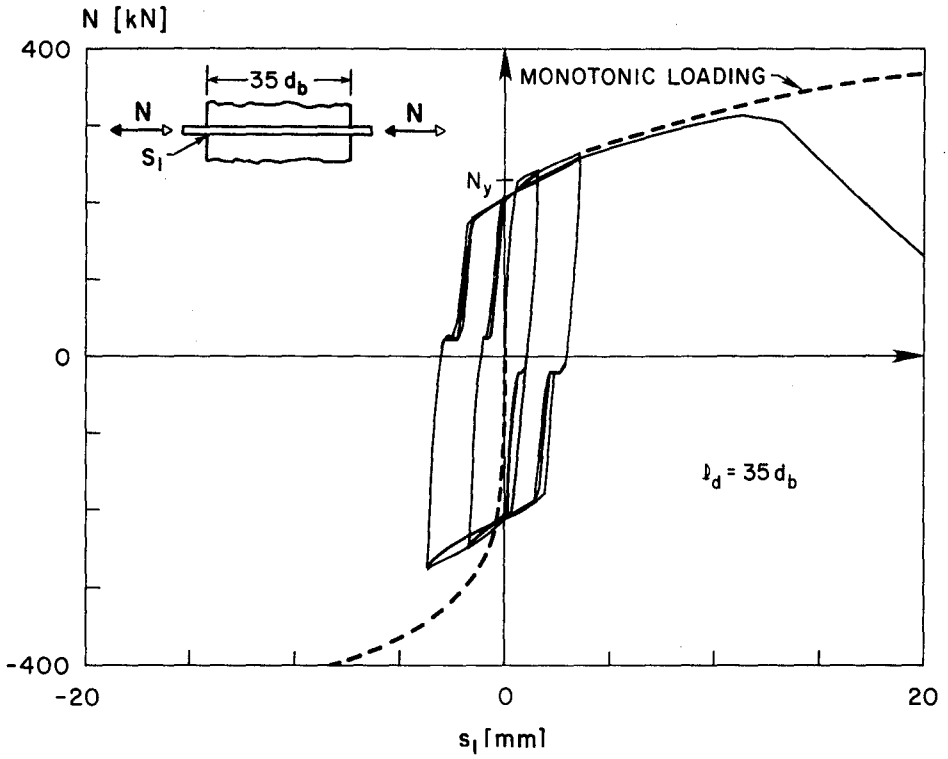

(c) CYCLIC LOADING, $l_d = 35d_b$

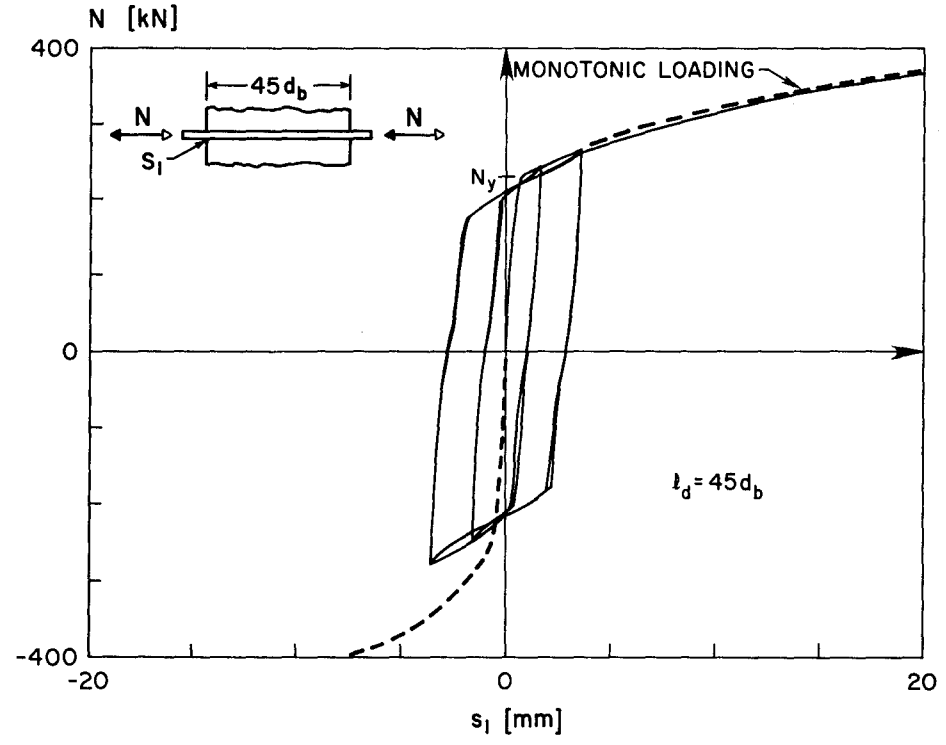

(d) CYCLIC LOADING, $l_d = 45d_b$

FIG. 6.7 - INFLUENCE OF EMBEDMENT LENGTH ON THE RESPONSE OF AN ANCHORED BEAM BAR

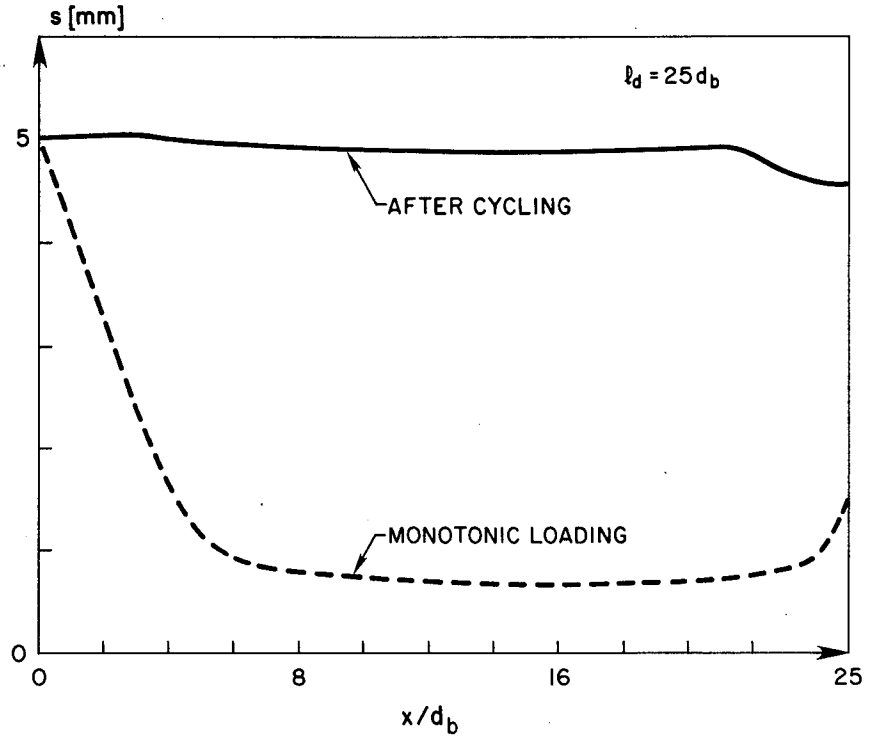

(a) $l_d = 25d_b$

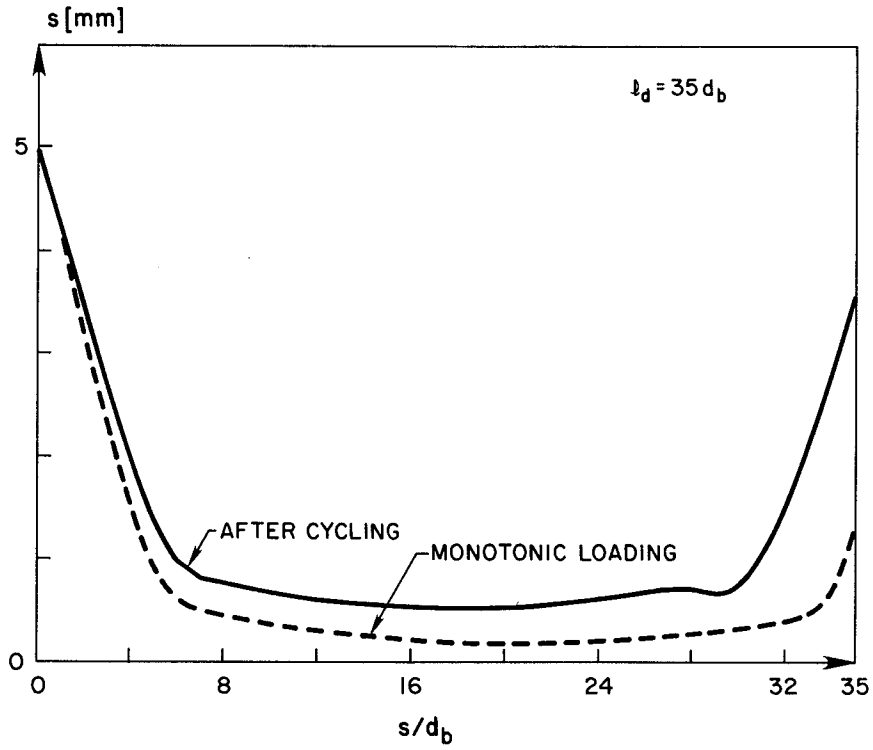

(b) $l_d = 35d_b$

FIG. 6.8 - INFLUENCE OF EMBEDMENT LENGTH ON THE DISTRIBUTION OF SLIP ALONG THE ANCHORAGE LENGTH AT A PEAK SLIP s_1 = 5.0 mm

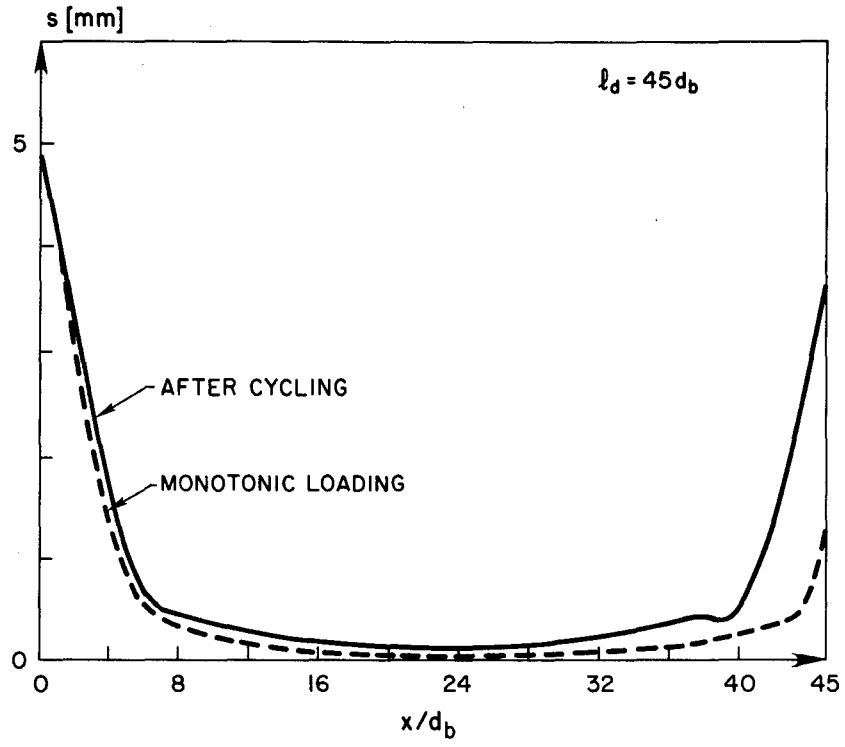

(c) $l_d = 45d_b$

FIG 6.8 - INFLUENCE OF EMBEDMENT LENGTH ON THE DISTRIBUTION OF SLIP ALONG THE ANCHORAGE LENGTH AT A PEAK SLIP S_1 = 5.0 MM.

TABLE 5.1 - INPUT FOR PROGRAM TO CALCULATE THE RESPONSE OF TESTED BARS

(a) Subdivision of Bar

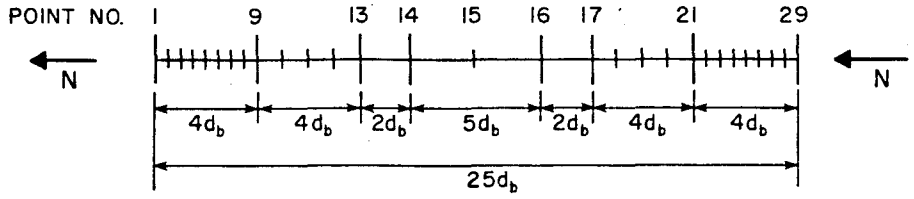

(b) Local Bond Laws

Region	Length	Points	Direction of Loading	Monotonic Envelope*						Cyclic Parameter α
				s_1 mm	s_2 mm	s_3 mm	τ_1 N/mm²	τ_3 N/mm²	β	
1	2 d_b	1-5	Positive Negative	1.0 0.3	3.0 0.3	10.5 1.0	20.0 5.0	7.5 0.0		1.0 114.0
2	2 d_b	6-9	Positive Negative	1.0 0.475	3.0 0.975	10.5 3.375	18.4 7.1	6.9 1.25		1.0 11.0
3	1 d_d	10	Positive Negative	1.0 0.825	3.0 7.325	10.5 8.125	15.1 11.4	5.6 3.75		1.0 3.5
4	15 d_b	11-19	Positive Negative	1.0	3.0	10.5	13.5	5.0	0.4	1.0 1.0
5	1 d_b	20	Positive Negative	0.825 1.0	2.325 3.0	8.125 10.5	11.4 15.1	3.75 5.6		3.5 1.0
6	2 d_b	21-24	Positive Negative	0.475 1.0	0.975 3.0	3.375 10.5	7.1 18.4	1.25 6.9		11.0 1.0
7	2 d_b	25-29	Positive Negative	0.3 1.0	0.3 3.0	1.0 10.5	5.0 20.0	0.0 7.5		114.0 1.0

*For definition of terms see Fig. 2.1.

α^+, α^- are amplification (scaling) factors for computing, respectively, relative damage in positive and negative directions (see Section 2.4).

Damage Parameters: Reduced Envelope - $b_1 = 0.5$, $b_2 = 1.2$, $b_3 = 1.1$;
Friction Branch - $f_1 = 0.1$, $f_2 = 1.8$, $f_3 = 1.2$, $f_4 = 0.67$.

(c) Characteristics of Steel

$E_0 = 2.05 \times 10^5$ N/mm² $\quad b = E_1/E_0 = 0.017 \quad f_y = 475$ N/mm² $\quad A_s = 453$ mm²

$u = 66$ mm² (circumference of bar)

EARTHQUAKE ENGINEERING RESEARCH CENTER REPORTS

NOTE: Numbers in parentheses are Accession Numbers assigned by the National Technical Information Service; these are followed by a price code. Copies of the reports may be ordered from the National Technical Information Service, 5285 Port Royal Road, Springfield, Virginia, 22161. Accession Numbers should be quoted on orders for reports (PB --- ---) and remittance must accompany each order. Reports without this information were not available at time of printing. The complete list of EERC reports (from EERC 67-1) is available upon request from the Earthquake Engineering Research Center, University of California, Berkeley, 47th Street and Hoffman Boulevard, Richmond, California 94804.

UCB/EERC-77/01 "PLUSH - A Computer Program for Probabilistic Finite Element Analysis of Seismic Soil-Structure Interaction," by M.P. Romo Organista, J. Lysmer and H.B. Seed - 1977 (PB81 177 651)A05

UCB/EERC-77/02 "Soil-Structure Interaction Effects at the Humboldt Bay Power Plant in the Ferndale Earthquake of June 7, 1975," by J.E. Valera, H.B. Seed, C.F. Tsai and J. Lysmer - 1977 (PB 265 795)A04

UCB/EERC-77/03 "Influence of Sample Disturbance on Sand Response to Cyclic Loading," by K. Mori, H.B. Seed and C.K. Chan - 1977 (PB 267 352)A04

UCB/EERC-77/04 "Seismological Studies of Strong Motion Records," by J. Shoja-Taheri - 1977 (PB 269 655)A10

UCB/EERC-77/05 Unassigned

UCB/EERC-77/06 "Developing Methodologies for Evaluating the Earthquake Safety of Existing Buildings," by No. 1 - B. Bresler; No. 2 - B. Bresler, T. Okada and D. Zisling; No. 3 - T. Okada and B. Bresler; No. 4 - V.V. Bertero and B. Bresler - 1977 (PB 267 354)A08

UCB/EERC-77/07 "A Literature Survey - Transverse Strength of Masonry Walls," by Y. Omote, R.L. Mayes, S.W. Chen and R.W. Clough - 1977 (PB 277 933)A07

UCB/EERC-77/08 "DRAIN-TABS: A Computer Program for Inelastic Earthquake Response of Three Dimensional Buildings," by R. Guendelman-Israel and G.H. Powell - 1977 (PB 270 693)A07

UCB/EERC-77/09 "SUBWALL: A Special Purpose Finite Element Computer Program for Practical Elastic Analysis and Design of Structural Walls with Substructure Option," by D.Q. Le, H. Peterson and E.P. Popov - 1977 (PB 270 567)A05

UCB/EERC-77/10 "Experimental Evaluation of Seismic Design Methods for Broad Cylindrical Tanks," by D.P. Clough (PB 272 280)A13

UCB/EERC-77/11 "Earthquake Engineering Research at Berkeley - 1976," - 1977 (PB 273 507)A09

UCB/EERC-77/12 "Automated Design of Earthquake Resistant Multistory Steel Building Frames," by N.D. Walker, Jr. - 1977 (PB 276 526)A09

UCB/EERC-77/13 "Concrete Confined by Rectangular Hoops Subjected to Axial Loads," by J. Vallenas, V.V. Bertero and E.P. Popov - 1977 (PB 275 165)A06

UCB/EERC-77/14 "Seismic Strain Induced in the Ground During Earthquakes," by Y. Sugimura - 1977 (PB 284 201)A04

UCB/EERC-77/15 Unassigned

UCB/EERC-77/16 "Computer Aided Optimum Design of Ductile Reinforced Concrete Moment Resisting Frames," by S.W. Zagajeski and V.V. Bertero - 1977 (PB 280 137)A07

UCB/EERC-77/17 "Earthquake Simulation Testing of a Stepping Frame with Energy-Absorbing Devices," by J.M. Kelly and D.F. Tsztoo - 1977 (PB 273 506)A04

UCB/EERC-77/18 "Inelastic Behavior of Eccentrically Braced Steel Frames under Cyclic Loadings," by C.W. Roeder and E.P. Popov - 1977 (PB 275 526)A15

UCB/EERC-77/19 "A Simplified Procedure for Estimating Earthquake-Induced Deformations in Dams and Embankments," by F.I. Makdisi and H.B. Seed - 1977 (PB 276 820)A04

UCB/EERC-77/20 "The Performance of Earth Dams during Earthquakes," by H.B. Seed, F.I. Makdisi and P. de Alba - 1977 (PB 276 821)A04

UCB/EERC-77/21 "Dynamic Plastic Analysis Using Stress Resultant Finite Element Formulation," by P. Lukkunapvasit and J.M. Kelly - 1977 (PB 275 453)A04

UCB/EERC-77/22 "Preliminary Experimental Study of Seismic Uplift of a Steel Frame," by R.W. Clough and A.A. Huckelbridge 1977 (PB 278 769)A08

UCB/EERC-77/23 "Earthquake Simulator Tests of a Nine-Story Steel Frame with Columns Allowed to Uplift," by A.A. Huckelbridge - 1977 (PB 277 944)A09

UCB/EERC-77/24 "Nonlinear Soil-Structure Interaction of Skew Highway Bridges," by M.-C. Chen and J. Penzien - 1977 (PB 276 176)A07

UCB/EERC-77/25 "Seismic Analysis of an Offshore Structure Supported on Pile Foundations," by D.D.-N. Liou and J. Penzien 1977 (PB 283 180)A06

UCB/EERC-77/26 "Dynamic Stiffness Matrices for Homogeneous Viscoelastic Half-Planes," by G. Dasgupta and A.K. Chopra - 1977 (PB 279 654)A06

UCB/EERC-77/27 "A Practical Soft Story Earthquake Isolation System," by J.M. Kelly, J.M. Eidinger and C.J. Derham - 1977 (PB 276 814)A07

UCB/EERC-77/28 "Seismic Safety of Existing Buildings and Incentives for Hazard Mitigation in San Francisco: An Exploratory Study," by A.J. Meltsner - 1977 (PB 281 970)A05

UCB/EERC-77/29 "Dynamic Analysis of Electrohydraulic Shaking Tables," by D. Rea, S. Abedi-Hayati and Y. Takahashi 1977 (PB 282 569)A04

UCB/EERC-77/30 "An Approach for Improving Seismic - Resistant Behavior of Reinforced Concrete Interior Joints," by B. Galunic, V.V. Bertero and E.P. Popov - 1977 (PB 290 870)A06

UCB/EERC-78/01 "The Development of Energy-Absorbing Devices for Aseismic Base Isolation Systems," by J.M. Kelly and D.F. Tsztoo - 1978 (PB 284 978)A04

UCB/EERC-78/02 "Effect of Tensile Prestrain on the Cyclic Response of Structural Steel Connections, by J.G. Bouwkamp and A. Mukhopadhyay - 1978

UCB/EERC-78/03 "Experimental Results of an Earthquake Isolation System using Natural Rubber Bearings," by J.M. Eidinger and J.M. Kelly - 1978 (PB 281 686)A04

UCB/EERC-78/04 "Seismic Behavior of Tall Liquid Storage Tanks," by A. Niwa - 1978 (PB 284 017)A14

UCB/EERC-78/05 "Hysteretic Behavior of Reinforced Concrete Columns Subjected to High Axial and Cyclic Shear Forces," by S.W. Zagajeski, V.V. Bertero and J.G. Bouwkamp - 1978 (PB 283 858)A13

UCB/EERC-78/06 "Three Dimensional Inelastic Frame Elements for the ANSR-I Program," by A. Riahi, D.G. Row and G.H. Powell - 1978 (PB 295 755)A04

UCB/EERC-78/07 "Studies of Structural Response to Earthquake Ground Motion," by O.A. Lopez and A.K. Chopra - 1978 (PB 282 790)A05

UCB/EERC-78/08 "A Laboratory Study of the Fluid-Structure Interaction of Submerged Tanks and Caissons in Earthquakes," by R.C. Byrd - 1978 (PB 284 957)A08

UCB/EERC-78/09 Unassigned

UCB/EERC-78/10 "Seismic Performance of Nonstructural and Secondary Structural Elements," by I. Sakamoto - 1978 (PB81 154 593)A05

UCB/EERC-78/11 "Mathematical Modelling of Hysteresis Loops for Reinforced Concrete Columns," by S. Nakata, T. Sproul and J. Penzien - 1978 (PB 298 274)A05

UCB/EERC-78/12 "Damageability in Existing Buildings," by T. Blejwas and B. Bresler - 1978 (PB 80 166 978)A05

UCB/EERC-78/13 "Dynamic Behavior of a Pedestal Base Multistory Building," by R.M. Stephen, E.L. Wilson, J.G. Bouwkamp and M. Button - 1978 (PB 286 650)A08

UCB/EERC-78/14 "Seismic Response of Bridges - Case Studies," by R.A. Imbsen, V. Nutt and J. Penzien - 1978 (PB 286 503)A10

UCB/EERC-78/15 "A Substructure Technique for Nonlinear Static and Dynamic Analysis," by D.G. Row and G.H. Powell - 1978 (PB 288 077)A10

UCB/EERC-78/16 "Seismic Risk Studies for San Francisco and for the Greater San Francisco Bay Area," by C.S. Oliveira - 1978 (PB 81 120 115)A07

UCB/EERC-78/17 "Strength of Timber Roof Connections Subjected to Cyclic Loads," by P. Gülkan, R.L. Mayes and R.W. Clough - 1978 (HUD-000 1491)A07

UCB/EERC-78/18 "Response of K-Braced Steel Frame Models to Lateral Loads," by J.G. Bouwkamp, R.M. Stephen and E.P. Popov - 1978

UCB/EERC-78/19 "Rational Design Methods for Light Equipment in Structures Subjected to Ground Motion," by J.L. Sackman and J.M. Kelly - 1978 (PB 292 357)A04

UCB/EERC-78/20 "Testing of a Wind Restraint for Aseismic Base Isolation," by J.M. Kelly and D.E. Chitty - 1978 (PB 292 833)A03

UCB/EERC-78/21 "APOLLO - A Computer Program for the Analysis of Pore Pressure Generation and Dissipation in Horizontal Sand Layers During Cyclic or Earthquake Loading," by P.P. Martin and H.B. Seed - 1978 (PB 292 835)A04

UCB/EERC-78/22 "Optimal Design of an Earthquake Isolation System," by M.A. Bhatti, K.S. Pister and E. Polak - 1978 (PB 294 735)A06

UCB/EERC-78/23 "MASH - A Computer Program for the Non-Linear Analysis of Vertically Propagating Shear Waves in Horizontally Layered Deposits," by P.P. Martin and H.B. Seed - 1978 (PB 293 101)A05

UCB/EERC-78/24 "Investigation of the Elastic Characteristics of a Three Story Steel Frame Using System Identification," by I. Kaya and H.D. McNiven - 1978 (PB 296 225)A06

UCB/EERC-78/25 "Investigation of the Nonlinear Characteristics of a Three-Story Steel Frame Using System Identification," by I. Kaya and H.D. McNiven - 1978 (PB 301 363)A05

UCB/EERC-78/26 "Studies of Strong Ground Motion in Taiwan," by Y.M. Hsiung, B.A. Bolt and J. Penzien - 1978 (PB 298 436)A06

UCB/EERC-78/27 "Cyclic Loading Tests of Masonry Single Piers: Volume 1 - Height to Width Ratio of 2," by P.A. Hidalgo, R.L. Mayes, H.D. McNiven and R.W. Clough - 1978 (PB 296 211)A07

UCB/EERC-78/28 "Cyclic Loading Tests of Masonry Single Piers: Volume 2 - Height to Width Ratio of 1," by S.-W.J. Chen, P.A. Hidalgo, R.L. Mayes, R.W. Clough and H.D. McNiven - 1978 (PB 296 212)A09

UCB/EERC-78/29 "Analytical Procedures in Soil Dynamics," by J. Lysmer - 1978 (PB 298 445)A06

UCB/EERC-79/01 "Hysteretic Behavior of Lightweight Reinforced Concrete Beam-Column Subassemblages," by B. Forzani, E.P. Popov and V.V. Bertero - April 1979(PB 298 267)A06

UCB/EERC-79/02 "The Development of a Mathematical Model to Predict the Flexural Response of Reinforced Concrete Beams to Cyclic Loads, Using System Identification," by J. Stanton & H. McNiven - Jan. 1979(PB 295 875)A10

UCB/EERC-79/03 "Linear and Nonlinear Earthquake Response of Simple Torsionally Coupled Systems," by C.L. Kan and A.K. Chopra - Feb. 1979(PB 298 262)A06

UCB/EERC-79/04 "A Mathematical Model of Masonry for Predicting its Linear Seismic Response Characteristics," by Y. Mengi and H.D. McNiven - Feb. 1979(PB 298 266)A06

UCB/EERC-79/05 "Mechanical Behavior of Lightweight Concrete Confined by Different Types of Lateral Reinforcement," by M.A. Manrique, V.V. Bertero and E.P. Popov - May 1979(PB 301 114)A06

UCB/EERC-79/06 "Static Tilt Tests of a Tall Cylindrical Liquid Storage Tank," by R.W. Clough and A. Niwa - Feb. 1979 (PB 301 167)A06

UCB/EERC-79/07 "The Design of Steel Energy Absorbing Restrainers and Their Incorporation into Nuclear Power Plants for Enhanced Safety: Volume 1 - Summary Report," by P.N. Spencer, V.F. Zackay, and E.R. Parker - Feb. 1979(UCB/EERC-79/07)A09

UCB/EERC-79/08 "The Design of Steel Energy Absorbing Restrainers and Their Incorporation into Nuclear Power Plants for Enhanced Safety: Volume 2 - The Development of Analyses for Reactor System Piping,""Simple Systems" by M.C. Lee, J. Penzien, A.K. Chopra and K, Suzuki "Complex Systems" by G.H. Powell, E.L. Wilson, R.W. Clough and D.G. Row - Feb. 1979(UCB/EERC-79/08)A10

UCB/EERC-79/09 "The Design of Steel Energy Absorbing Restrainers and Their Incorporation into Nuclear Power Plants for Enhanced Safety: Volume 3 - Evaluation of Commercial Steels," by W.S. Owen, R.M.N. Pelloux, R.O. Ritchie, M. Faral, T. Ohhashi, J. Toplosky, S.J. Hartman, V.F. Zackay and E.R. Parker - Feb. 1979(UCB/EERC-79/09)A04

UCB/EERC-79/10 "The Design of Steel Energy Absorbing Restrainers and Their Incorporation into Nuclear Power Plants for Enhanced Safety: Volume 4 - A Review of Energy-Absorbing Devices," by J.M. Kelly and M.S. Skinner - Feb. 1979(UCB/EERC-79/10)A04

UCB/EERC-79/11 "Conservatism In Summation Rules for Closely Spaced Modes," by J.M. Kelly and J.L. Sackman - May 1979(PB 301 328)A03

UCB/EERC-79/12 "Cyclic Loading Tests of Masonry Single Piers; Volume 3 - Height to Width Ratio of 0.5," by P.A. Hidalgo, R.L. Mayes, H.D. McNiven and R.W. Clough - May 1979(PB 301 321)A08

UCB/EERC-79/13 "Cyclic Behavior of Dense Course-Grained Materials in Relation to the Seismic Stability of Dams," by N.G. Banerjee, H.B. Seed and C.K. Chan - June 1979(PB 301 373)A13

UCB/EERC-79/14 "Seismic Behavior of Reinforced Concrete Interior Beam-Column Subassemblages," by S. Viwathanatepa, E.P. Popov and V.V. Bertero - June 1979(PB 301 326)A10

UCB/EERC-79/15 "Optimal Design of Localized Nonlinear Systems with Dual Performance Criteria Under Earthquake Excitations," by M.A. Bhatti - July 1979(PB 80 167 109)A06

UCB/EERC-79/16 "OPTDYN - A General Purpose Optimization Program for Problems with or without Dynamic Constraints," by M.A. Bhatti, E. Polak and K.S. Pister - July 1979(PB 80 167 091)A05

UCB/EERC-79/17 "ANSR-II, Analysis of Nonlinear Structural Response, Users Manual," by D.P. Mondkar and G.H. Powell July 1979(PB 80 113 301)A05

UCB/EERC-79/18 "Soil Structure Interaction in Different Seismic Environments," A. Gomez-Masso, J. Lysmer, J.-C. Chen and H.B. Seed - August 1979(PB 80 101 520)A04

UCB/EERC-79/19 "ARMA Models for Earthquake Ground Motions," by M.K. Chang, J.W. Kwiatkowski, R.F. Nau, R.M. Oliver and K.S. Pister - July 1979(PB 301 166)A05

UCB/EERC-79/20 "Hysteretic Behavior of Reinforced Concrete Structural Walls," by J.M. Vallenas, V.V. Bertero and E.P. Popov - August 1979(PB 80 165 905)A12

UCB/EERC-79/21 "Studies on High-Frequency Vibrations of Buildings - 1: The Column Effect," by J. Lubliner - August 1979 (PB 80 158 553)A03

UCB/EERC-79/22 "Effects of Generalized Loadings on Bond Reinforcing Bars Embedded in Confined Concrete Blocks," by S. Viwathanatepa, E.P. Popov and V.V. Bertero - August 1979(PB 81 124 018)A14

UCB/EERC-79/23 "Shaking Table Study of Single-Story Masonry Houses, Volume 1: Test Structures 1 and 2," by P. Gülkan, R.L. Mayes and R.W. Clough - Sept. 1979 (HUD-000 1763)A12

UCB/EERC-79/24 "Shaking Table Study of Single-Story Masonry Houses, Volume 2: Test Structures 3 and 4," by P. Gülkan, R.L. Mayes and R.W. Clough - Sept. 1979 (HUD-000 1836)A12

UCB/EERC-79/25 "Shaking Table Study of Single-Story Masonry Houses, Volume 3: Summary, Conclusions and Recommendations," by R.W. Clough, R.L. Mayes and P. Gülkan - Sept. 1979 (HUD-000 1837)A06

UCB/EERC-79/26 "Recommendations for a U.S.-Japan Cooperative Research Program Utilizing Large-Scale Testing Facilities," by U.S.-Japan Planning Group - Sept. 1979(PB 301 407)A06

UCB/EERC-79/27 "Earthquake-Induced Liquefaction Near Lake Amatitlan, Guatemala," by H.B. Seed, I. Arango, C.K. Chan, A. Gomez-Masso and R. Grant de Ascoli - Sept. 1979(NUREG-CR1341)A03

UCB/EERC-79/28 "Infill Panels: Their Influence on Seismic Response of Buildings," by J.W. Axley and V.V. Bertero Sept. 1979(PB 80 163 371)A10

UCB/EERC-79/29 "3D Truss Bar Element (Type 1) for the ANSR-II Program," by D.P. Mondkar and G.H. Powell - Nov. 1979 (PB 80 169 709)A02

UCB/EERC-79/30 "2D Beam-Column Element (Type 5 - Parallel Element Theory) for the ANSR-II Program," by D.G. Row, G.H. Powell and D.P. Mondkar - Dec. 1979(PB 80 167 224)A03

UCB/EERC-79/31 "3D Beam-Column Element (Type 2 - Parallel Element Theory) for the ANSR-II Program," by A. Riahi, G.H. Powell and D.P. Mondkar - Dec. 1979(PB 80 167 216)A03

UCB/EERC-79/32 "On Response of Structures to Stationary Excitation," by A. Der Kiureghian - Dec. 1979(PB 80166 929)A03

UCB/EERC-79/33 "Undisturbed Sampling and Cyclic Load Testing of Sands," by S. Singh, H.B. Seed and C.K. Chan Dec. 1979(ADA 087 298)A07

UCB/EERC-79/34 "Interaction Effects of Simultaneous Torsional and Compressional Cyclic Loading of Sand," by P.M. Griffin and W.N. Houston - Dec. 1979(ADA 092 352)A15

UCB/EERC-80/01 "Earthquake Response of Concrete Gravity Dams Including Hydrodynamic and Foundation Interaction Effects," by A.K. Chopra, P. Chakrabarti and S. Gupta - Jan. 1980(AD-A087297)A10

UCB/EERC-80/02 "Rocking Response of Rigid Blocks to Earthquakes," by C.S. Yim, A.K. Chopra and J. Penzien - Jan. 1980 (PB80 166 002)A04

UCB/EERC-80/03 "Optimum Inelastic Design of Seismic-Resistant Reinforced Concrete Frame Structures," by S.W. Zagajeski and V.V. Bertero - Jan. 1980(PB80 164 635)A06

UCB/EERC-80/04 "Effects of Amount and Arrangement of Wall-Panel Reinforcement on Hysteretic Behavior of Reinforced Concrete Walls," by R. Iliya and V.V. Bertero - Feb. 1980(PB81 122 525)A09

UCB/EERC-80/05 "Shaking Table Research on Concrete Dam Models," by A. Niwa and R.W. Clough - Sept. 1980(PB81 122 368)A06

UCB/EERC-80/06 "The Design of Steel Energy-Absorbing Restrainers and their Incorporation into Nuclear Power Plants for Enhanced Safety (Vol 1A): Piping with Energy Absorbing Restrainers: Parameter Study on Small Systems," by G.H. Powell, C. Oughourlian and J. Simons - June 1980

UCB/EERC-80/07 "Inelastic Torsional Response of Structures Subjected to Earthquake Ground Motions," by Y. Yamazaki April 1980(PB81 122 327)A08

UCB/EERC-80/08 "Study of X-Braced Steel Frame Structures Under Earthquake Simulation," by Y. Ghanaat - April 1980 (PB81 122 335)A11

UCB/EERC-80/09 "Hybrid Modelling of Soil-Structure Interaction," by S. Gupta, T.W. Lin, J. Penzien and C.S. Yeh May 1980(PB81 122 319)A07

UCB/EERC-80/10 "General Applicability of a Nonlinear Model of a One Story Steel Frame," by B.I. Sveinsson and H.D. McNiven - May 1980(PB81 124 877)A06

UCB/EERC-80/11 "A Green-Function Method for Wave Interaction with a Submerged Body," by W. Kioka - April 1980 (PB81 122 269)A07

UCB/EERC-80/12 "Hydrodynamic Pressure and Added Mass for Axisymmetric Bodies," by F. Nilrat - May 1980(PB81 122 343)A08

UCB/EERC-80/13 "Treatment of Non-Linear Drag Forces Acting on Offshore Platforms," by B.V. Dao and J. Penzien May 1980(PB81 153 413)A07

UCB/EERC-80/14 "2D Plane/Axisymmetric Solid Element (Type 3 - Elastic or Elastic-Perfectly Plastic) for the ANSR-II Program," by D.P. Mondkar and G.H. Powell - July 1980(PB81 122 350)A03

UCB/EERC-80/15 "A Response Spectrum Method for Random Vibrations," by A. Der Kiureghian - June 1980(PB81 122 301)A03

UCB/EERC-80/16 "Cyclic Inelastic Buckling of Tubular Steel Braces," by V.A. Zayas, E.P. Popov and S.A. Mahin June 1980(PB81 124 885)A10

UCB/EERC-80/17 "Dynamic Response of Simple Arch Dams Including Hydrodynamic Interaction," by C.S. Porter and A.K. Chopra - July 1980(PB81 124 000)A13

UCB/EERC-80/18 "Experimental Testing of a Friction Damped Aseismic Base Isolation System with Fail-Safe Characteristics," by J.M. Kelly, K.E. Beucke and M.S. Skinner - July 1980(PB81 148 595)A04

UCB/EERC-80/19 "The Design of Steel Energy-Absorbing Restrainers and their Incorporation into Nuclear Power Plants for Enhanced Safety (Vol 1B): Stochastic Seismic Analyses of Nuclear Power Plant Structures and Piping Systems Subjected to Multiple Support Excitations," by M.C. Lee and J. Penzien - June 1980

UCB/EERC-80/20 "The Design of Steel Energy-Absorbing Restrainers and their Incorporation into Nuclear Power Plants for Enhanced Safety (Vol 1C): Numerical Method for Dynamic Substructure Analysis," by J.M. Dickens and E.L. Wilson - June 1980

UCB/EERC-80/21 "The Design of Steel Energy-Absorbing Restrainers and their Incorporation into Nuclear Power Plants for Enhanced Safety (Vol 2): Development and Testing of Restraints for Nuclear Piping Systems," by J.M. Kelly and M.S. Skinner - June 1980

UCB/EERC-80/22 "3D Solid Element (Type 4-Elastic or Elastic-Perfectly-Plastic) for the ANSR-II Program," by D.P. Mondkar and G.H. Powell - July 1980(PB81 123 242)A03

ERC-80/23 "Gap-Friction Element (Type 5) for the ANSR-II Program," by D.P. Mondkar and G.H. Powell - July 1980 (PB81 122 285)A03

UCB/EERC-80/24 "U-Bar Restraint Element (Type 11) for the ANSR-II Program," by C. Oughourlian and G.H. Powell July 1980(PB81 122 293)A03

UCB/EERC-80/25 "Testing of a Natural Rubber Base Isolation System by an Explosively Simulated Earthquake," by J.M. Kelly - August 1980(PB81 201 360)A04

UCB/EERC-80/26 "Input Identification from Structural Vibrational Response," by Y. Hu - August 1980(PB81 152 308)A05

UCB/EERC-80/27 "Cyclic Inelastic Behavior of Steel Offshore Structures," by V.A. Zayas, S.A. Mahin and E.P. Popov August 1980(PB81 196 180)A15

UCB/EERC-80/28 "Shaking Table Testing of a Reinforced Concrete Frame with Biaxial Response," by M.G. Oliva October 1980(PB81 154 304)A10

UCB/EERC-80/29 "Dynamic Properties of a Twelve-Story Prefabricated Panel Building," by J.G. Bouwkamp, J.P. Kollegger and R.M. Stephen - October 1980(PB82 117 128)A06

UCB/EERC-80/30 "Dynamic Properties of an Eight-Story Prefabricated Panel Building," by J.G. Bouwkamp, J.P. Kollegger and R.M. Stephen - October 1980(PB81 200 313)A05

UCB/EERC-80/31 "Predictive Dynamic Response of Panel Type Structures Under Earthquakes," by J.P. Kollegger and J.G. Bouwkamp - October 1980(PB81 152 316)A04

UCB/EERC-80/32 "The Design of Steel Energy-Absorbing Restrainers and their Incorporation into Nuclear Power Plants for Enhanced Safety (Vol 3): Testing of Commercial Steels in Low-Cycle Torsional Fatigue," by P. Spencer, E.R. Parker, E. Jongewaard and M. Drory

UCB/EERC-80/33 "The Design of Steel Energy-Absorbing Restrainers and their Incorporation into Nuclear Power Plants for Enhanced Safety (Vol 4): Shaking Table Tests of Piping Systems with Energy-Absorbing Restrainers," by S.F. Stiemer and W.G. Godden - Sept. 1980

UCB/EERC-80/34 "The Design of Steel Energy-Absorbing Restrainers and their Incorporation into Nuclear Power Plants for Enhanced Safety (Vol 5): Summary Report," by P. Spencer

UCB/EERC-80/35 "Experimental Testing of an Energy-Absorbing Base Isolation System," by J.M. Kelly, M.S. Skinner and K.E. Beucke - October 1980(PB81 154 072)A04

UCB/EERC-80/36 "Simulating and Analyzing Artificial Non-Stationary Earthquake Ground Motions," by R.F. Nau, R.M. Oliver and K.S. Pister - October 1980(PB81 153 397)A04

UCB/EERC-80/37 "Earthquake Engineering at Berkeley - 1980," - Sept. 1980(PB81 205 874)A09

UCB/EERC-80/38 "Inelastic Seismic Analysis of Large Panel Buildings," by V. Schricker and G.H. Powell - Sept. 1980 (PB81 154 338)A13

UCB/EERC-80/39 "Dynamic Response of Embankment, Concrete-Gravity and Arch Dams Including Hydrodynamic Interaction," by J.F. Hall and A.K. Chopra - October 1980(PB81 152 324)A11

UCB/EERC-80/40 "Inelastic Buckling of Steel Struts Under Cyclic Load Reversal," by R.G. Black, W.A. Wenger and E.P. Popov - October 1980(PB81 154 312)A08

UCB/EERC-80/41 "Influence of Site Characteristics on Building Damage During the October 3, 1974 Lima Earthquake," by P. Repetto, I. Arango and H.B. Seed - Sept. 1980(PB81 161 739)A05

UCB/EERC-80/42 "Evaluation of a Shaking Table Test Program on Response Behavior of a Two Story Reinforced Concrete Frame," by J.M. Blondet, R.W. Clough and S.A. Mahin

UCB/EERC-80/43 "Modelling of Soil-Structure Interaction by Finite and Infinite Elements," by F. Medina - December 1980(PB81 229 270)A04

UCB/EERC-81/01 "Control of Seismic Response of Piping Systems and Other Structures by Base Isolation," edited by J.M. Kelly - January 1981 (PB81 200 735)A05

UCB/EERC-81/02 "OPTNSR - An Interactive Software System for Optimal Design of Statically and Dynamically Loaded Structures with Nonlinear Response," by M.A. Bhatti, V. Ciampi and K.S. Pister - January 1981 (PB81 218 851)A09

UCB/EERC-81/03 "Analysis of Local Variations in Free Field Seismic Ground Motions," by J.-C. Chen, J. Lysmer and H.B. Seed - January 1981 (AD-A099508)A13

UCB/EERC-81/04 "Inelastic Structural Modeling of Braced Offshore Platforms for Seismic Loading," by V.A. Zayas, P.-S.B. Shing, S.A. Mahin and E.P. Popov - January 1981(PB82 138 777)A07

UCB/EERC-81/05 "Dynamic Response of Light Equipment in Structures," by A. Der Kiureghian, J.L. Sackman and B. Nour-Omid - April 1981 (PB81 218 497)A04

UCB/EERC-81/06 "Preliminary Experimental Investigation of a Broad Base Liquid Storage Tank," by J.G. Bouwkamp, J.P. Kollegger and R.M. Stephen - May 1981(PB82 140 385)A03

UCB/EERC-81/07 "The Seismic Resistant Design of Reinforced Concrete Coupled Structural Walls," by A.E. Aktan and V.V. Bertero - June 1981(PB82 113 358)A11

UCB/EERC-81/08 "The Undrained Shearing Resistance of Cohesive Soils at Large Deformations," by M.R. Pyles and H.B. Seed - August 1981

UCB/EERC-81/09 "Experimental Behavior of a Spatial Piping System with Steel Energy Absorbers Subjected to a Simulated Differential Seismic Input," by S.F. Stiemer, W.G. Godden and J.M. Kelly - July 1981

UCB/EERC-81/10 "Evaluation of Seismic Design Provisions for Masonry in the United States," by B.I. Sveinsson, R.L. Mayes and H.D. McNiven - August 1981

UCB/EERC-81/11 "Two-Dimensional Hybrid Modelling of Soil-Structure Interaction," by T.-J. Tzong, S. Gupta and J. Penzien - August 1981(PB82 142 118)A04

UCB/EERC-81/12 "Studies on Effects of Infills in Seismic Resistant R/C Construction," by S. Brokken and V.V. Bertero - September 1981

UCB/EERC-81/13 "Linear Models to Predict the Nonlinear Seismic Behavior of a One-Story Steel Frame," by H. Valdimarsson, A.H. Shah and H.D. McNiven - September 1981(PB82 138 793)A07

UCB/EERC-81/14 "TLUSH: A Computer Program for the Three-Dimensional Dynamic Analysis of Earth Dams," by T. Kagawa, L.H. Mejia, H.B. Seed and J. Lysmer - September 1981(PB82 139 940)A06

UCB/EERC-81/15 "Three Dimensional Dynamic Response Analysis of Earth Dams," by L.H. Mejia and H.B. Seed - September 1981 (PB82 137 274)A12

UCB/EERC-81/16 "Experimental Study of Lead and Elastomeric Dampers for Base Isolation Systems," by J.M. Kelly and S.B. Hodder - October 1981 (PB82 166 182)A05

UCB/EERC-81/17 "The Influence of Base Isolation on the Seismic Response of Light Secondary Equipment," by J.M. Kelly - April 1981 (PB82 255 266)A04

UCB/EERC-81/18 "Studies on Evaluation of Shaking Table Response Analysis Procedures," by J. Marcial Blondet - November 1981 (PB82 197 278)A10

UCB/EERC-81/19 "DELIGHT.STRUCT: A Computer-Aided Design Environment for Structural Engineering," by R.J. Balling, K.S. Pister and E. Polak - December 1981 (PB82 218 496)

UCB/EERC-81/20 "Optimal Design of Seismic-Resistant Planar Steel Frames," by R.J. Balling, V. Ciampi, K.S. Pister and E. Polak - December 1981 (PB82 220 179)

UCB/EERC-82/01 "Dynamic Behavior of Ground for Seismic Analysis of Lifeline Systems," by T. Sato and A. Der Kiureghian - January 1982 (PB82 218 926)A05

UCB/EERC-82/02 "Shaking Table Tests of a Tubular Steel Frame Model," by Y. Ghanaat and R. W. Clough - January 1982 (PB82 220 161)A07

UCB/EERC-82/03 "Experimental Behavior of a Spatial Piping System with Shock Arrestors and Energy Absorbers under Seismic Excitation," by S. Schneider, H.-M. Lee and G. W. Godden - May 1982

UCB/EERC-82/04 "New Approaches for the Dynamic Analysis of Large Structural Systems," by E. L. Wilson - June 1982

UCB/EERC-82/05 "Model Study of Effects of Damage on the Vibration Properties of Steel Offshore Platforms," by F. Shahrivar and J. G. Bouwkamp - June 1982

UCB/EERC-82/06 "States of the Art and Practice in the Optimum Seismic Design and Analytical Response Prediction of R/C Frame-Wall Structures," by A. E. Aktan and V. V. Bertero - July 1982

UCB/EERC-82/07 "Further Study of the Earthquake Response of a Broad Cylindrical Liquid-Storage Tank Model," by G. C. Manos and R. W. Clough - July 1982

UCB/EERC-82/08 "An Evaluation of the Design and Analytical Seismic Response of a Seven Story Reinforced Concrete Frame - Wall Structure," by A. C. Finley and V. V. Bertero - July 1982

UCB/EERC-82/09 "Fluid-Structure Interactions: Added Mass Computations for Incompressible Fluid," by J. S.-H. Kuo - August 1982

UCB/EERC-82/10 "Joint-Opening Nonlinear Mechanism: Interface Smeared Crack Model," by J. S.-H. Kuo - August 1982

UCB/EERC-82/11 "Dynamic Response Analysis of Techi Dam," by R. W. Clough, R. M. Stephen and J. S.-H. Kuo - August 1982

UCB/EERC-82/12 "Prediction of the Seismic Responses of R/C Frame-Coupled Wall Structures," by A. E. Aktan, V. V. Bertero and M. Piazza - August 1982

UCB/EERC-82/13 "Preliminary Report on the SMART 1 Strong Motion Array in Taiwan," by B. A. Bolt, C. H. Loh, J. Penzien, Y. B. Tsai and Y. T. Yeh - August 1982

UCB/EERC-82/14 "Shaking-Table Studies of an Eccentrically X-Braced Steel Structure," by M. S. Yang - September 1982

UCB/EERC-82/15 "The Performance of Stairways in Earthquakes," by C. Roha, J. W. Axley and V. V. Bertero - September 1982

UCB/EERC-82/16 "The Behavior of Submerged Multiple Bodies in Earthquakes," by W.-J. Liao - September 1982

UCB/EERC-82/17 "Effects of Concrete Types and Loading Conditions on Local Bond-Slip Relationships," by A. D. Cowell, E. P. Popov and V. V. Bertero - September 1982

UCB/EERC-82/18 "Mechanical Behavior of Shear Wall Vertical Boundary Members: An Experimental Investigation," by M. T. Wagner and V. V. Bertero - October 1982

UCB/EERC-82/19 "Experimental Studies of Multi-support Seismic Loading on Piping Systems," by J. M. Kelly and A. D. Cowell - November 1982

UCB/EERC-82/20 "Generalized Plastic Hinge Concepts for 3D Beam-Column Elements," by P. F.-S. Chen and G. H. Powell - November 1982

UCB/EERC-82/21 "ANSR-III: General Purpose Computer Program for Nonlinear Structural Analysis," by C. V. Oughourlian and G. H. Powell - November 1982

UCB/EERC-82/22 "Solution Strategies for Statically Loaded Nonlinear Structures," by J. W. Simons and G. H. Powell - November 1982

UCB/EERC-82/23 "Analytical Model of Deformed Bar Anchorages under Generalized Excitations," By V. Ciampi, R. Eligehausen, V. V. Bertero and E. P. Popov - November 1982